In Vitro and *In Vivo* Antitumor Activities of Allyl Isothiocyanate

LAU, Wing Sze

A Thesis Submitted in Partial Fulfilment
of the Requirements for the Degree of
Doctor of Philosophy
in
Biology

The Chinese University of Hong Kong

September 2010

ProQuest LLC
789 East Eisenhower Parkway
P.O. Box 1346
Ann Arbor, MI 48106-1346

Thesis/ Assessment Committee

Professor Cheung Chi-Keung, Peter (Chair)
Professor Wong Yum-Shing (Thesis Supervisor)
Professor Chung Hau-Yin, Anthony (Committee Member)
Professor Wu Jian-Yong (External Examiner)

Acknowledgements

I sincerely thank Prof. Wong Yum-Shing for being my supervisor. Besides giving me pinpoint, elaborate guidance and valuable advice, he is patient, kind and considerate.

I am grateful to Prof. Cheung Chi-Keung and Prof. Chung Hau-Yin for being my internal examiners, giving me invaluable advice and encouragement in my research project and thesis. I would like to thank Prof. Wu Jian-Yong, for his willingness to serve as my external examiner.

I would like to express my gratitude to my laboratory collaborators. Their encouragement and support made this study possible. Thanks are also given to all the staff of the Department of Biology, The Chinese University of Hong Kong, for their assistance in my project. Last but not least, I would like to express my appreciation to my family for their love and emotional support.

Abstract of thesis entitled:

In Vitro and *In Vivo* Antitumor Activities of Allyl Isothiocyanate

Submitted by LAU Wing Sze

for the degree of Doctor of Philosophy in Biology

at The Chinese University of Hong Kong in Sept 2010

Many epidemiological studies indicate that a high intake of cruciferous vegetables, such as cabbage, broccoli and Brussels sprouts, may reduce the risk of certain types of cancer. Glucosinolates in cruciferous vegetables and their digested products are suggested to play an important role in such chemoprevention. When plant tissue is physically damaged, glucosidic bonds are cleaved by endogenous myrosinase to produce various products. Among these products, isothiocyanates (ITCs) draw most of the attention because of their potent antitumor activities. But the molecular mechanism leading to such effects has not yet been defined.

The objective of this study was to investigate the chemotherapeutic potential of allyl isothiocyanate (AITC) towards human colorectal adenocarcinoma cells. Another commonly founded ITC, phenylethyl isothiocyanate (PEITC) was employed as a reference sample. The growth inhibitory effects of ITCs on different colorectal adenocarcinoma cells were investigated using *in vitro* cell models. Both AITC and PEITC were found to inhibit the growth and proliferation of Caco-2, COLO 201 and SW620 cells in a time- and dose-dependent manner. Based on sensitivity, the most vulnerable SW620 cells were chosen for further studies. In the following BrdU assay, IC_{50} values for 24-h AITC and PEITC treatments were determined to be 30.2 and 9.21 μM, respectively. At the same time, the effects of ITCs on human normal skin fibroblast Hs68 cells were also investigated. It was found that the survival of Hs68

cells was not affected by the treatments of AITC. However, the survival of Hs68 cells was greatly affected by PEITC-treatments in a dose- and time-dependent manner.

In order to gain insights into the underlying mechanisms, several methods including, flow cytometric, western blot and quantitative real-time PCR analyses were employed. AITC-induced cell growth inhibition in SW620 cells was mainly caused by G2/M arrest, which was accompanied by regulatory proteins modifications. Results of western blot and quantitative real-time PCR analysis showed clear downregulation of pivotal phosphatases Cdc25B and Cdc25C at both transcriptional and post-translational levels in AITC-treated cells. Subsequently, accumulation of inhibitory phosphorylation of Cdc2 on Thr14 and Tyr15 were resulted. Furthermore, an AITC induced apoptosis after prolonged exposure was observed. It was a caspase-mediated apoptosis as evidenced by the activation of initiator caspases (-8 and -9), effector caspases (-3 and -7) and cleavage of Poly (ADP-ribose) polymerase (PARP). Besides *in vitro* studies, the antitumor activity of AITC was further illustrated by a nude mice xenografts experiment. Treatment with 10 μmol AITC could effectively suppress the growth of SW620 xenografts *in vivo.* Taken together, our results suggest that AITC is an attractive candidate for future research in chemotherapy and chemoprevention.

摘要

根據近年的流行病學研究顯示，多進食十字花科類蔬菜，例如: 捲心菜、西蘭花和球芽甘藍等，能有助減低患上癌症的機會。科學家更相信，蔬菜中所含的硫配糖體及其轉化物擁有抗癌的作用。當植物組織遇到物理破壞時，植物內部的芥子酶便會對硫配糖體產生作用，分解出各種轉化物。而在人類進食這些植物後，餘下的硫配糖體更會被人體腸道內的細菌所分解。其中的轉化物異硫氰酸酯，更被視爲重要的有效成份。不過，我們現時仍未能充份了解它們在抗癌效果上的分子基理改變。

在本論文研究中，將對常見的異硫氰酸酯，異硫氰酸烯丙酯，在人類大腸直腸癌細胞抗癌作用上作深入的探討。同時地，也選取了另一種常見的異硫氰酸酯，異硫氰酸苯乙酯，作出對比。在抑制人類癌細胞增殖的離體測試中，異硫氰酸烯丙酯和異硫氰酸苯乙酯皆能有效地抑制類大腸直腸癌細胞的增生，包括：Caco-2、COLO201 和 SW620，並且表現出劑量上和時間上的依賴性。根據這些細胞對於異硫氰酸酯的敏感度，SW620 細胞被選取作更深入的研究。在溴脫氧尿苷合併的實驗中所得，異硫氰酸烯丙酯和異硫氰酸苯乙酯的 IC_{50} 值分別爲 30.2 及 9.21 μM。另外，對於正常人類皮膚纖維母細胞 Hs68，它們卻產生顯著不同的效果，異硫氰酸烯丙酯並沒有毒性，相反地，異硫氰酸苯乙酯則擁有相當強的毒性。

對於異硫氰酸烯丙酯抑制癌細胞增殖的作用機理，本研究透過流式細胞儀、蛋白質電泳和即時定量聚合酶鏈鎖反應作進一步檢測。異硫氰酸烯丙酯導致 SW620 細胞的細胞周期停滯於 G_2/M 期，也影響了其中控制蛋白的調節。在異硫氰酸烯丙酯作用下，蛋白磷酸酶 Cdc25B 和 Cdc5C 的信使核糖核酸和蛋白

量，皆被減量調節，導致不能活化重要的 Cdc2 蛋白。此外，加以延長暴露於異硫氰酸烯丙酯的時間，更會誘導 SW620 細胞的凋亡。而其凋亡途徑是透過活化特定的凋亡蛋白，包括：caspase-8、9、3、7 和最後的 PARP 分裂。除了在的細胞模型上的活性測試，本研究亦利用了裸鼠作動物性的成效評估。異硫氰酸烯丙酯(10 μmol)能有效地抑制 SW620 異種皮移植的生長。綜合以上的實驗結果，我們相信異硫氰酸烯丙酯在抗癌療效上有很大的發展潛力。

Table of Contents

List of Tables

List of Figures

List of Abbreviations

AITC	Allyl isothiocyanate
BITC	Benzyl isothiocyanate
BrdU	5-bromo-2'-deoxyuridine
BSA	Albumin bovine serum
CRC	Colorectal cancer
DMEM	Dulbecco's modified Eagle's medium
DMSO	Dimethylsulfoxide
ELISA	Enzyme linked immunosorbent assay
FBS	Fetal bovine serum
GC-MS	Gas chromatography-electrospray mass spectrometry
HPLC-MS	High performance liquid chromatography-electrospray
IC_{50}	Half maximal inhibitory concentration
IP	Intraperitoneal injection
ITCs	Isothiocyanates
MTT	3-(4,5-dimethylthiazoly-2)-2,5-diphenl tetrazolium
PARP	Poly(ADP-ribose) polymerase
PBS	Dulbecco's phosphate buffered saline
PCR	Polymerase chain reaction
PEITC	Phenylethyl isothiocyanate
PI	Propidium iodide
RT	Room temperature
RT-PCR	Reverse transcription polymerase chain reaction
SDS	Sodium dodecyl sulfate
SFN	Sulforaphane

Chapter One

Introduction

1.1 Introduction to cancer

Cancer is a leading cause of death in human populations over the world. It may affect people at all ages, while the risk of having this disease increases with age. In terms of cellular origin, cancer cells can be divided into four main groups; carcinoma (from epithelium), sarcoma (from mesenchyme), leukaemia (from white blood cells) and cells from the nervous system (Franks and Teich, 1997a; King, 2000a). Unfortunately, the exact causes of cancer are still unknown. It is the end point of a sequence of events, and mutations of cellular DNA are the bases of the change. These mutations can be arisen from the interactions with exogenous agents, such as ionizing radiation and chemical carcinogens, or due to errors occurred during DNA replications (Franks and Teich, 1997a; King, 2000b; Tannock *et al.*, 2004a). Eventually, normal cells are transformed into malignant cancer cells that invade surrounding tissue and even spread to distant locations (metastasis). The whole process can be generalized into three main steps, initiation, promotion and progression. Among these processes, initiation is primarily the most critical step, whereas the following processes may take a long time to be completed (Franks and Teich, 1997a; King, 2000b).

Cancer is usually characterized as a mass of cells called tumor. It is a result of uncontrolled growth of cells which are no longer responding to the normal growth control mechanisms. Therefore, balance between cell proliferation and cell death is disrupted. Several possible mechanisms are suggested to be involved, including DNA

repair genes alternation, oncogenes activation, tumor suppressor genes inactivation and growth factor binding modulation (Franks and Teich, 1997a; King, 2000c; Sherr, 2004; Tannock *et al.*, 2004b). It is generally believed that oncogenes and tumor suppressor genes play a critical role in the cancer development. Originally, proto-oncogenes are very important regulatory elements, especially the *ras* and *myc*. They are encoding proteins that regulate normal cell growth and proliferation. After mutation, they become activated oncogenes, whereas a gain of function is usually resulted. On the other hand, inactivated the tumor suppressor genes, such as *Rb* and *p53*, will lead to the lost of functional inhibitory proteins, and hence deregulating normal control mechanisms. In addition, the formation of new blood vessels (angiogenesis), which usually stimulated by endothelial cell growth factors, is also necessary for the expansion of tumor (Franks and Teich, 1997b; King, 2000d; Sherr, 2004; Tannock *et al.*, 2004c).

Fortunately, some cases of cancers can be controlled and cured after proper treatments. The success rate depends on the specific type, location, and stage of cancer. With the help of doctors and pathologists, patients can have definitive diagnosis of cancer through detailed histological and cytological examinations. Once a diagnosis is made, patients can receive different cancer therapies, including physical surgery, chemotherapy and radiotherapy. In additional to traditional therapies, it is now hypothesized that various naturally occurring phytochemicals from edible plants possess different antitumor activities (Baer-Dubowska *et al.*, 2006a-c; He, 2008; Ramos, 2007; Ramos 2008; Steinmetz and Potter, 1996; Surh, 2003). Representative chemopreventive phytochemicals and their dietary sources are shown in Table 1.1. As a result, studies on the phytochemicals become a new direction in the anticancer drugs development.

1.1.1 Colorectal cancer

Colorectal cancer (CRC) is the third most common cancer worldwide (Stewart and Kleihues, 2003). It has arisen from cells lining of the large intestine including colon and rectum, and therefore collectively called 'colorectal'. In both developing and developed countries, there are increases in the number of cases and deaths because of expanding and aging of the population. For instance, around 5.5 % of American people will develop the disease at some time in their lives (Berg, 2001a). One of the reasons why colorectal cancer created such a big problem, it is because the symptoms of disease are often minimal at the beginning (Berk and Macrae, 2006a). When people noticed about the disease, the tumor has spread outside the intestine that maybe too late to be cured. According to the depth of tumor invasion into the intestine wall, the development of CRC is divided into different stages under Dukes' classification (Figure 1.1). Recent research has intense investigations on its genetic development. It involved number molecular changes, with a detailed conceptual model as shown in Figure 1.2. Furthermore, there are some risk factors that are believed to be associated with the development of CRC, which included genetic syndromes, lifestyle and age (Berg, 2001a; Berk and Macrae, 2006b; Faivre *et al.*, 2002; Marques-Vidal *et al.*, 2006; Winawer, 2007). Firstly, there are two main genetic syndromes associated with CRC. Possessing the familial adenomatous polyposis (FAP) and the hereditary non-ployposis colorectal cancer (HNPCC) are considered as high risk factors (Berg, 2001a; Berk and Macrae, 2006b; Faivre *et al.*, 2002; Winawer, 2007). Secondly, improper lifestyle such as having high fat diet, alcohol consumption and cigarette smoking will also increase the rick (Berg, 2001a; Berk and Macrae, 2006b; Marques-Vidal *et al.*, 2006). Lastly, the chance of CRC greatly increased with age, especially over the age of 50 (Berg, 2001a; Berk and Macrae, 2006b; Faivre *et al.*, 2002).

In this project, three human colorectal adenocarcinoma cell lines obtained from American Type Culture Collection (ATCC), including SW620, COLO 201 and Caco-2, were selected for investigation. For SW620 cells, they are categorized as stage C according to Dukes' classification. These cells were derived form metastasis site of the lymph-node from a 51-year-old male Caucasian. Mutations of important genes, *myc*, *ras* and *p53* were found. For COLO 201 cells, they are categorized as stage D according to Dukes' classification. These cells were derived form metastasis site of the ascites from a 70-year-old male Caucasian. Mutations of important genes, *myc*, *ras* and *p53* were observed. Lastly, Caco-2 cells were derived form the colon of a 72-year-old male Caucasian. These cells were also tumorigenic.

1.2 The relationship between dietary vegetables and cancer

Human beings have always depended on food for survival. Food provides us with the required energy and nutrients, which can promote our growth and keep us health. Many epidemiological studies indicate that a high intake of vegetables may reduce the risk of certain types of cancer, including the gastrointestinal, lung and breast cancers (Bingham and Riboli, 2004; Lin *et al.*, 1998; Steinmetz and Potter, 1996; Verhoeven *et al.*, 1996). Dietary fiber, vitamins and minerals are believed to be associated with these antitumor activities (Ames and Wakimoto, 2002; Borek, 2005; Klein *et al.*, 2003; Kune and Watson, 2006; Lowe and Frazee, 2006). It is suggested that the antitumor effects of dietary fiber were related to the modified bowel habits, which minimized exposure time to potential carcinogens (Alabaster *et al.*, 1996; Reddy, 1999; Terry *et al.*, 2001). For vitamins like vitamin C and E, their potential effects may be connected with their high antioxidant activities (Borek, 2005; Klein *et al.*, 2003; Kune and Watson, 2006; Lowe and Frazee, 2006). Moreover, one of the representative mineral, selenium, has widely reported to possess potent antitumor

activities (Borek, 2005; Klein *et al.*, 2003; Kune and Watson, 2006; Lowe and Frazee, 2006). In additional to these dietary food components, researchers have also proved that various naturally occurring phytochemicals, including polyphenols, carotenoids and glucosinolates, from edible plants also possessed well documented antitumor activities, as illustrated by various *in vitro* and *in vivo* experiments (Baer-Dubowska *et al.*, 2006a-c; He, 2008; Lin *et al.*, 1998; Ramos, 2007; Ramos 2008; Steinmetz and Potter, 1996; Surh, 2003; Verhoeven *et al.*, 1996).

1.3 Dietary glucosinolates

Glucosinolates are a class of sulphur-containing compounds. We can found them in various commonly consumed cruciferous vegetables, including cauliflower, cabbage, watercress, broccoli, Brussels sprouts and radish, etc. All these glucosinolates share a basic structure, which composed of a sulphonated moiety, a β-D-thioglucose group, and a variable side-chain (Fenwick *et al.*, 1983). The basic structure of glucosinolates is shown in Figure 1.3. Depending on the chemical structure, they can be divided into three main groups, the aliphatic, aromatic and indolyl (Fahey *et al.*, 2001; Mithen *et al.*, 2000; Verkerk *et al.*, 2009). The actual chemical composition and total glucosinolates content vary between different species. In addition, cultivating status including, soil contents and weather conditions, could also greatly affect these profiles (Fenwick *et al.*, 1983; Verkerk *et al.*, 2009). In our daily life, inclusion of cruciferous vegetables in both Eastern and Western cuisines is very common (McNaughton and Marks, 2003). On average, the daily intake of cruciferous vegetables was about 11.3 g, which contributed for about 5% of the total consumed vegetables. Hence, the average daily intake of glucosinolates is around 6.5 mg (Agudo *et al.*, 2008). But, the actual intake varies between people from different ethnic origin and socio-economic level.

In the past, glucosinolates and/ or their breakdown products were regarded as natural pesticides (Fahey *et al.*, 2001; Fenwick *et al.*, 1983; Mithen *et al.*, 2000). Certain reports even revealed their undesirable antinutritional effects in higher animals, especially in rodents having rape seeds as their major feedstuff (Fenwick *et al.*, 1983; Mithen *et al.*, 2000). Although we may concern about the potential side-effects in the consumption of cruciferous vegetables, but there was little or no direct evidence indicated these vegetables and their phytochemicals content as a cause of human disease (Fowke *et al.*, 2003; Lin *et al.*, 1998; McMillan *et al.*, 1986; Steinmetz and Potter, 1996; Verhoeven *et al.*, 1996). On the other hand, glucosinolates and/ or their breakdown products started to attract scientists' interest because of their potential antitumor effects (Gamet-Payrastre *et al.*, 2000; Hu *et al.*, 2003; Kuang *et al.*, 2004; Pappa *et al.*, 2007; Rose *et al.*, 2003; Satyan *et al.*, 2006; Singh *et al.*, 2004a; Singh *et al.*, 2004b; Tang *et al.*, 2004; Xiao *et al.*, 2003; Xiao *et al.*, 2004).

1.4 Bioconversion of glucosinolates into their related metabolites

Originally, glucosinolates are very stable and stored within subcellular compartments of cruciferous vegetables (Johnson, 2002; Mithen *et al.*, 2000). When plant tissue is physically damaged, glucosidic bonds of glucosinolates are cleaved by the action of endogenous enzyme myrosinase, producing various breakdown products, including thiocyanates, nitriles and isothiocyanates (ITCs). A generalized breakdown process of glucosinolates is shown in Figure 1.4 (Fenwick *et al.*, 1983). Upon human ingestion, intact glucosinolates remaining in the plant tissue may also be broken down by colonial bacterial myrosinase (Cheung *et al.*, 2004; Elfoul *et al.*, 2001; Krul *et al.*, 2002). Among these breakdown products, ITCs draw the most attention. They are commonly called 'mustard oils' in the food industry because of

their characteristic hot and bitter taste (Fenwick *et al.*, 1983). Examples of commonly found ITCs are shown in Figure 1.5. In recent years, scientists tried to understand the conversion and absorptive fate of glucosinolates and their metabolites through various methods. With the development of modern analytical technologies, the detection sensitive can be greatly increased. High-performance liquid chromatography-electrospray mass spectrometry (HPLC-MS) and gas chromatography-electrospray mass spectrometry (GC-MS) are commonly employed for the quantification of glucosinolates. While for the quantification of their related breakdown products, different pre-treatments are usually required. Pre-treated samples are further subjected to HPLC-MS and GC-MS analysis. Various studies suggested that ITCs are the major breakdown products of glucosinolates (Fenwick *et al.*, 1983; Getahun and Chung, 1999; Krul *et al.*, 2002). Therefore, majority of the analytical experiments are focus on the detection of glucosinolates and their respective ITCs.

1.5 Analysis of glucosinolates and their related metabolites

Back to 1880s, one of the major dietary glucosinolates, sinigrin, had already been isolated from black mustard (B. *nigra* Koch) and its' structural was formulated subsequently (Fenwick *et al.*, 1983). Now, about 120 different glucosinolates have been identified (Fahey *et al.*, 2001). Examples of identified glucosinolates in major cruciferous vegetables are listed Table 1.2. Furthermore, the contents of glucosinolates in major cruciferous vegetables are listed in Table 1.3. For the analysis of the major breakdown products of glucosinolates, different *in vitro* studies were employed. At first, the conversion abilities of the human gastrointestinal symbiotic *Lactobacillus* species were tested. After 17 h of incubation under anaerobic conditions, about 55% of sinigrin was found to be converted into its corresponding

ITC, allyl isothiocyanate (AITC). Eventually, the conversion activities were ceased after 20 h (Palop *et al.*, 1995). In another test employing a dynamic *in vitro* large-intestinal model, the conversion condition inside human colon was simulated. It was found that about 19% of sinigrin was converted into its corresponding ITC in a dynamic *in vitro* large-intestinal model (Krul *et al.*, 2002).

Beside *in vitro* experiments, various *in vivo* studies were further used to reveal the metabolic fates of glucosinolates. In a recent study, gnotobiotic rats were employed to study the ability of the inoculated human gastrointestinal bacteria to convert singirn into its metabolites. Instantaneous production of its respective ITC, AITC, was measured at different parts of the digestive tract. Peak production of AITC was found in the caecum and colon after 12 h of gavage (Elfoul *et al.*, 2001). After that, the conversion of glucosinolates was further verified in human. Volunteers were given 200 g of raw broccoli, and then blood was taken from the peripheral vein after 3 h of consumption. It was found that the total ITCs content was up to about 660 ηM (Song, 2005). The detailed contents of glucosinolates in fresh broccoli and concentrations of the respective ITCs detected in plasma after consumption are shown in Table 1.4 and 1.5, respectively. Similarly, peak concentrations of ITCs were detected in plasma, serum and erythrocytes in the blood samples of other human volunteers after consumption of broccoli sprout extracts (Ye *at al.*, 2002). Moreover, recent reports suggested that cooking time of cruciferous vegetables would alter the production of ITCs (Getahun and Chung, 1999; Rungapamestry *et al.*, 2007). It was estimated that the yield of ITC, sulforaphane, from lightly cooked broccoli was three times higher than fully cooked broccoli after human ingestions (Rungapamestry *et al.*, 2007). This difference might be due to severe loss of glucosinolates from the vegetables during cooking, and together with prolonged cooking time which had

denatured the endogenous plant myrosinase.

In additional to studies about the dynamic conversion of glucosinolates into their metabolites, the uptake actions of their major products, ITCs, by mammalian cells were also being investigated. Recent studies indicated that the ITCs could be rapidly accumulated in several tested cell types (Zhang, 2000; Zhang, 2001; Zhang and Callaway, 2002). It was suggested that such accumulation was resulted from the conjugations of ITCs with different intracellular compounds, especially glutathione. In another study using MCF-7 cells as model, it showed a nearly proportional increase of cellular ITCs uptake upon elevating level of cellular glutathione. At the same time, in a modified MCF-7 cells with an overexpression of glutathione transferases, the rate of ITCs uptake was linearly increased with the specific activities of these enzymes (Zhang, 2001). Further investigations are required to reveal the actual cellular uptake mechanisms of these compounds.

1.6 Anti-carcinogenic process by ITCs

In recent years, ITCs attract more and more scientists' attention because of their potent antitumor activities. Various reports showed that several ITCs, exerted significant growth inhibitory effects on different types of human cancer cells (Gamet-Payrastre *et al.*, 2000; Hu *et al.*, 2003; Kuang and Chen, 2004; Pappa *et al.*, 2007; Rose *et al.*, 2003; Satyan *et al.*, 2006; Singh *et al.*, 2004a; Singh *et al.*, 2004b; Tang *et al.*, 2004; Xiao *et al.*, 2003; Xiao *et al.*, 2004). In fact, ITCs caused regression of the development of cancer in different stages of the carcinogenic processes. The related mechanisms, including the carcinogens inactivation, modulation of xenobiotic metabolizing enzymes, antiproliferation and induction of apoptosis in cancer cells and preservation of intracellular matrices integrity.

1.6.1 Modulation on initiation phase

In the process of cancer prevention, blockage of genotoxic damage is the first line of defense. This can be achieved by the modulation on the activities of carcinogen-activating and carcinogen-detoxifying enzymes in the xenobiotic metabolisms. Phase I enzymes, such as cytochrome P450 oxidases, can perform the activation of carcinogens through chemical modifications. On the other hand, phase II enzymes, such as glutathione *S*-transferases, can detoxify these compounds and leads to protection (Johnson *et al.*, 1994). *In vivo* studies revealed that ITCs, including AITC, benzyl isothiocyanate (BITC), phenethyl isothiocyanate (PEITC) and sulforaphane (SFN) exerted their antitumor effects through inhibiting the activities phase I enzymes and enhancing the activities of phase II enzymes. In an *in vivo* experiment, a single dose of 1 mmol/kg BW PEITC could modify both xenobiotic enzymes in the F334 rats. Only after 2 h of PEITC treatment, there was about 30% decreased of liver microsomal total P450 content and 30% decreased of the activity of P450 reductase. Moreover, there was a maximal of 1.5-fold elevation of the glutathione *S*-tansferase activities in liver (Guo *et al.*, 1992). Similar results were observed in other animal experiments employing potent carcinogens. It was shown that treatments with ITCs could retard the process of carcinogenic activations and inhibit tumorigenesis in lung (Boysen *et al.*, 2003; Nishikawa *et al.*, 1996; Staretz *et al.*, 1997).

1.6.2 Modulation on promotion phase

In the second stage of cancer development, transformed cells will continue to grow into a clone and premalignant lesion may form. Interference on the growth of the transformed cells is an anticarcinogenic strategy at this stage. Recent *in vitro* studies showed that several ITCs possessed growth inhibitory effects on different

human cancer cell types at a relatively low dosage, ranged from 1 to 30 μM (Gamet-Payrastre *et al.*, 2000; Hu *et al.*, 2003; Kuang and Chen, 2004; Pappa *et al.*, 2007; Rose *et al.*, 2003; Satyan *et al.*, 2006; Singh *et al.*, 2004a; Singh *et al.*, 2004b; Tang and Zhang, 2004; Xiao *et al.*, 2003; Xiao *et al.*, 2004). Several methods are used to determine cell survival/ proliferation, such as trypan blue dye exclusion, sulforhodamin B staining, 3-(4,5-dimethylthiazol-2-yl)-2,5,dipheyl tetrazolum bromide (MTT) and 5-bromo-2-deoxyuridine (BrdU) assays.

It was suggested that the inhibitory effects of ITCs on different cancer cells were associated with the induction of apoptosis and induction of cell cycle arrest. Apoptosis is a form of programmed cell death. It involves a series of biochemical events, leading to a variety of morphological modifications and cellular biochemical changes. Several preliminary detection methods are commonly used, including the analysis of DNA content and examination on cellular histological appearance. The ITCs-induced cells death was demonstrated in different human cancer cells (Hu *et al.*, 2003; Kuang and Chen, 2004; Satyan *et al.*, 2006; Singh *et al.*, 2004a; Tang and Zhang, 2004; Wu *et al.*, 2005 Yeh and Yen, 2005). For instant, it was showed that PEITC inhibited the growth of human gynecological cancer cells in a dose-dependent manner. After treatment of 5-20 μM PEITC with OVCAR-3 cells for 48 h, signs of apoptosis were found as detected by the gel-electrophorisis or annexin V stating assays (Satyan *et al.*, 2006). In order to reveal the underling molecular mechanisms involved, the expression of important apoptotic marker proteins, including poly(ADP-Ribose) polymerase (PARP), caspase-cascades and Bcl-2 families were also studied. Western blot analysis clearly illustrated ITCs-induced caspase-mediated apoptosis in human cancer cells (Hu *et al.*, 2003; Satyan *et al.*, 2006; Singh *et al.*, 2004a; Tang and Zhang, 2004; Wu *et al.*, 2005). In order to further verify the

importance of caspases, different caspases inhibitors were included for test. In the addition of pan caspase inhibitor z-VADfmk, specific inhibitors of caspase 9 (z-LEHDfmk) and caspase 8 (z-IETDfmk) could effectively block the cleavage procaspae 3 or PARP. These blockages further confirmed the importance of caspase 8 and 9 in this pathway (Singh *et al.*, 2004a).

On the other hand, the growth inhibitory effects of ITCs were also governed by the impairment of cell cycle in human cancer cells. Whereas, the ITCs-mediated cell cycle arrest was predominantly at G_2/M phase (Gamet-Payrastre *et al.*, 2000; Pappa *et al.*, 2007; Singh *et al.*, 2004b; Tang and Zhang, 2004; Xiao *et al.*, 2003; Xiao *et al.*, 2004). Western blot analysis was employed to reveal the expression of key regulatory proteins in the G_2/M checkpoint, including Cyclin B1, Cdc2, Cdc25B and Cdc25C (Molinari, 2000; Shackelford *et al.*, 20002; Strausfeld *et al.*, 1991). After treatment with ITCs, the expressions of these regulatory proteins were significantly affected (Gamet-Payrastre *et al.*, 2000; Pappa *et al.*, 2007; Singh *et al.*, 2004b; Tang and Zhang, 2004; Xiao *et al.*, 2003; Xiao *et al.*, 2004). Besides *in vitro* studies, the ITCs were also found to be effectively retarding the growth of xenograft models *in vivo*. Treatment of AITC or SFN significantly inhibited the growth of PC-3 xenograft in mice (Singh *et al.*, 2004a; Srivastava *et al.*, 2003). Taken together, combination of different mode of actions was usually found in the anti-carcinogenic mechanisms of ITCs. Further investigations are required in order to reveal the actual cross-linkages involved.

1.6.3 Modulation on progression phase

In the final stage of cancer development, benign tumors will transform into life-threatening invasive malignant tumors. It is important to stop the invasion and

spreading process, otherwise it will be too late to be cured. Angiogenesis is a normal physiological process which involved the growth of new blood vessels from pre-existing ones. Since the development of tumor cells needs extra supply of nutrients, angiogenesis becomes the critical step for the transition of benign to malignant tumors (King, 2000d). In an *in vitro* rat aortic ring assay, both AITC and PEITC (1-5 μg/ml) treatments could inhibit the microvessel outgrowth (Thejass and Kuttan, 2007). Similar result was also observed in human umbilical vein endothelial cells model. Treatment of SFN decreased the proliferation of the endothelial cells and inhibited vessels tube formation (Asakage *et al.*, 2006). Besides *in vitro* studies, recent *in vivo* study also demonstrated that the ITCs could inhibit tumor-specific angiogenesis effectively. In this experiment, B16F-10 melanoma cells were intradermally injected into the C57BL/6 mice. Only five consecutive doses (25 μg/day) of AITC or PEITC could significantly inhibit the formation of tumor-directed capillaries in the C57BL/6 mice. At the same time, the levels of angiogenic factors, including serum nitric oxide (NO) and tumor necrosis factor-α (TNF-α) levels were also reduced after treatment. Despite all these findings, the sequences of molecular events leading to the antitumor effects of ITCs are not yet well defined. Further investigations are required to fully elucidate the cellular signaling pathways involved.

1.7 Project objectives and long-term significance

According to epidemiological and animal studies, it is suggested that high intake of cruciferous vegetables may reduce the risk of cancer (Steinmetz and Potter, 1996; Verhoeven *et al.*, 1996), in which glucosinolates and their digested products are believed to play an important role (Fowke *et al.*, 2003; Lin *et al.*, 1998). However, little is known about the actual antitumor mechanism, and further investigations are required to fully elucidate the cellular signaling pathways involved. Therefore, objectives of this proposed project are:

(1) To determine the antiproliferative activity of sinigrin, one of the major glucosinolates

(2) To evaluate the antiproliferative activity of allyl isothiocyanate (AITC), a digested product of sinigrin, and the possible mechanism involved in its action

(3) To investigate the *in vivo* antitumor effect of AITC

The importance of our research is the trial to reveal the antitumor mechanism on one of the major glucosinolates, sinigrin, and its main digested product, AITC. This study is warranted for the future development of cruciferous vegetables as a dietary chemotherapeutic agent.

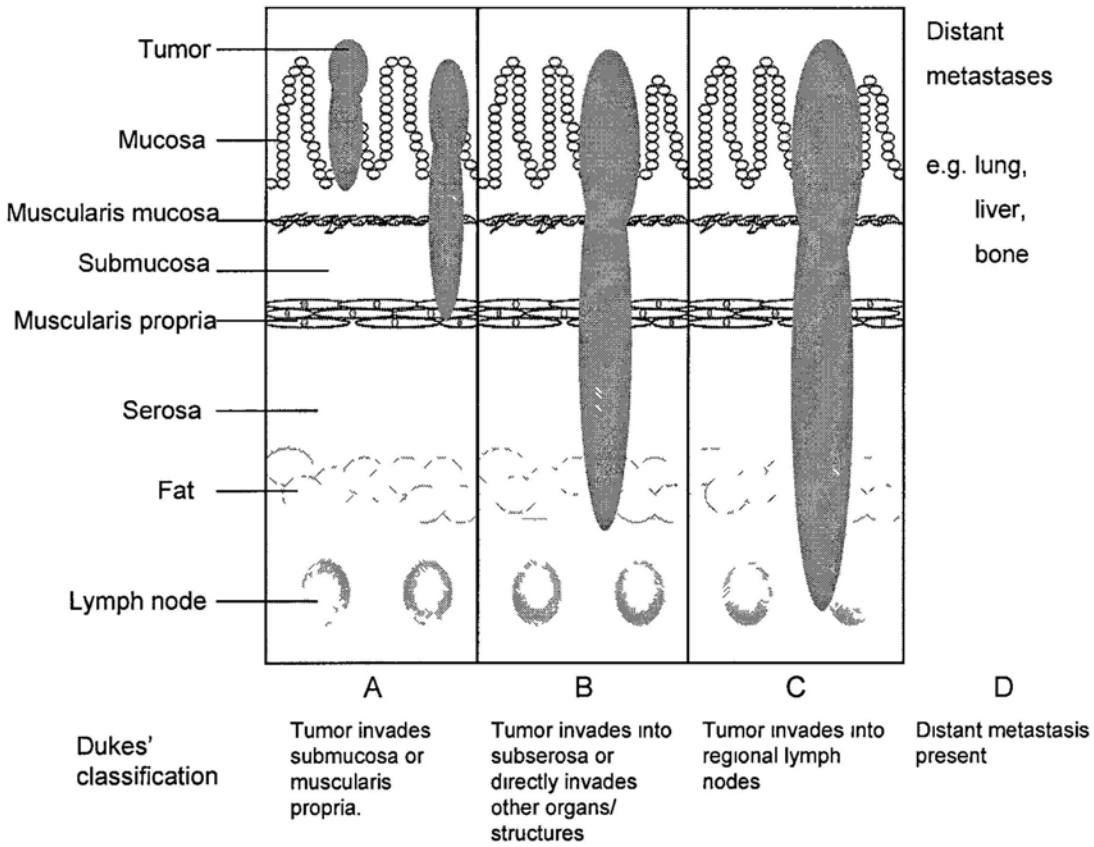

Figure 1.1 Development of CRC is divided into different stages under Dukes' classification (Adapted from: Berg, 2001c).

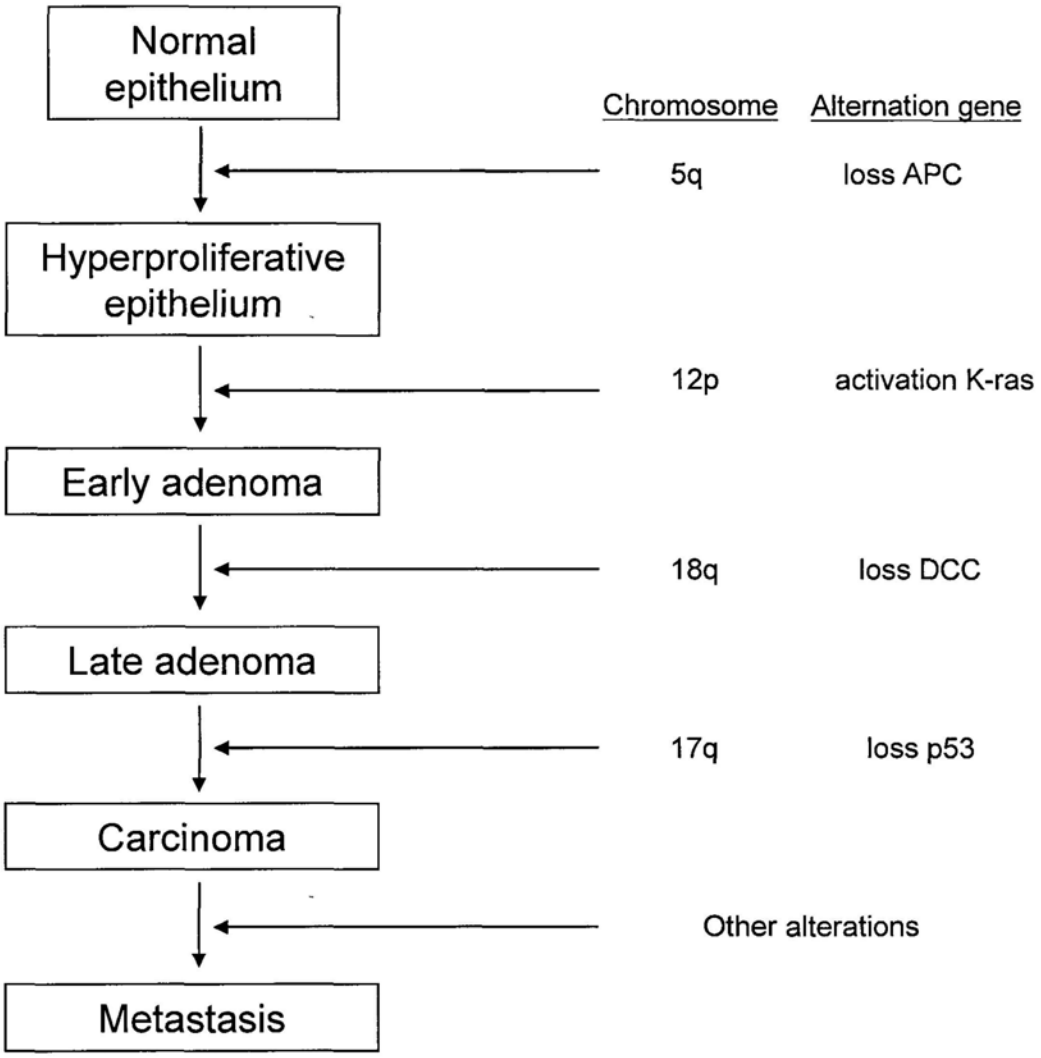

Figure 1.2 A conceptual genetic model for the development of CRC (Adapted from: Berg, 2001c).

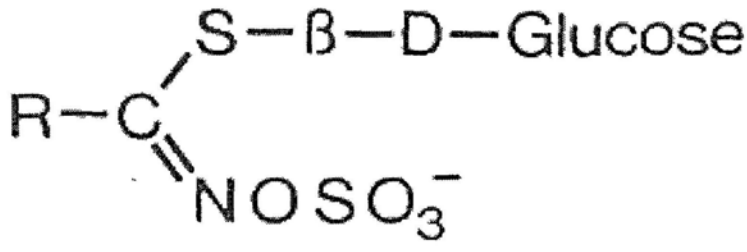

Figure 1.3 The basic structure of glucosinolates (Adapted from: Fenwick *et al.*, 1983).

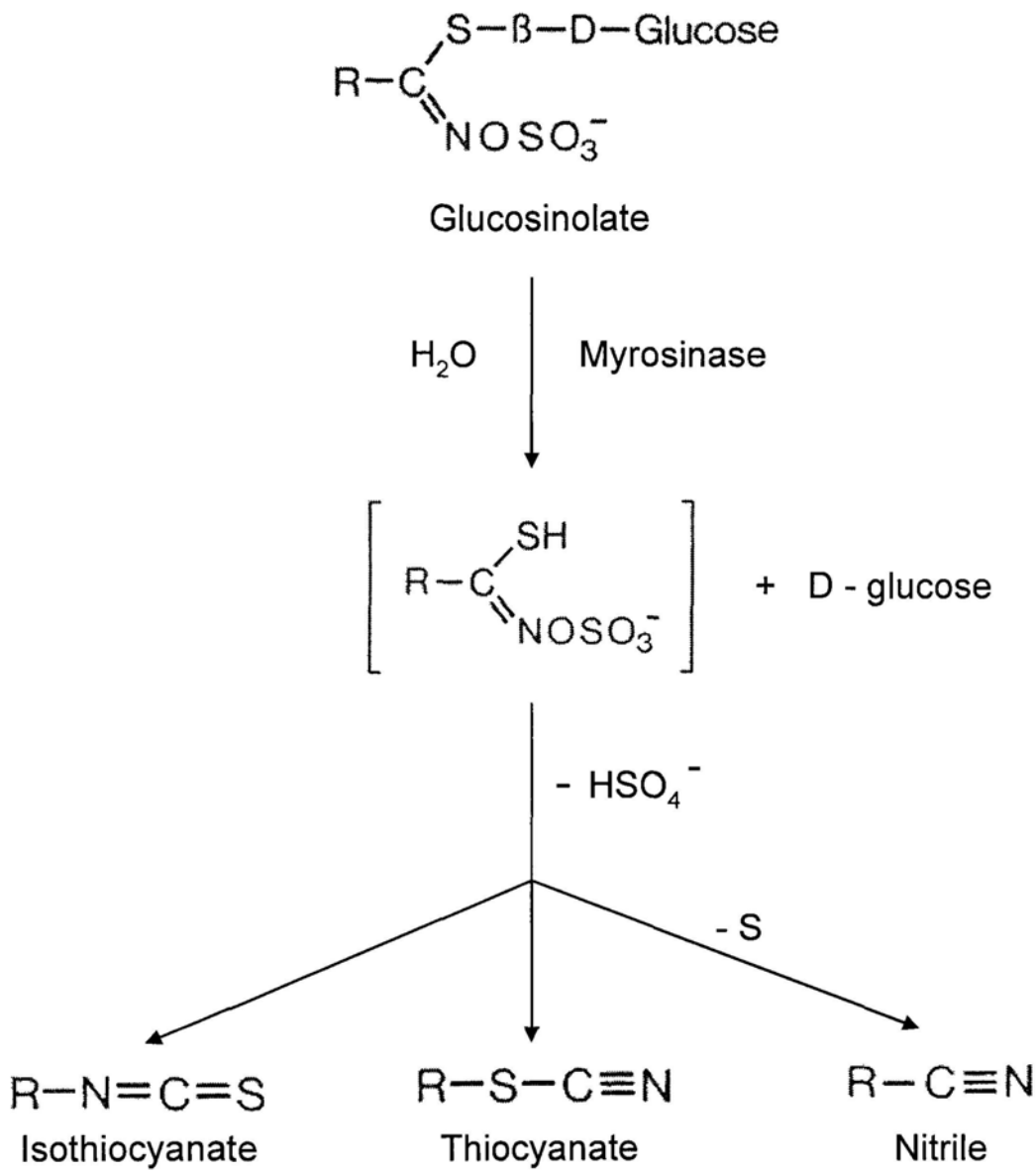

Figure 1.4 A generalized breakdown process of glucosinolates (Adapted from: Fenwick *et al.*, 1983)

Allyl isothiocyanate

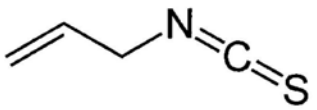

Benzyl isothiocyanate

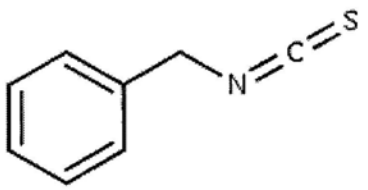

Phenylethyl isothiocyanate

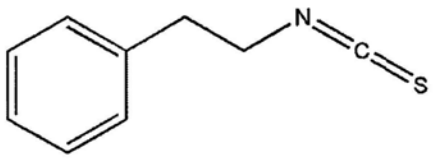

Sulforaphane

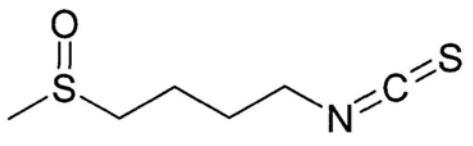

Figure 1.5 Examples of commonly found ITCs.

Table 1.1 Representative chemopreventive phytochemicals and their dietary sources (With source of data: Surh, 2003).

Dietary source	Chemopreventive phytochemicals
Tumeric	**Curcumin**
Chili peppers	**Capsaicin**
Ginger	**[6]-Gingerol**
Green tea	**Epigallocatechin-3-gallate**
Soybeans	**Genistein**
Tomatoes	**Lycopene**
Grapes	**Resveratrol**
Honey	**Caffeic acid phenethyl ester**
Garlic	**Diallyl sulphide**
Cabbage	**Indole-3-carbinol**
Broccoli	**Sulphoraphane**

Table 1.2 Trivial and chemical names of commonly found glucosinolates

Trivial names	Chemical names of R-groups 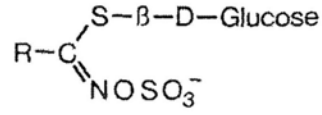
Aliphatic	
Sinigrin	2-Propenyl
Gluconapin	3-Butenyl
Glucobrassicanapin	4-Phentenyl
Progoitrin	2-(R)-2-Hydroxy-3-butenyl
Epiprogoitrin	2-(S)-2-Hydroxy-3-butenyl
Gluconapoleiferin	2-Hydroxy-4-pentenyl
Glucoubervirin	3-Methylthiopropyl
Glucoerucin	4-Methylthiobutyl
Dehydroerucin	4-Methylthio-3-butenyl
Glucoiberin	3-Methylsulphinylpropyl
Glucoraphanin	4-Methylsulphinylbutyl
Glucoraphenin	4-Methylsulphinyl-3-butenyl
Glucoalyssin	5-Methylsulphinylpentenyl
Indole	
Glucobrassicin	3-Indolylmethyl
Neoglucobrasscin	1-Methoxy-3-indolylmethyl
Aromatic	
Glucotropaeolin	Benzyl
Gluconasturtiin	2-Phenylethyl

(With source of data: Verkerk *et al.*, 2009)

Table 1.3 Contents of glucosinolates in major cruciferous vegetables

	Broccoli sprouts (μmol/ g FW)		Broccoli (μmol/ g FW)		Brussels sprouts (μmol/ g FW)		Cauliflower (μmol/ g FW)	
	Mean ± SD		Mean ± SD		Mean ± SD		Mean ± SD	
Glucoiberin	5.99E-01	1.06E-01	1.29E-01	8E-03	5.87E-01	8.9E-02	4.16E-01	6.3E-02
Glucoraphanin	1.33	2.8E-01	1.05	1.0E-01	1.51E-01	3.7E-02	4.54E-02	1.36E-02
Progoitrin	1.06E-01	4E-03	8.75E-04	8.8E-05	1.33	7E-02	8.57E-02	1.10E-02
Gluconapin	2.44E-02	2.5E-03	6.60E-04	3.34E-04	1.08	3.4E-01	1.34E-02	1.1E-03
Sinigrin	3.74E-02	1.7E-03	1.51E-03	1.6E-04	1.55	8E-02	4.20E-01	7.5E-02
Glucoalysin	1.12E-03	2.1E-04	1.05E-02	9E-04	1.10E-01	1.9E-02	4.67E-02	5.3E-03
Glucoerucin	1.02	1.3E-01	1.01E-02	1.8E-03	0.00	0.00	2.59E-02	7.2E-03
Glucobrassicin	3.96E-02	7.4E-03	3.77E-01	4.7E-02	3.74	5.55E-01	1.53	1.8E-01
Neoglucobrassicin	3.12E-01	3.9E-02	1.14E-01	1.1E-02	0.00	0.00	2.34E-01	3.3E-02
4-Methoxyglucobrassicin	5.54E-01	8.7E-02	3.85E-01	4.8E-02	8.44E-01	4.4E-02	4.04E-01	7.0E-02
Total	4.02	6.6E-01	2.08	2.2E-01	9.40	1.2	3.22	4.6E-01

Data were means ± SDs (n=3)

(With source of data: Tian, 2005)

Table 1.4 Contents of glucosinolates in fresh broccoli

	Glucosinolate content (μmol/ 100 g fresh weight)
Sinigrin	1.7 ± 1.1
Gluconapin	3.4 ± 1.0
Progoitrin	3.9 ± 1.3
Glucoiberin	19.7 ± 2.7
Glucoraphanin	29.8 ± 2.8
Glucoalyssin	3.9 ± 1.1
Gluconasturiin	4.4 ± 1.0
Total glucosinolates	66.8

Data were means ± SDs (n=3)

(With source of data: Song, 2005)

Table 1.5 Concentrations of ITCs in plasma 3 h after consumption of 200g of raw broccoli (ηM)

	Grouped plasma sample (ηM)
Allyl isothiocyanate	136 ± 16
3-Butenyl isothiocyanate	173 ± 56
3-Methylsulfinylpropyl isothiocyanate	87 ± 42
4-Methylsulfinylbutyl isothiocyanate	114 ± 48
5-Methylsulfinylpentyl isothiocyanate	43 ± 15
Phenethyl isothiocyanate	19#
Total isothiocyanates	549 ± 115

Group data were estimated for all human volunteers (Means ± SDs, n = 5).

Only one plasma sample has detectable level of phenethyl isothiocyanate, SD could not be obtained.

(With source of data: Song, 2005)

Chapter Two

Materials and methods

2.1 Materials

AITC (> 95% purity) was purchased from International Laboratory Limited (San Bruno, CA, USA). Cell proliferation ELISA 5-bromo-2'-deoxyuridine (BrdU) colorimetric assay kit was purchased from Roche Diagnostics GmbH (Mannheim, Germany). Antibodies against β-actin, Cdc2, p-Cdc2(Thr14), p-Cdc2(Tyr15), p-Cdc25C(Ser216), Cdc25C, caspase-3, -6, -7, -8, -9, poly(ADP-ribose) polymerase (PARP), and secondary antibodies horseradish peroxidase-conjugated goat anti-rabbit IgG and horse anti-mouse IgG were purchased from Cell Signaling Technology (Danvers, MA, USA). Antibodies against Cdc25B, CyclinB1, and secondary antibody horseradish peroxidase-conjugated goat anti-chicken IgY were purchased from Abcam (Cambridge, MA, USA). Fetal bovine serum (FBS) was purchased from HyClone (Logan, UT, USA). Phosphate buffered saline (PBS), penicillin-streptomycin, Leibovitz's -15 (L-15) and Dulbecco's modified Eagle's medium (DMEM) were purchased from Gibco (Rockville, MD, USA). Bicinchoninic acid protein assay kit, PEITC (> 95% purity), sinigrin, bovine serum albumin (BSA), propidium iodide (PI), protease inhibitor cocktail, myrosinase, ribonulease A (RNase A), RPMI-1640 medium, 3-(4,5-dimethylthiazol-2-yl) -2,5-diphenyltetrazolium bromide (MTT), propylene glycol and dimethyl sulfoxide (DMSO) were purchased from Sigma Chemical (St. Louis, MO, USA). Trifluoroacetic acid was purchased from J. T. Baker (Phillipsburg, NJ, USA). Methanol was purchased from Merck (Darmstadt, Germany).

2.2 Samples preparation

Sinigrin was prepared by diluting in PBS with a final concentration of PBS employed in all assays was 1%. An equivalent amount of PBS was used as control. On the other hand, AITC and PEITC solutions were prepared by diluting in DMSO with the final concentration of DMSO employed in all assays were 0.5%. An equivalent amount of DMSO was used as control.

2.3 Cell lines and cell cultures

Human skin fibroblast Hs68, human colorectal adenocarcinoma Caco-2, COLO 201 and SW620 cells were obtained from American Type Culture Collection (ATCC) (Manassas, VA, USA). Caco-2 and Hs68 cells were cultured in DMEM, whereas COLO 201 and SW620 cells were cultured in RPMI-1640 and L-15 medium, respectively. All cells were supplemented with 10% FBS and 1% penicillin (10,000 unit/ml)-streptomycin (10,000 μg/ml). Monolayer cultures of Caco-2 and COLO cells were regularly maintained at 37°C in a humidified atmosphere of 95% air and 5% CO_2, whereas SW620 cells were cultured without CO_2.

2.4 Cell viability/ proliferation and quantification assays

The effects of different samples on the survival and proliferation on various cell lines were determined by cell viability MTT and cell proliferation BrdU colorimetric assays. Moreover, a high-performance liquid chromatography (HPLC) determination was employed for the quantification of sinigrin content after *in vitro* enzyme digestion assay.

2.4.1 MTT assay of sinigrin on colorectal adenocarcinoma cells

The effect of sinigrin, one of the major glucosinolates (Fahey *et al.*, 2001; Fenwick *et al.*, 1983; Moreno *et al.*, 2006; Song *et al.*, 2005; Verkerk *et al.*, 2009), on the survival of two human colorectal adenocarcinoma cells (SW620 and Caco-2) were determined by MTT assay. MTT assay is a quick quantitative colorimetric method for the determination of mitochondrial impairment. It is based on the ability of mitochondrial dehydrogenases in viable cells to convert soluble pale yellow tetrazolium salt (MTT) into dark blue formazan product. Since mitochondrial activities of viable cells are proportional to the amount of formazan produced, cell growth and survival can be reflected by the color intensity of formazan product. In brief, Caco-2 and SW620 cells at concentrations of 2.5×10^3 and 1×10^4 cells/well, respectively, were pre-seeded into 96-well tissue culture plates for 24 h. Cells were then exposed to a range of sinigrin (0 - 500 μM) for different incubation periods. After incubation, 20 μl freshly prepared MTT solution (5 mg/ml in PBS) was added into each well and re-incubated for 5 h. Culture medium was removed afterwards, and 150 μl acid-isopropanol (0.04 N HCl in isopropanol) was added to dissolve the formazan products. Absorbance was determined by microplate reader SpectraMax250 (Molecular Devices, CA, USA.) at 570 ηm (Mosmann, 1983).

2.4.2 MTT assay of the co-incubation of sinigrin and myrosinase on colorectal adenocarcinoma cells

Besides investigating the effect of sinigrin, a co-incubation assay of sinigrin and myrosinase was performed. Before starting the experiment, no alerting effect of myrosinase on SW620 and Caco-2 cells was counter proved. By using the MTT assay with detailed procedures as described in chapter 2.4.1, both Caco-2 and SW620 cells were challenged with 0 - 0.025 unit/ml myrosinase for 72 h. Subsequently,

different concentrations of sinigrin (0 - 500 μM) were co-treated with a constant dose of 0.025 unit/mL myrosinase. Simultaneous production of digested products was carried out in contact with colorectal adenocarcinomas cells in the culture medium directly (Fimognari *et al.*, 2002; Leoni *et al.*, 1997; Pappa *et al.*, 2006). Incubation periods of 24, 48 and 72-h were employed in order to reveal the time-dependent effect of these *in situ* mixtures. The effects of co-treatments on the survival of SW620 and Caco-2 cells were determined by MTT assay with detailed procedures as described in chapter 2.4.1.

2.4.3 High-performance liquid chromatography (HPLC) determination of sinigrin after *in vitro* enzyme digestion

In order to elucidate the digestion profile of sinigrin, an *in vitro* digestion of sinigrin by myrosinase was simulated. Different concentrations of sinigrin (0 - 500 μM) were co-incubated with 0.025 unit/mL myrosinase in PBS at 37°C for 24, 48 and 72 h. After incubation, the presence of sinigrin was detected by HPLC analysis according to Song *et al.*, 2005 with some modifications. HPLC analysis was performed using a Waters 2690 separation module system, with the chromatographic separation was carried out using a 150 x 2.1 mm i.d., 5 μm SymmetryShield C_{18} steel column with a 10 x 2.1 mm i.d. 3.5 μm Symmetry C_{18} guard column (Waters Associates, Milford, MA). The operation temperature was at 25°C. Mobile phase of the HPLC system was consisted of 0.1% trifluoroacetic acid in water with gradient of 0 - 10% methanol over 0 - 30 min, and the flow rate was 0.2 ml/min. All samples were filtered through 0.2 μm pore size syringe filter (Millipore Corp., Bedford, MA) prior to analysis. The injection volume of all samples was 10 μl. The UV-vis absorption spectra of column eluant were recorded from 200 to 400 ηm and the response at 227 ηm was plotted.

2.4.4 MTT assay of ITCs on colorectal adenocarcinoma cells

Besides studying the effects of sinigirn and the co-treatment of sinigrin with myrosinase, activity of the corresponding ITC of sinigrin, AITC, on different colorectal adenocarcinoma cells was also determined. In additional to AITC, another commonly founded ITC, PEITC, was employed as a reference sample. In brief, Caco-2, COLO 201 and SW620 cells at concentrations of 2.5×10^3, 2.5×10^3 and 1×10^4 cells/well, respectively, were pre-seeded into 96-well tissue culture plates for 24 h. Cells were then exposed to various ranges of AITC and PEITC (0 - 150 μM). Incubation periods of 24, 48 and 72-h were employed to reveal the time-dependent effects of the samples. The effects of these treatments on the survival of Caco-2, COLO 201 and SW620 cells were determined by MTT assay with detailed procedures as described in chapter 2.4.1.

2.4.5 BrdU colorimetric assay of ITCs on colorectal adenocarcinoma cells

In additional to MTT assay, the growth inhibitory effects of AITC and PEITC were further confirmed by BrdU assay. It is a colorimetric immunoassay based on the measurement of BrdU incorporation during DNA synthesis. As cellular proliferation requires the replication of cellular DNA, monitoring DNA synthesis is an indirect parameter for the quantification of cell proliferation. In fact, BrdU is a pyrimidine analogue, it will incorporate into cellular DNA during S phase in the same way as thymidine (Huong *et al.*, 1991; Porstmann *et al.*, 1985). In brief, SW620 cells at concentration of 1×10^4 cells/well were pre-seeded into 96-well tissue culture plates for 24 h. Cells were then exposed to various ranges of AITC and PEITC (0 - 150 μM) for 24 h and/ or 48 h. After incubation, BrdU assay was performed according to manufacturer's protocol (Roche; Mannheim, Germany). Ten microliter BrdU labeling solution was added into each well and re-incubated for 4 h. Culture medium

was removed and the micoplate was dried at 60°C for 1 h. Then, two hundred microliter Fix- Denat solution was added, and allowed to stand for 30 min at room temperature (RT). After removing Fix-Denant solution, the plate was allowed to stand in RT for 30 min again. One hundred microliter freshly prepared anti-BrdU-POD working solution was added to each well and further incubated for 90 min. Afterwards, the plate was rinsed with 200 µl washing solutions for 3 times. Lastly, one hundred microliter freshly prepared substrate solution was added and allowed to react for 30 min at RT. Absorbance was determined by microplate reader SpectraMax250 (Molecular Devices, CA, USA.) at 370 ηm.

2.4.6 Determination of half maximal inhibitory concentration (IC_{50})

Half maximal inhibitory concentration (IC_{50}) value was determined in the BrdU assay. It was determined graphically from the plot of percentage cell proliferation against ITCs concentrations.

2.4.7 MTT assay of ITCs on normal skin fibroblast

Besides investigating the growth inhibitory effects of ITCs on different colorectal adenocarcinoma cells, their effects on normal cells were also worth to be studied. The effects of AITC and PEITC on the survival of human skin fibroblast Hs68 were determined by MTT assay. In brief, Hs68 cells at concentration of 4×10^3 cells/well were pre-seeded into 96-well tissue culture plates for 24 h. Cells were then exposed to various range of AITC or PEITC (0 - 150 µM) for two different incubation periods (24 and 72-h). After incubation, the effects of these treatments on the survival of Hs68 cells were determined by MTT assay with detailed procedures as described in chapter 2.4.1.

2.5 Determination of cell cycle distribution by flow cytometry assay

After assessing the growth inhibitory effects of ITCs on different colorectal adenocarcinoma cells, their effects on cell cycle distribution were elevated by flow cytometry analysis. With the use of DNA specific fluorescence dye (PI) which binds to cellular double stranded DNA, DNA content can be measured at single cell level. Cells at different phases of cell cycle (G_0/G_1, S, G_2/M) containing different DNA content are displayed in a flow cytometric diagram (Pucillo *et al.*, 1990). This pattern gives us information on the cell cycle distribution in a cell population.

Firstly, SW620 cells (1×10^6) were pre-seeded in T75 tissue culture flasks for 24 h. After 24 h, cells were subjected to designated ITCs treatments. In order to study the dose-dependent effect, different dosages of AITC (10, 20 and 40 μM) or PEITC (2.5, 5 and 10 μM) were tested. At same time, different incubation periods (0, 4, 16, 24 and 48-h) were chosen to study the time-dependent effect of AITC (20 μM). Subsequently, designated ITCs treated cells were harvested by trypsination. Harvested cells were washed with PBS and fixed with ice-cold 70% ethanol at -20°C overnight. Fixed cells were washed twice with PBS, once with 1% BSA in PBS, and then re-suspended in DNA-binding PI solution (700 U/ml RNase A, 50.1 μg/ml PI, pH 8.0) in darkness at 4°C overnight. After labeling with PI, cells were analyzed with a Beckman Coulter Epics XL•MCL flow cytometer (Miami, FL, USA). Cell cycle distribution was analyzed by the MuliCycle software (Phoenix Flow Systems, San Diego, CA, USA). For all the assays, 10 000 events per samples were recorded.

2.6 Western blot analysis on checkpoint regulatory proteins

In order to gain insights into the underlying mechanisms, the expression profile of checkpoint regulatory proteins in SW620 cells after different AITC treatments were revealed by western blot analysis. Firstly, SW620 cells (1×10^6) were pre-seeded in T75 tissue culture flasks for 24 h. After 24 h, cells were subjected to designated AITC treatments. In order to study the dose-dependent effect, different dosages of AITC (10, 20 and 40 μM) with an incubation period of 24-h were tested. At the same time, different incubation periods (0, 1, 2, 4, 8, 12 and 24-h) were chosen for the study of time-dependent effect of AITC (20 μM).

2.6.1 Preparation of protein lysate

Designated AITC-treated cells were harvested by trypsination and washed with PBS. Proteins were extracted by incubating the collected cells with lysis buffer (Cell Signaling Technology, Danvers, MA, USA), containing protease inhibitor cocktail. After incubation on ice for 50 min, samples were centrifuged at 14000 rpm for 15 min at 4°C. Clear supernatants were collected after centrifugation.

2.6.2 Determination of protein content

Protein content of each cell lysate samples were determined by bicinchoninic acid protein assay kit according to manufacture's protocol (Sigma Chemical, St. Louis, MO, USA). A protein standard curve was prepared by using different concentrations of BSA (0, 200, 400, 600, 800 and 1000 μg/ml), whereas the cell lysate samples were diluted with PBS (1: 24; Sample: PBS). After transferring 25 μl of each samples into 1.5 ml microcentrifuge tubes, 200 μl freshly prepared reagent (Bicinichoninic acid solution: Copper (II) sulfate solution; 50: 1) was added. Gently mixed samples were incubated at 37°C for 30 min, and the absorbance was

determined by microplate reader SpectraMax250 (Molecular Devices, CA, USA.) at 562 ηm. Afterwards, equal volume of cell lysate samples were mixed with 2X Laemmli sample buffer (Sigma Chemical, St. Louis, MO, USA) and stored at -80°C until use.

2.6.3 SDS-polyacrylamide gel electrophoresis

Samples containing 10 - 60 μg protein were resolved by SDS-polyacrylamide gel electrophoresis (4% stacking; 10% resolving) and then transferred onto nitrocellulose membrane (Amersham Life Science, Buckinghamshire, UK) (Towbin *et al.*, 1979). Membrane was raised gently with 1 X Tris-buffered saline.

2.6.4 Immunoblotting and detection

Membrane was firstly blocked with blocking buffer (1 X Tris-buffered saline, 0.1% Tween-20, 5% (w/v) non-fat dry milk) for 1 h at RT. It was then incubated with desired primary antibody at 4°C overnight. Primary antibodies p-Cdc2(Thr14), p-Cdc2(Tyr15), p-Cdc25C(Ser216), Cdc25B and Cdc25C, were diluted with blocking buffer at 1:1000. Primary antibodies against β-actin, Cdc2 and CyclinB1, were diluted with blocking buffer at 1:2000. After washing with TBST (1 X Tris-buffered saline with 0.1% Tween-20), membrane was incubated with corresponding secondary antibodies. Secondary antibodies horseradish peroxidase-conjugated goat anti-rabbit IgG, horse anti-mouse IgG and goat anti-chicken IgY were diluted with blocking buffer at dilution of 1:2000. Immune detection was achieved by using LumiGLO reagent® (Cell Signaling Technology, Danvers, MA, USA) with the emitted light captured on X-ray film. Each membrane was stripped and re-probed with β-actin for checking the uniformity of protein loading.

2.7 Analysis of gene expression level on checkpoint proteins

The effect of AITC on SW620 cells towards transcriptional regulation of representative genes in G_2 checkpoint were further investigated by quantitative real-time PCR analysis.

2.7.1 Extraction of total RNA

Firstly, SW620 cells (1×10^6) were pre-seeded in T75 tissue culture flasks for 24 h. Cells were then exposed to 20 μM AITC for different incubation periods (0, 2, 4, 8, 12 and 24-h). Total RNA was extracted from AITC-treated cells using TRI-Reagent (Molecular Research Center, Cincinnati, OH, USA) according to manufacturer's instruction. Treated cells were collected and transferred into 1.5ml microcentrifuge tube and 1 ml TRI-Reagent was added. The mixture was incubated at RT for 5min. Afterwards, 0.2 ml chloroform was added, shook vigorously for 15s and then re-incubated at RT for 2-3 min. The mixture was centrifuged at 4°C for 15 min at 12000 g. Upper aqueous phase was transferred to new tube after centrifugation. In order to precipitate the RNA, 0.5 ml of isopropanol was added and re-incubated in RT for about 30 min. Supernatant was removed after centrifuged at 7500 g for 10 min at 4°C. Pellet was washed by 1 ml 75 % ethanol and centrifuged again at 7500 g for 5 min at 4°C. Lastly, pellet was allowed to dry up at RT and stored in -80°C until use. Furthermore, RNA concentration was determined by spectrophotometric measurement and the quality of RNA samples was further checked by formaldehyde agarose gel electrophoresis.

2.7.2 Preparation of cDNA from total RNA sample

The cDNA sample was prepared by reverse transcription of DNase I-treated RNA using Superscript™ III reverse transcriptase according to manufacturer's

instruction (Invitrogen Corp., CA, USA). In brief, Oligo dT (200 μM) and dNTPs (10 mM) were added to the treated sample and incubated at 65°C for 5 min. Afterwards, it was allowed to cool on ice. Reaction mixture (5X first strand buffer, 0.1 M DTT and RNase OUT) was added and incubated at 50°C for 2 min. Superscript™ III RNaseH was then added to the mixture and incubated at 50°C for 2 h, followed by 70°C for 15 min. Final cDNA samples were stored in -20°C until use.

2.7.3 Primer design for quantitative real-time PCR assay

Primers of selected genes for quantitative real-time quantitative PCR assay were designed according to Ismail *et al.*, 2007 and Primer3 software (http://frodo.wi.mit.edu/cgi-bin/primer3/ primer3_www.cgi) based on the sequence data obtained from NCBI database (http://www.ncbi.nlm.nih.gov/). Designed primers are shown in Table 2.1.

2.7.4 Quantitative real-time PCR assay

Real-time PCR amplification of cDNA was carried out using BioRad iQ™5 real-time PCR detection system (BioRad Laboratories, Hercules, CA, USA) in 96-well PCR plate with a dome cap at the cycling conditions: 3 min at 95°C, and 40 cycles at 95°C for 10 s followed by 30 s at 55°C. Reaction mixture was comprised of 10 μl of iQ™ SYBR Green Supermix (BioRad Laboratories, Hercules, CA, USA), 0.4 μM each of the forward and reverse primers in a total reaction volume of 20 μl. Expression level of each gene was normalized by glyceraldehyde 3-phosphate dehydrogenase (GAPDH) as a house keeping gene. Relative gene expression was calculated using the $2^{-\Delta\Delta CT}$ method (Livak and Schmittgen, 2001). At the same time, a single sharp peak was noted in the dissociation curve for the confirmation of accuracy.

2.8 Detection of apoptosis by flow cytometry assay

Besides studying the effect of ITCs on cell cycle distribution, the presence of apoptosis was also detected by flow cytometry assay. Flow cytometric pattern of the ITCs-treated cells obtained in chapter 2.5 could also give information on the sign of apoptosis. Cells with hypodiploid DNA content were quantified as apoptotic cells population.

2.9 Western blot analysis on apoptotic proteins

In order to gain insights into the mechanisms, the expressions of important apoptotic proteins in SW620 cells after AITC treatments were revealed by western blot analysis. Different incubation periods (0, 4, 16, 24 and 48-h) were chosen to study the time-dependent effect of AITC (20 μM). Treated cells were harvested and then subjected to western blot analysis with detailed procedures as described in chapter 2.6. Primary antibodies against caspase-3, -6, -7, -8, -9 and PARP were diluted with blocking buffer at 1:2000.

2.10 Nude mice xenograft assay

Besides performing various *in vitro* experiments, a nude mice xenograft assay was also employed to determine the *in vivo* antitumor effect of AITC. The experimental design was based on Srivastava *et al.*, 2003 with some modifications. This experiment was carried out following the approval and guidelines from the Animal Experimental Ethical Committee, The Chinese University of Hong Kong.

2.10.1 Animals

Male BALB/c nude mice (nu/nu) at 6-7 weeks were obtained from the Laboratory Animal Services Centre, The Chinese University of Hong Kong. All mice

were housed in filtered cages and maintained in a controlled environment (22-25°C) with 12 hour of light and dark cycle. They were freely accessible to sterile rodent chow and water. An acclimation period was 4 days prior to the experiment.

2.10.2 Preparation of sample

Sample was prepared freshly by diluting AITC in 8% propylene glycol in PBS (v/v). An equivalent amount of propylene glycol in PBS was employed as control.

2.10.3 Experimental design

At the beginning of experiment, SW620 cells (2 x 10^6 cells) were injected subcutaneously onto the back of twenty-four mice. They were randomly divided into three groups. Staring from the day of cells inoculation, two treatment groups received intraperitoneal injection (i.p.) three times per week (Monday, Wednesday and Friday), comprised of 5 and 10 μmol AITC, respectively. At the same time, control group received an equal volume of vehicle. Tumor size of each mouse was measured periodically using a caliper when palpable tumor appeared, whereas tumor volume was calculated by using the equation: tumor volume (mm^3) = (length x $width^2$)/2 (Singh *et al.*, 1996). In order to assess the health condition, all mice were monitored and their body weight was measured periodically.

2.10.4 Post-experimental assays

At the end of the experiment, mice were scarified using CO_2 asphyxiation. Wet tumor weights were obtained. All tumor tissues were raised with ice-cold PBS and divided into two parts. One part was subjected to western blot analysis and the second part was used for histological analysis.

2.10.4.1 Western blot analysis

Before performing western blot analysis, tumor tissues were minced and homogenized using a polytron. Proteins extracted from tumor tissues were used for western blot analysis with detailed procedures as described in chapter 2.6.

2.10.4.2 Histological analysis

Tumor tissues collected for histological analysis were fixed in 10% neutral-buffered formalin for 3 - 4 days. Fixed tissues were dehydrated and embedded in paraffin wax with detailed procedures were listed in Table 2.2. Afterwards, tumor specimens were sectioned into 4 μm thick. Hematoxylin and eosin were used for the staining process with detailed procedures were listed in Table 2.3. The stained slides were mounted on cover slides coated with Canada Balsam and stored in RT until use. Morphology of the tumor tissues was observed under Nikon upright microscope 80i (Nikon USA, Melville, NY).

2.11 Statistical analysis

Experimental results are expressed as mean $\pm$ S.D. of at least three independently performed experiments, unless indicated otherwise. Statistical differences between control and treatment groups were determined using two-tailed Student's t-test. The P-value of <0.05(*) or <0.01(**) was considered statistically significant.

Gene	Forward primer (5' - 3')	Reverse primer (5' - 3')
GAPDH	AGATCATCAGCAATGCCTCCTG	ATGGCATGGACTGTGGTCATG
Cdc25B	ACGATGGTGGCCCTATTGAC	GCAAGTTCACCGCAGTCTTG
Cdc25C	TTTTTCCAAGGTATGTGCGCTG	TGGAACTTCCCCGACAGTAAGG
Cdc2	GCATCCCATGTCAAAAACTTGG	GGATGATTCAGTGCCATTTTGC
CyclinB1	TCGAGCAACATACTTTGGCCA	GCAAAAAGCTCCTGCTGCAA

Table 2.1 Primers used for real-time quantitative PCR

Table 2.2 Dehydrating and embedding procedures for the histological analysis of mice tumor tissue

Procedure	Reagent	Time
Rinsing	50 % Ethanol	5 min x 3
Dehydration	50 % Ethanol	1.5 h
	70 % Ethanol	1.5 h
	85 % Ethanol	1.5 h
	95 % Ethanol	2 h
	100 % Ethanol	30 min x 3
Clearing	Xylene : Ethanol (1:1)	30 min
	Xylene	30 min x 2
Infiltration	Paraffin wax	45 min x 2
Embedding	Paraffin wax	Cool rapidly

Table 2.3 Staining procedures for the histological analysis of mice tumor tissue

Procedure	Reagent	Time
De-wax	Xylene	5 min x 2
Hydration	100 % Ethanol	1 min
	95 % Ethanol	1 min
	70 % Ethanol	1 min
	50 % Ethanol	1 min
	30 % Ethanol	1 min
	Running tap water	1 min
Staining	Mayer's hematoxylin	~ 15 min
	Running tap water	1 min
	Acid ethanol	~ 1-5 s
	Running tap water	1 min
	Scott's tap water	~2 min
	Running tap water	1 min
	0.5 % aqueous eosin	~ 1 min
	Running tap water	~1 min
Dehydration	70 % Ethanol	as short as possible
	95 % Ethanol	as short as possible
	100 % Ethanol	2 min x 2
	Xylene: Ethanol (1:1)	2 min
	Xylene	2 min x 2

Chapter Three

Results

3.1 Cytotoxic effect of sinigrin products on colorectal adenocarcinoma cells

As shown in MTT assay, there was no significant effect of sinigrin on the survival of both colorectal adenocarcinoma cells, Caco-2 and SW620. The treatment concentration was up to 500 μM for a 72-h period of incubation (Figures 3.1 and 3.2).

3.2 Cytotoxic effect of the co-incubation of sinigrin and myrosinase on colorectal adenocarcinoma cells

Since treatment of sinigrin did not affect the survival of both colorectal adenocarcinoma cells (SW620 and Caco-2), a co-incubation assay of sinigrin and myrosinase was further performed. Before starting the experiment, no alerting effect of myrosinase on the cells was counter proved by MTT assay. The treatment concentration of myrosinase was up to 0.025 unit/ml for a 72-h period of incubation (Figures 3.3 and 3.4). Interestingly, the co-incubation of different concentrations of sinigirn with a constant dose of myrosinase (0.025 unit/ml) could exert significant cytotoxic effect on different colorectal adenocarcinoma cells as determined by MTT assay (Figures 3.5 -3.8). As shown in Figures 3.5 - 3.6, there was a clear dose- and time-dependent cytotoxic effect of the co-treatments on Caco-2 cells. The percentages of survival Caco-2 cells in the co-treatment of 50 μM sinigrin and myrosinase after 24, 48 and 72 h were 72.0, 57.4 and 48.1%, respectively. Similarly, a clear dose- and time-dependent cytotoxic effect of the co-treatment was also found in SW620 cells (Figures 3.7 and 3.8). The percentages of survival SW620 cells in the

co-treatment of 50 μM sinigrin and myrosinase after the 24, 48 and 72 h were 70.4, 59.3 and 43.2 %, respectively.

3.3 HPLC determination of sinigrin after *in vitro* enzyme digestion

In order to elucidate the digestion profile of sinigrin, an *in vitro* digestion of sinigrin by myrosinase was simulated. Firstly, a standard curve of sinigrin was prepared. As shown in the HPLC-vis chromatograms, sinigrin standard ranged from 0.64 - 2000 μM were appeared as sharp peaks with an average retention time of 4.55 min (Figure 3.9). In the *in vitro* digestion assay, only after 24 h of co-incubation of sinigrin with myrosinase, no detectable peak at retention time of 4.55 min was observed. Therefore, no sinigrin could be detected (Figure 3.10). Thus, the starting sinigrin should be broken down by myrosinase effectively.

3.4 Cytotoxic effects of AITC on colorectal adenocarcinoma cells

Besides studying the effects of sinigirn and the co-treatment of sinigrin with myrosinase, the effect of corresponding ITC of sinigrin, AITC, on different colorectal adenocarcinoma cells was also investigated. The effect of AITC on the survival of different colorectal adenocarcinoma cells were determined by MTT assay. Upon 72-h of exposure, AITC exerted significant cytotoxic effect on all the tested cancer cells. For instance, the percentages of survival cells after 50 μM AITC treatments in Caco-2, COLO 201 and SW620 were 50.7, 64.6 and 42.0%, respectively (Figure 3.11). Based on sensitivity of these cells, the most vulnerable SW620 cells were chosen for further studies. As shown in Figure 3.13, a clear dose- and time-dependent cytotoxic effect of AITC on SW620 cells was observed. The percentages of survival cells after 50 μM AITC treatment for 24, 48 and 72 h were 79.6, 46.7 and 42.0%, respectively. Moreover, microscopic observation also illustrated an apparent decrease

in SW620 cells density after 10, 20 and 40 μM AITC treatments for 24 h (Figure 3.15).

3.5 Cytotoxic effect of PEITC on colorectal adenocarcinoma cells

As shown in Figure 3.12, PEITC also greatly affected the survival of different colorectal adenocarcinoma cells. Upon 72-h of exposure, PEITC exerted a significant cytotoxic effect on all the tested cancer cells. The percentages of survival cells after 50 μM PEITC treatments were 9.75, 18.2 and 6.36% in Caco-2, COLO 201 and SW620, respectively. In paralleled with the studies on AITC, SW620 cells were also subjected to further investigations. A clear dose- and time-dependent cytotoxic effect of PEITC on SW620 cells was observed (Figure 3.14). The percentage of survival cells after 50 μM PEITC treatment for 24, 48 and 72 h were 20.0, 5.13 and 6.36%, respectively. In general, PEITC possessed a much stronger cytotoxic effect on the tested cancer cells when compared with AITC.

3.6 Antiproliferative effects of AITC on colorectal adenocarcinoma cells

In additional to MTT assay, the growth inhibitory effects of AITC and PEITC were further confirmed by the BrdU assay. As shown in Figure 3.13, AITC started to exert cyotoxic effect on SW620 cells at 24 h of treatment and progressed with time. Therefore, the antiproliferative effect of AITC on both 24 and 48-h of treatments were tested by BrdU assay. As shown in Figures 3.16 and 3.17, AITC inhibited the proliferation of SW620 cells effectively in a dose- and time-dependent manner. The percentages of cell proliferation after 25 μM AITC treatment for 24 and 48-h were 65.7 and 30.6%, respectively. By graphical method, IC_{50} values were determined to be 30.2 and 23.2 μM after 24 and 48-h of treatment, respectively.

3.7 Antiproliferative effect of PEITC on colorectal adenocarcinoma cells

As shown in Figure 3.18, a 24-h period of PEITC treatment could exert very strong cytotoxic effect on SW620 cells. Therefore, the antiproliferative effect of PEITC for a 24-h of treatment was tested by BrdU assay. After 24 h, the percentage of cell proliferation after 25 μM PEITC treatment was 20.6%. By graphical method, IC_{50} value was determined to be 9.21 μM. In general, PEITC possessed a much stronger antiproliferative effect on SW620 cells when compared with AITC

3.8 Cytotoxic effects AITC on skin fibroblast

Besides investigating the growth inhibitory effects of ITCs on different colorectal adenocarcinoma cells, their effects on normal cells were also worth to be studied. A human skin fibroblast, Hs68, was chosen for investigation. As shown in Figures 3.19 and 3.20, the survival of skin fibroblast Hs68 was not affected by the treatment of AITC (up to 150 μM) for both 24 and 72-h of exposure. The percentages of survival cells after 150 μM AITC treatment for 24 and 72 h were 103.2 and 105.9%, respectively. Thus, no cytotoxic effect could be observed.

3.9 Cytotoxic effect PEITC on skin fibroblast

On the other hand, the survival of skin fibroblast Hs68 was affected by the treatment of PEITC in a dose- and time-dependent manner (Figures 3.21 and 3.22). In a 24-h period of treatment, the percentages of cells after exposure to 50, 100 and 150 μM PEITC were 92.0, 43.7 and 17.0%, respectively. Subsequently, the percentage of survival was further reduced after prolonged exposure. Only 40.2, 13.4 and 11.6% of survival cells were found upon 50, 100 and 150 μM treatments for 72 h, respectively.

3.10 Effects of AITC on cell cycle progression in SW620 cells

After assessing the growth inhibitory effects of AITC on different colorectal adenocarcinoma cells, their effects on cell cycle distribution were elevated by flow cytometry analysis using PI staining. Based on the IC_{50} values determined in the BrdU assay (Figure 3.16 - 3.17), three comparable dosages (10, 20 and 30 μM) were chosen for assay. As shown in Figures 3.23 - 3.24 and 3.26, treatment of AITC induced a dramatic dose- and time-dependent accumulation of SW620 cells in G_2/M phase, together with a concomitant diminution of cells in G_0/G_1 phase. The percentages of cells at G_2/M phase upon 0, 10, 20 and 40 μM AITC treatments for 24 h were 12.6, 62.3, 81.8 and 56.9%, respectively (Figure 3.26 and Table 3.1). The actually process of cell cycle arrested at G_2/M phase was initiated at 4-16 h and reached a maximum at 24 h (Table 3.2). The percentages of cells at G_2/M phase increased dramatically by 6.5-fold after 24 h of treatment. At the same time, a consecutive increased of cells at S phase was also observed, which reflected an impaired cell cycle progression through blockage at the G_2/M transition.

3.11 Effects of PEITC on cell cycle progression in SW620 cells

Based on the IC_{50} value determined in the BrdU assay (Figure 3.18), three comparable dosages (2.50, 5 and 10 μM) were chosen for assay. As shown in Figures 3.25, treatment of PEITC induced a blockage at the G_2/M ransition in SW620 cells in the similar way of AITC. After 24 h, the percentages of cells at G_2/M phase upon 0, 2.5, 5 and 10 μM PEITC treatments were 9.75, 14.9, 32.4 and 26.4%, respectively (Table 3.3). At the same time, a consecutive decreased in cells at G_0/G_1 phase was also observed (Figure 3.28).

3.12 Effect of AITC on expression of checkpoint regulatory proteins in SW620 cells

In order to elucidate the underlying mechanisms for the G_2/M arrest in AITC-treated SW620 cells, the expression level of pivotal regulatory proteins was studied. In G_2 checkpoint, control of Cdc2/cyclinB kinase complex is the crucial step for cells to entry mitosis. It is governed by the actions of phosphatases Cdc25B and Cdc25C (Molinari, 2000; Shackeford *et al.*, 2000; Strausfeld *et al.*, 1991). Results of western blot analysis illustrated that AITC treatment led to a markedly reduce in Cdc25C protein in a dose- and time- dependent manner (Figures 3.29 and 3.30). Upon 20 μM AITC treatment, downregulation of Cdc25C protein was clearly observed after 8 h and kept remaining at a relatively low level. At the same time, AITC treatment caused an apparent but short-term upregulation of Cdc25C phosphorylation on Ser216 (negative regulatory site) at 1 - 4 h, and followed by a sustained downregulation. The later downregulation of p-Cdc25C(Ser216) could be explained by the concomitant decrease in the total Cdc25C at that time interval. Moreover, AITC treatment also resulted in a downregulation of another phosphatase Cdc25B dose- and time-dependently. Subsequently, Cdc2 protein kinase was modulated by inhibitory phoshorylations on Thr14 and Tyr15. Only 1 h after treatment, a rapid and sustained upregulation of p-Cdc2(Tyr15) was observed. Another inhibitory phosphorylation of Cdc2 on Thr14 was noticeable until 24 h of exposure. On the other hand, AITC did not affect the level of total Cdc2 protein, whereas an unusual upregulation of total CyclinB1 was found in the treated cells.

3.13 Effect of AITC on expression of checkpoint regulatory genes in SW620 cells

In order to verify whether the change in protein expression was related to the transcriptional level of control, the effect of AITC on SW620 cells towards transcriptional control of regulatory genes in G_2 checkpoint was also investigated. Results of the quantitative real-time PCR on Cdc25B, Cdc25C, Cdc2 and CyclinB1 mRNA expression are shown in Figure 3.31. In general, the pattern of mRNA expression was well correlated with the western blot results (Figures 3.29 and 3.30). After treatment with 20 μM AITC, significant downregulation of both Cdc25B and Cdc25C mRNA were initiated at 4 h and remained low afterwards (Figure 3.31 and Table 3.4). At the same time, no change in the expression of Cdc2 at transcriptional level was found. Interestingly, a consistently matched upregulation of CyclinB1 mRNA (2.81-fold) was observed after 24-h treatment. In addition, a sharp peak was noted in the dissociation curve of each assay for the confirmation of accuracy (Figure 3.32).

3.14 Effect of AITC on induction of apoptosis in SW620 cells

Besides arresting cell cycle progression, an induction of apoptosis in SW620 cells was observed after prolonged exposure to AITC (Figure 3.33). It was proved by a significant increase in subG1 population after treatment with 20 μM AITC for 48 h. The proportion of apoptotic cells was elevated by 12.8-fold when compared with time 0 (Table 3.5).

3.15 Effect of PEITC on induction of apoptosis in SW620 cells

As shown in Figure 3.34, an induction of apoptosis by PEITC was also observed. It was proved by an increase in subG1 population after treatment. After 10 μM PEITC-treatment, the percentage of apoptotic cells was elevated by 13.1-fold when compared with control (Table 3.6).

3.16 Effect of AITC on the expression of apoptotic proteins in SW620 cells

After 20 μM AITC treatment for 48 h, results of western blot analysis demonstrated a clear caspase-mediated apoptosis in the treated SW620 cells (Figure 3.35). Firstly, AITC-induced the activation of initiator caspases, and consequently led to the activation of downstream effector caspases. For initiator caspases, full length caspase 8 (57 kDa) were cleaved, with the formation of activated caspase 8 (43 kDa) after treatment. At the same time, full length caspase 9 (47 kDa) was also cleaved, which indicated by the presence of 35 and 37 kDa units. Subsequently, these events triggered the activation of effector caspase cascade (including caspase-3 and -7). For caspase-3, cleavages of 17 and 19 kDa were observed. Whereas, respective activated fragment (20 kDa) of caspase-7 was found. However, no cleavage of caspase-6 was shown in the cells exposed to AITC. Finally, an obvious proteolytic cleavage of full length PARP (116 kDa) into cleaved PARP (89 kDa) was observed, which served as an important hallmark for the presence of apoptosis (Lazebnik *et al.*, 1994).

3.17 Effect of AITC on body weight of animals

Besides performing various *in vitro* experiments, a nude mice xenograft assay was also employed to determine the *in vivo* antitumor effect of AITC. During the experiment, all mice were monitored regularly and their body weight was measured periodically in order to assess their health condition. Both groups of AITC-treated mice were marginally weighed less when compared with control, but these discrepancies were actually less than 7%. Briefly, body weight in control, 5 and 10 μmol AITC-treated mice were 21.2 ± 0.9, 19.7 ± 1.0 and 19.7 ± 1.3 g, respectively (Figure 3.36 and Table 3.7). At the same time, all mice were appeared healthy and did not show any impaired movement.

3.18 Effect of AITC on growth of xenograft

The effect of AITC treatment on the growth of SW620 xenograft is shown in Figure 3.37 and Table 3.8. Tumor size of all mice was measured when palpable tumors appeared on day 6 after cell implantation. In 10 μmol AITC-treated mice, a significant suppression of tumor growth was found throughout the whole experimental period. For instance, on day 17, the tumor volume of control and 10 μmol AITC-treated mice were 261 ± 129 and 127 ± 61 mm^3, respectively. These results reflected a more than 50% reduction in tumor volume after treatment. Continuous suppression efficiency was demonstrated with the increase of treatment time. At the end of experiment, the tumor volume in control and 10 μmol AITC-treated mice were 843 ± 372 and 421 ± 132 mm^3, respectively. There was about 50% of reduction in tumor volume after treatment, it was in consistent with the suppression effect as observed on day 17. Similarly, the wet tumor weight in the treated mice obtained at the end of experiment was about 53% lightered than control. The wet tumor weight in control and 10 μmol AITC-treated mice were 0.47 ± 0.24

and 0.22 ± 0.13 g, respectively (Figure 3.38 and Table 3.9). On the other hand, the 5 μmol AITC treatment on the mice was not effective. Retarded tumor growth was observed only at the early phase of experiment and started to diminish after day 13. At the end of experiment, no significant difference between tumor size and weight of the control and 5 μmol AITC-treated mice was observed (Figure 3.38 and Table 3.9).

3.19 Effect of AITC on regulatory proteins expression of xenograft

In order to gain insights into the mechanisms, lysates from the mice tumors were subjected to western blot analysis. Both checkpoint regulatory proteins including, Cdc2, p-Cdc2(Thr14), p-Cdc2(Tyr15), p-Cdc25C(Ser216), Cdc25C, Cdc25B and CyclinB1, and representative apoptotic protein PARP were subjected to analysis. The expression level of checkpoint regulatory Cdc2 protein was clearly reduced in 10 μmol AITC-treated mice when compared with control. While all the other tested proteins showed no difference after treatment (Figures 3.39 and 3.40).

3.20 Effect of AITC on xenograft under histological analysis

Besides western blot analysis, the tumor tissue was further assay by histological analysis. Sectioned tumor tissue was stained by hematoxylin and eosin. Representative photographs taken under light microscope are shown in Figure 3.41. Stained cells with similar cells density were observed in both control and treatment mice. Nuclei of the cells were stained into dark blue-purple, while cytoplasm of the cells was in pink-orange. In fact, there were limitations on the tissue sectioning process. It was due to the fragile nature of both tissues. Therefore, no further immnostaining procedure was performed.

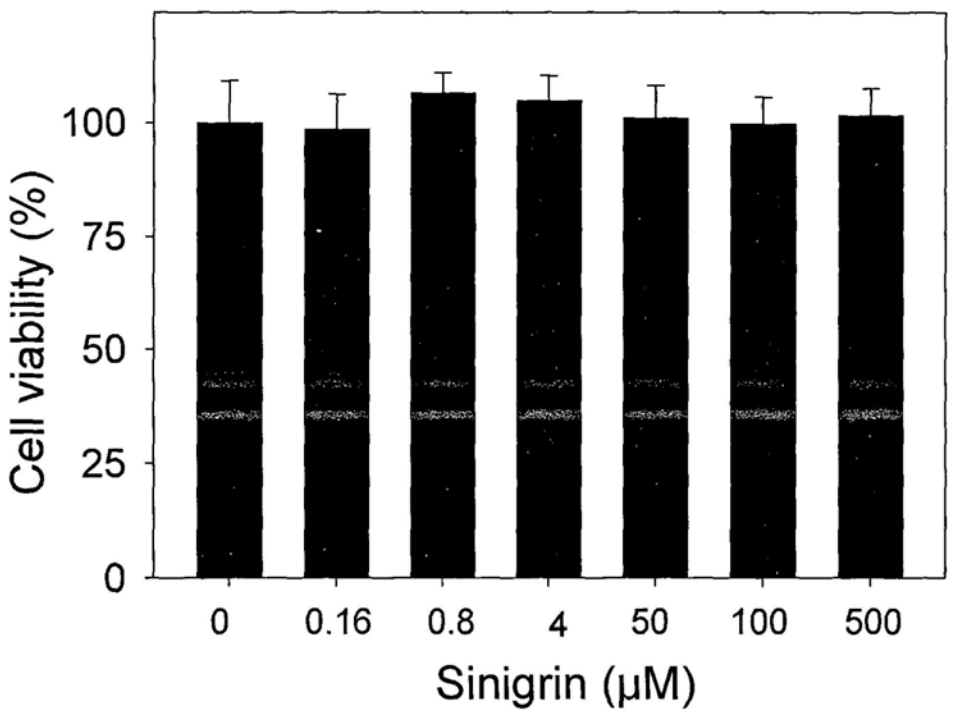

Figure 3.1 Effects of sinigrin treatments for 72 h on human colorectal adenocarcinoma Caco-2 cells as determined by MTT assay. Results were expressed as mean ± S.D. of three independent experiments.

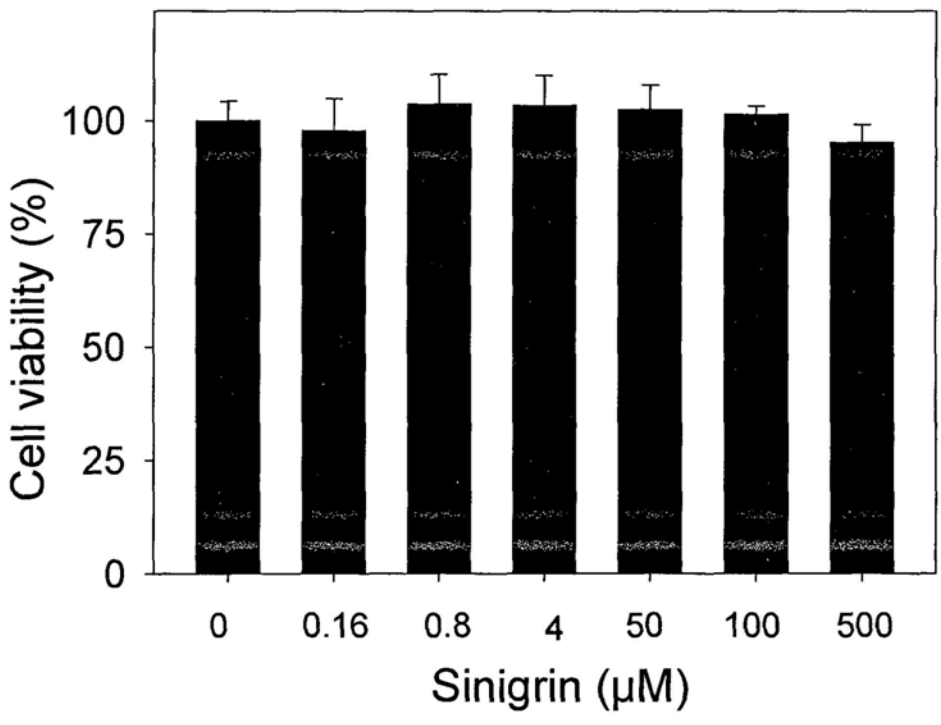

Figure 3.2 Effects of sinigrin treatments for 72 h on human colorectal adenocarcinoma SW620 cells as determined by MTT assay. Results were expressed as mean ± S.D. of three independent experiments.

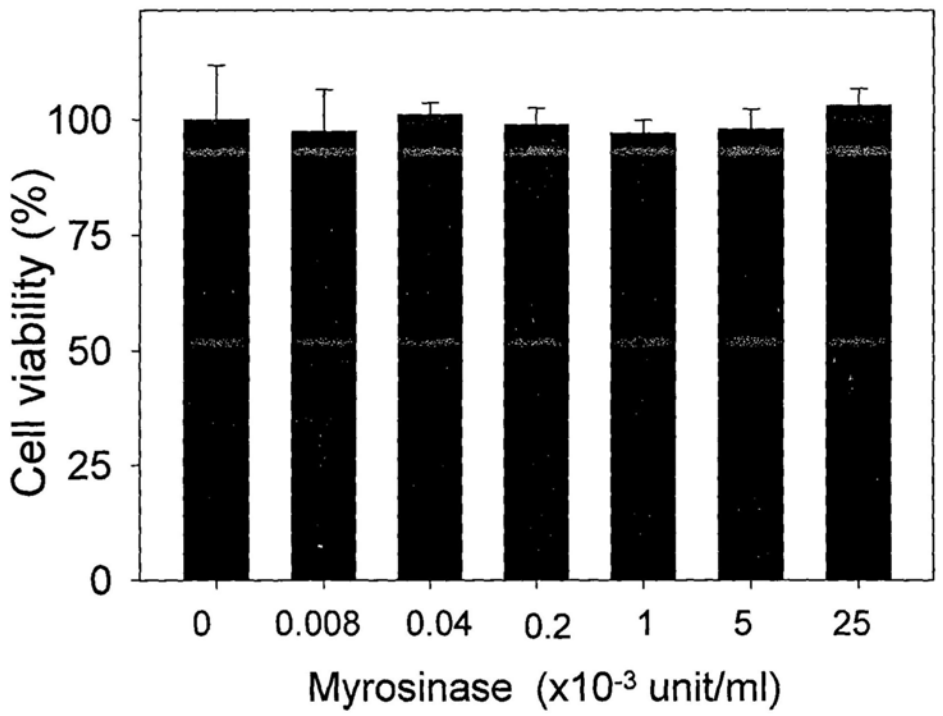

Figure 3.3 Effects of myrosinase treatments for 72 h on human colorectal adenocarcinoma Caco-2 cells as determined by MTT assay. Results were expressed as mean ± S.D. of three independent experiments.

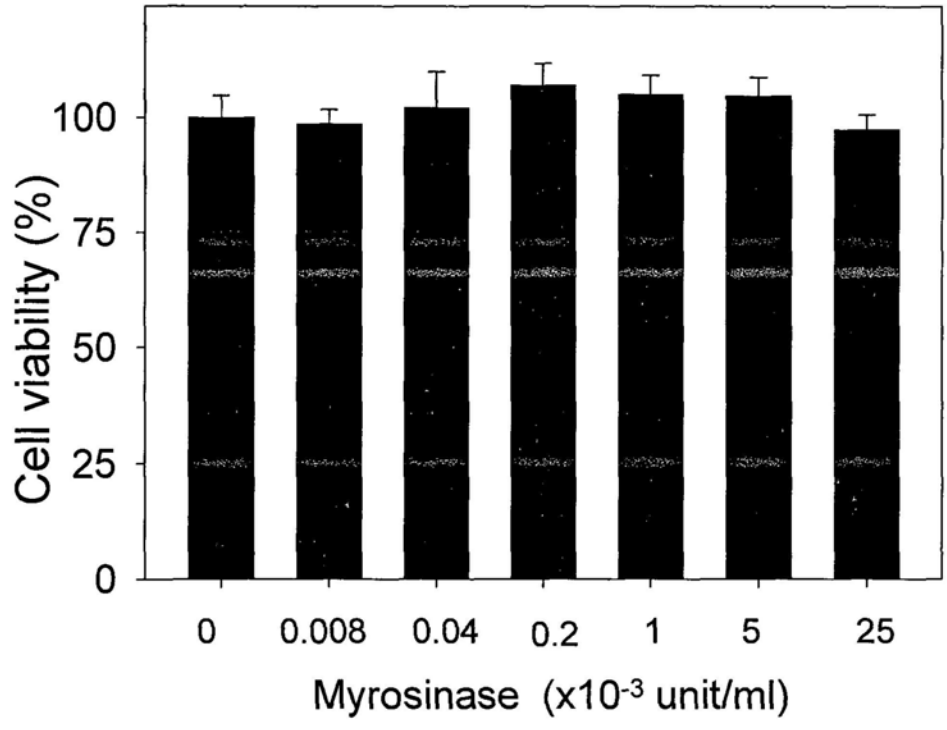

Figure 3.4 Effects of myrosinase treatments for 72 h on human colorectal adenocarcinoma SW620 cells as determined by MTT assay. Results were expressed as mean $\pm$ S.D. of three independent experiments.

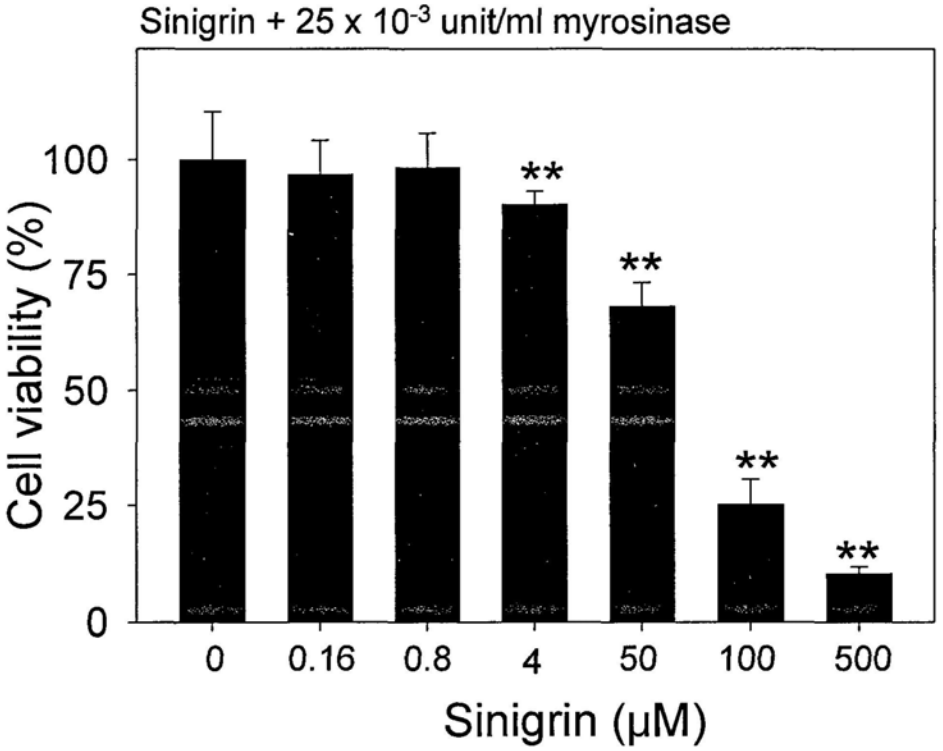

Figure 3.5 Effects of co-incubation of sinigrin and myrosinase for 72 h on Caco-2 cells as determined by MTT assay. Results were expressed as mean ± S.D. of three independent experiments. Statistical differences between control and treatment groups were determined using two-tailed Student's *t*-test. The P-value of <0.05(*) or <0.01(**) was considered statistically significant. At least one independent experiment was performed with similar results.

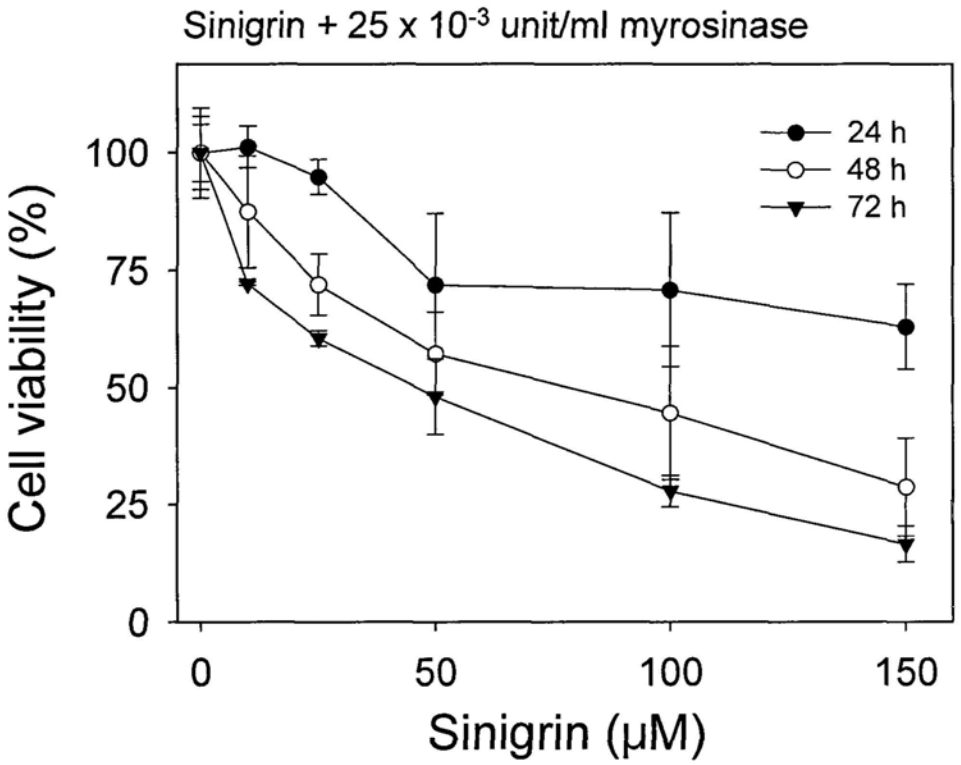

Figure 3.6 Dose- and time-dependent effects of co-incubation of sinigrin and myrosinase on Caco-2 cells as determined by MTT assay. Results were expressed as mean ± S.D. of three independent experiments. Statistical differences between control and treatment groups were determined using two-tailed Student's *t*-test. The P-value of <0.05(*) or <0.01(**) was considered statistically significant. At least one independent experiment was performed with similar results.

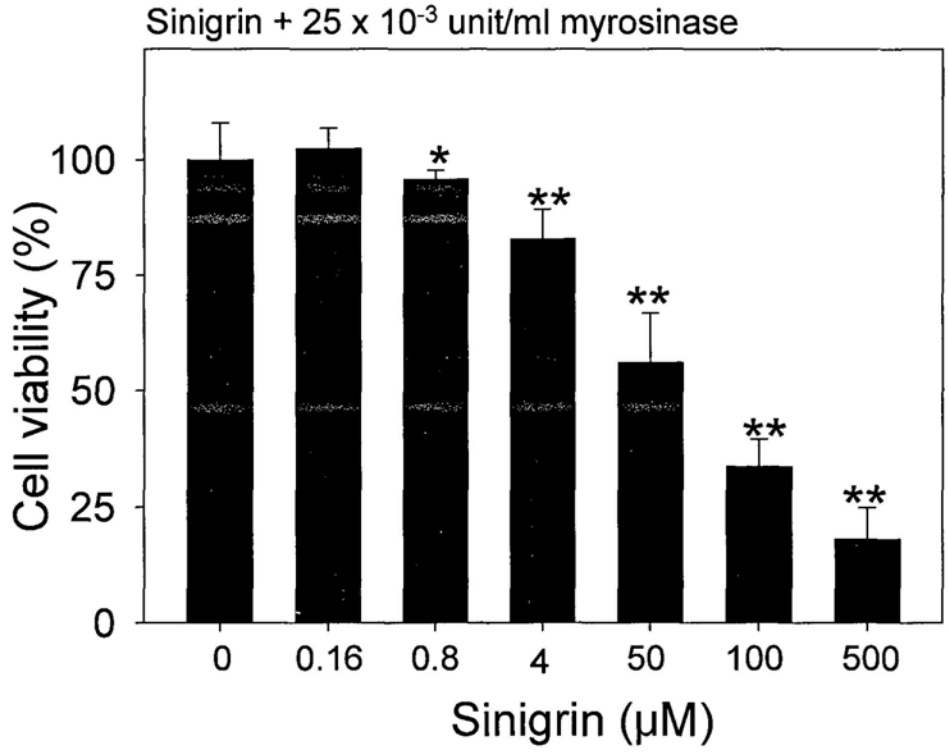

Figure 3.7 Effects of co-incubation of sinigrin and myrosinase for 72 h on SW620 cells as determined by MTT assay. Results were expressed as mean ± S.D. of three independent experiments. Statistical differences between control and treatment groups were determined using two-tailed Student's *t*-test. The P-value of <0.05(*) or <0.01(**) was considered statistically significant. At least one independent experiment was performed with similar results.

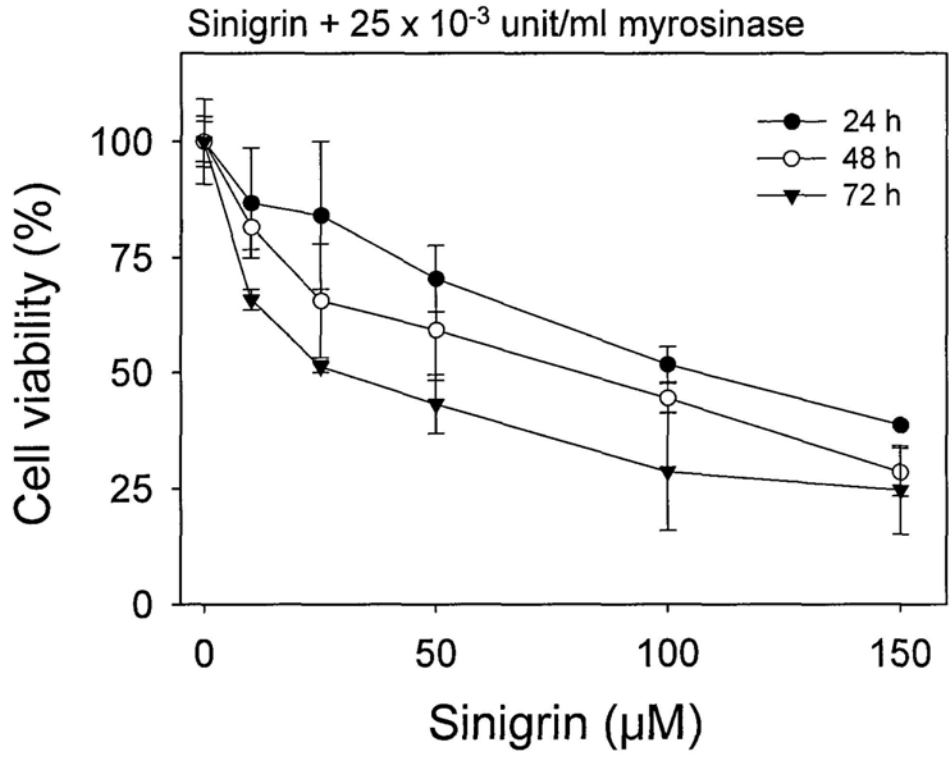

Figure 3.8 Dose- and time-dependent effects of co-incubation of sinigrin and myrosinase on SW620 cells as determined by MTT assay. Results were expressed as mean ± S.D. of three independent experiments. Statistical differences between control and treatment groups were determined using two-tailed Student's *t*-test. The P-value of <0.05(*) or <0.01(**) was considered statistically significant. At least one independent experiment was performed with similar results.

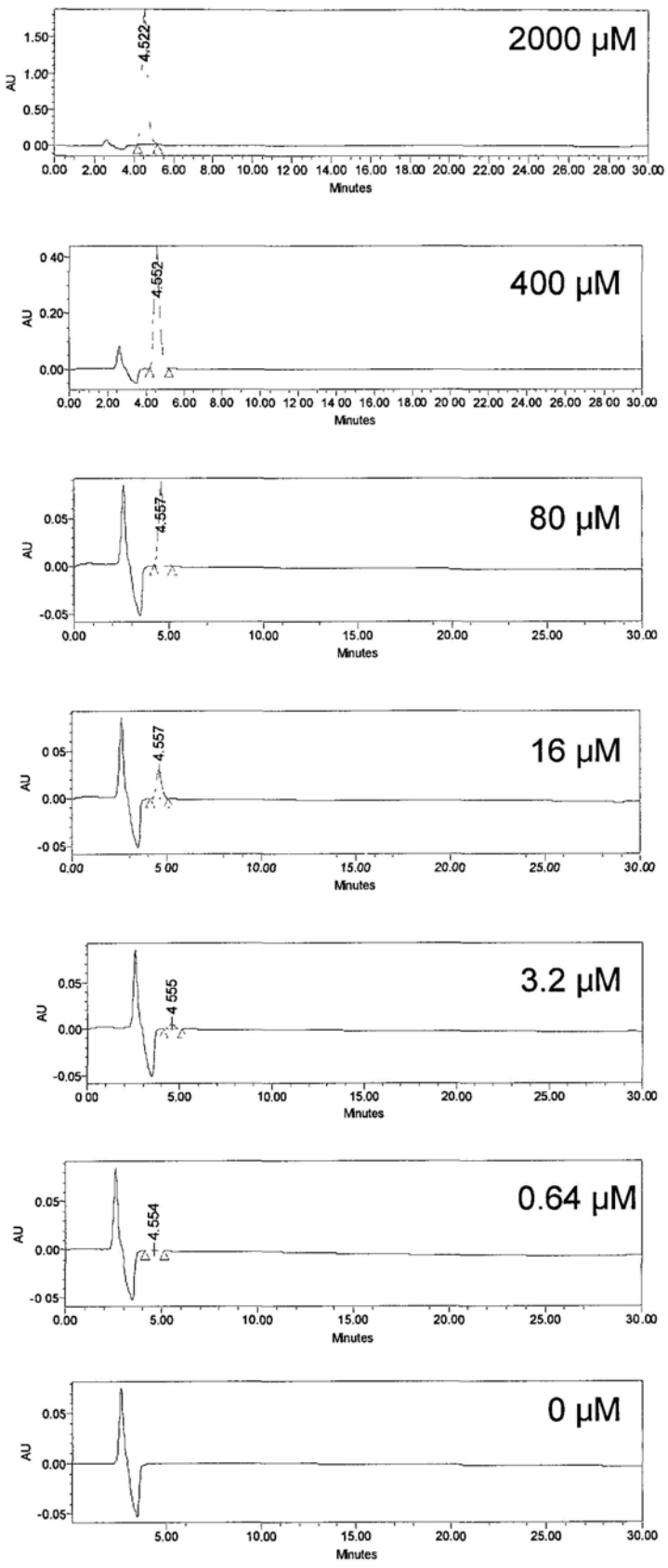

Figure 3.9 Representative HPLC-vis chromatogram (227 ηm) of sinigrin standard.

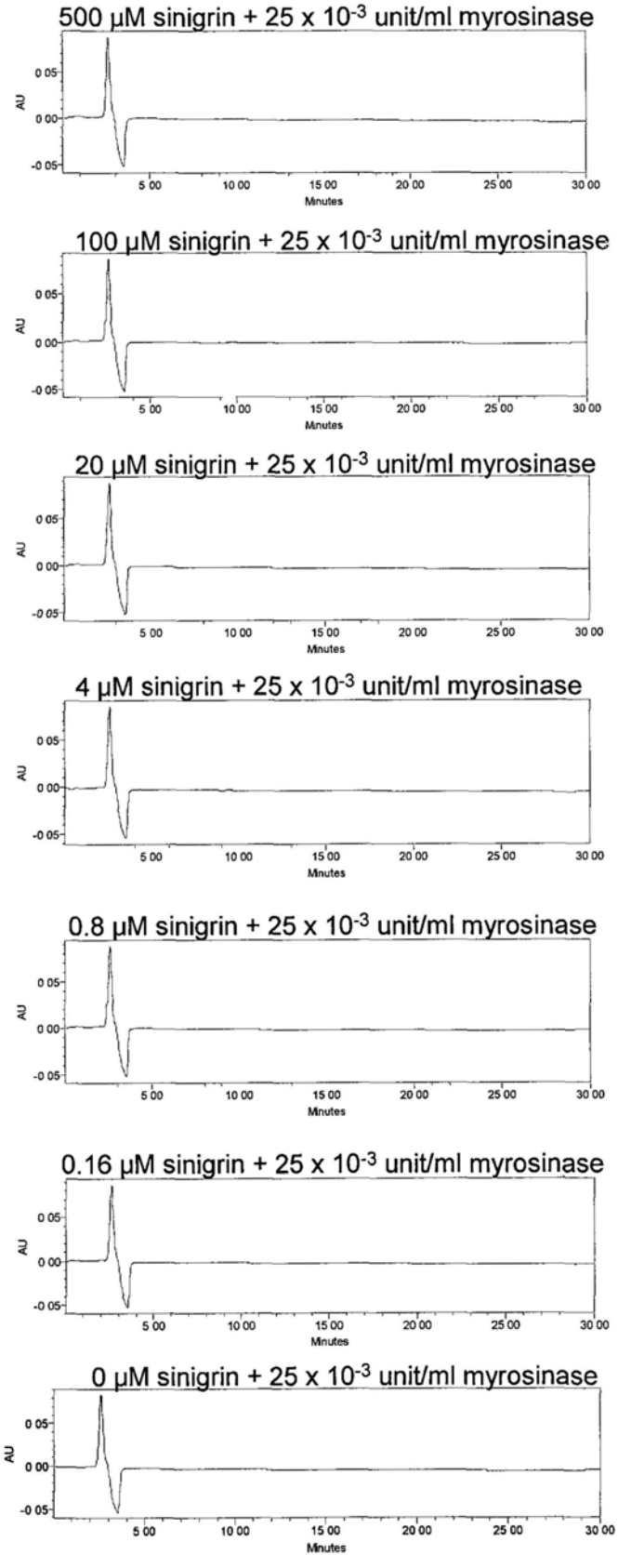

Figure 3.10 Representative HPLC-vis chromatogram (227 ηm) after co-incubation of sinigirn with myrosinase for 24 h.

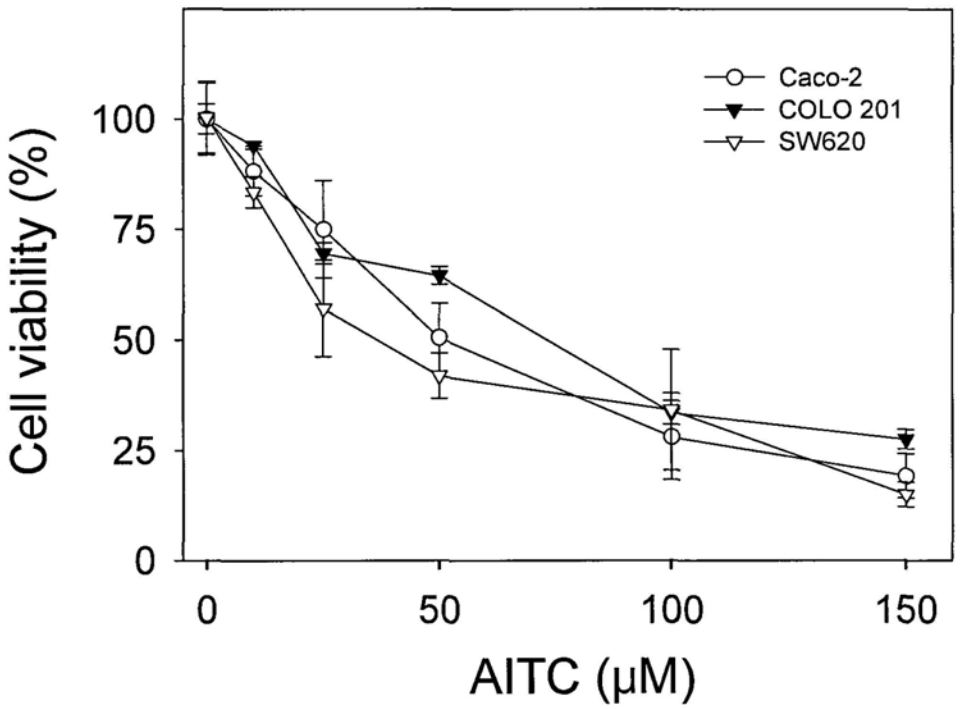

Figure 3.11 Effects of AITC treatments on different human colorectal adenocarcinoma cells (Caco-2, COLO 201 and SW620) for 72 h as determined by MTT assay. Results were expressed as mean ± S.D. of three independent experiments.

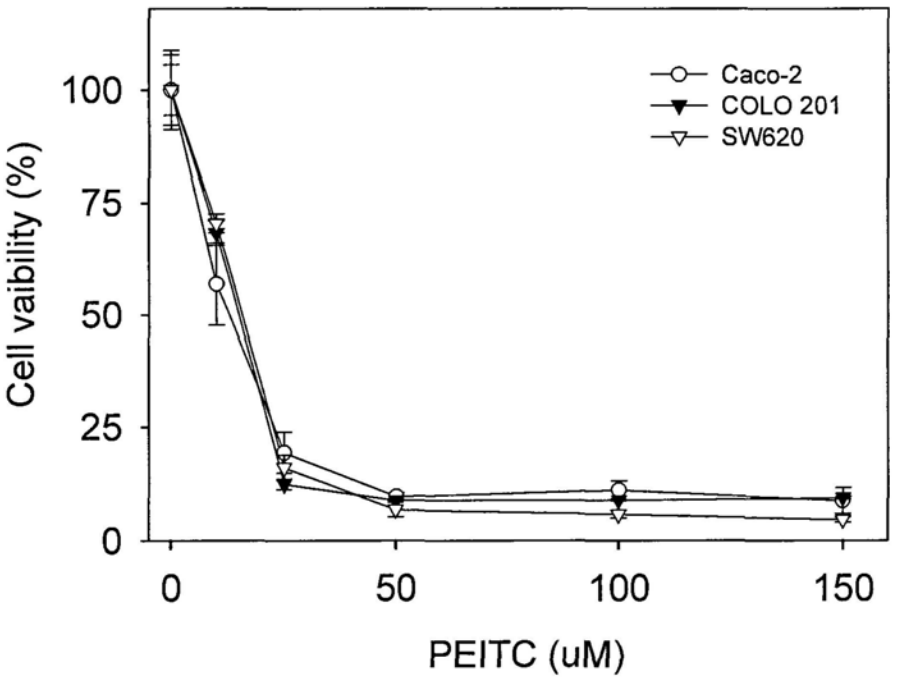

Figure 3.12 Effects of PEITC treatments on different human colorectal adenocarcinoma cells (Caco-2, COLO 201 and SW620) for 72 h as determined by MTT assay. Results were expressed as mean $\pm$ S.D. of three independent experiments.

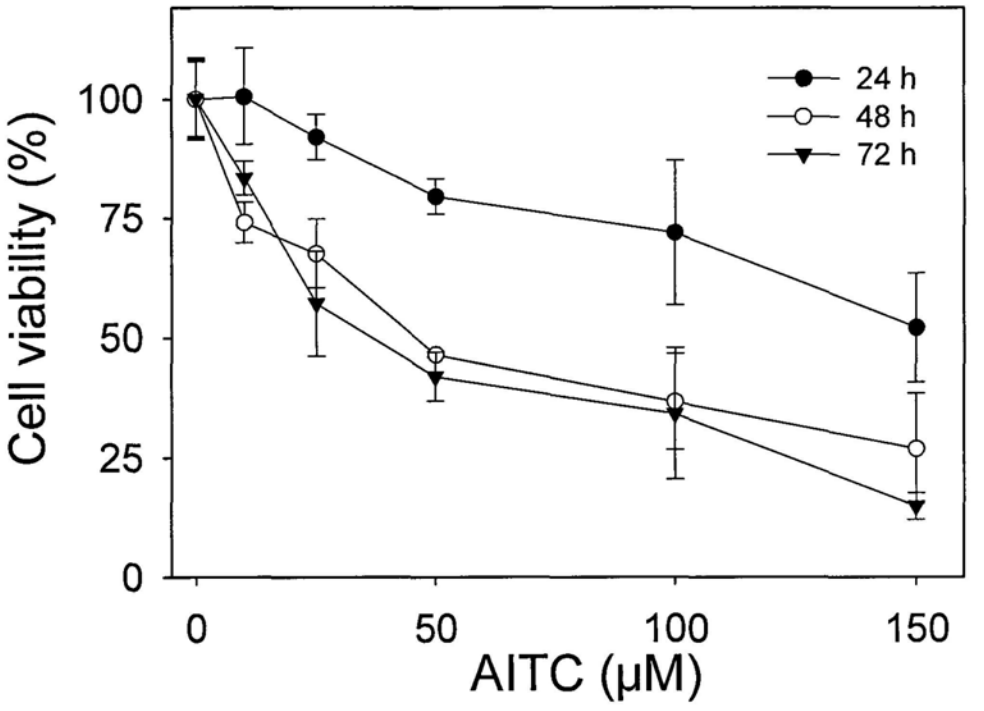

Figure 3.13 Dose- and time-dependent effects of AITC treatments on SW620 cells as determined by MTT assay. Results were expressed as mean ± S.D. of three independent experiments.

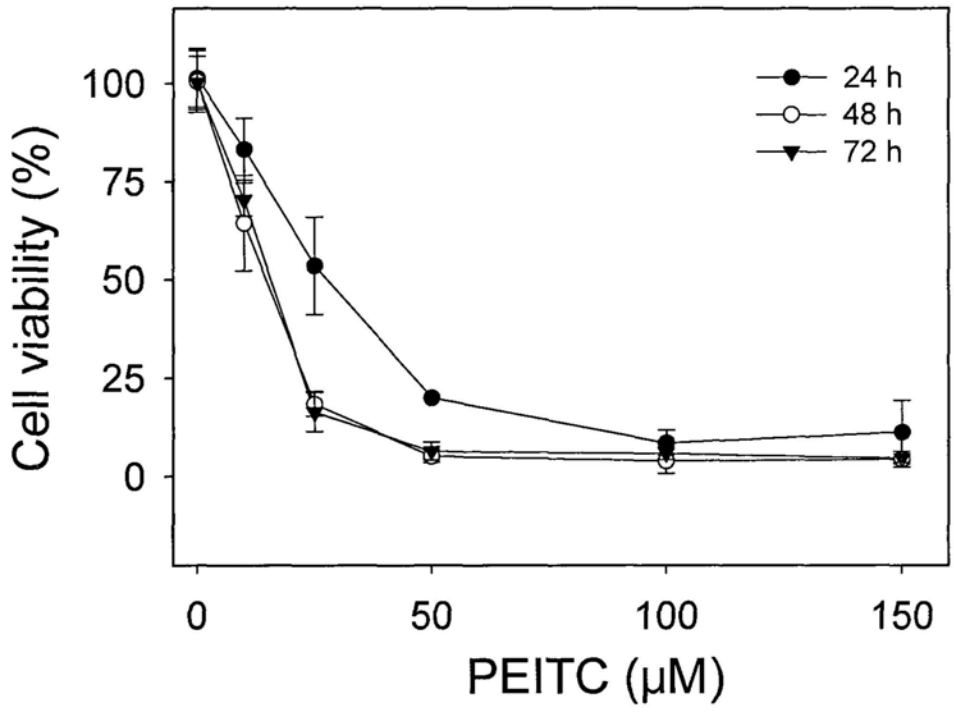

Figure 3.14 Dose- and time-dependent effects of PEITC treatments on SW620 cells as determined by MTT assay. Results were expressed as mean ± S.D. of three independent experiments.

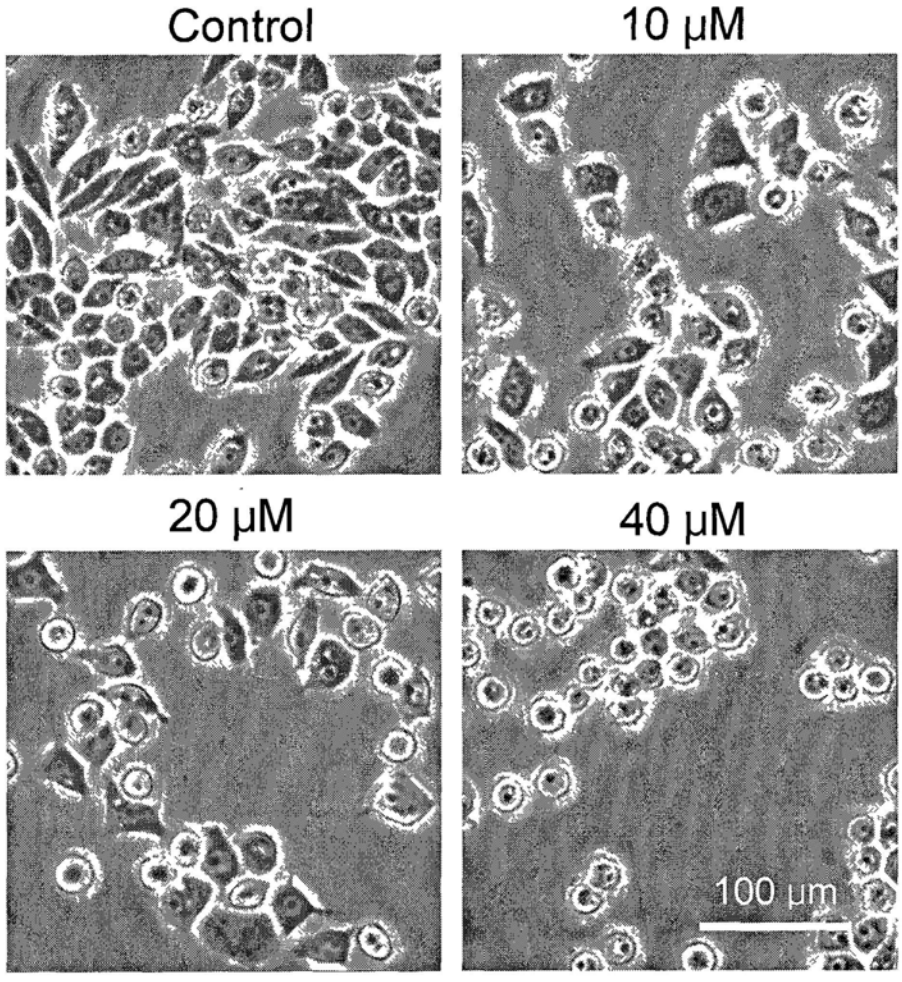

Figure 3.15 Representative photographs of SW620 cells exposed to AITC treatments for 24 h. Cells were observed under phase contrast microscope.

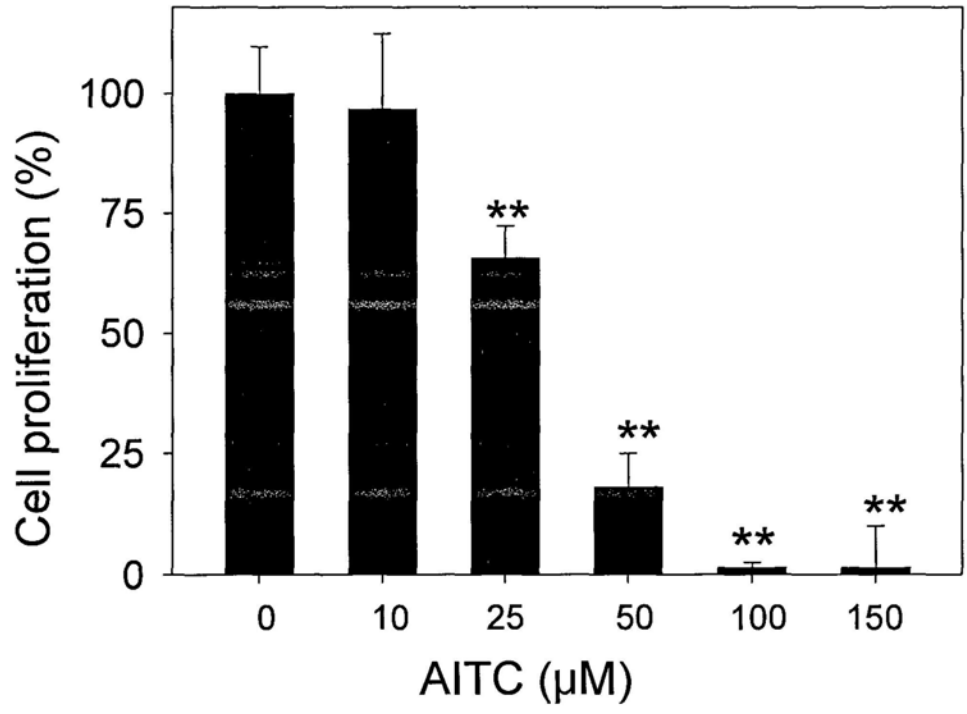

Figure 3.16 Effects of AITC treatments for 24 h on SW620 cells as determined by BrdU assay. Results were expressed as mean ± S.D. of three independent experiments. Statistical differences between control and treatment groups were determined using two-tailed Student's *t*-test. The P-value of <0.05(*) or <0.01(**) was considered statistically significant.

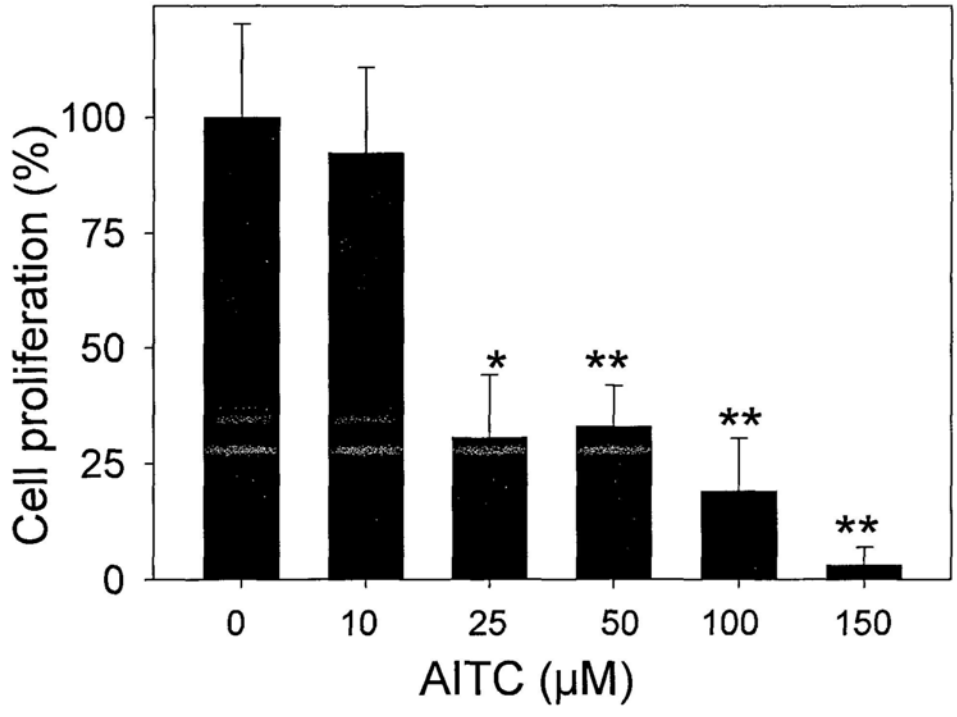

Figure 3.17 Effects of AITC treatments for 48 h on SW620 cells as determined by BrdU assay. Results were expressed as mean ± S.D.. Statistical differences between control and treatment groups were determined using two-tailed Student's *t*-test. The P-value of <0.05(*) or <0.01(**) was considered statistically significant. At least one independent experiment was performed with similar results.

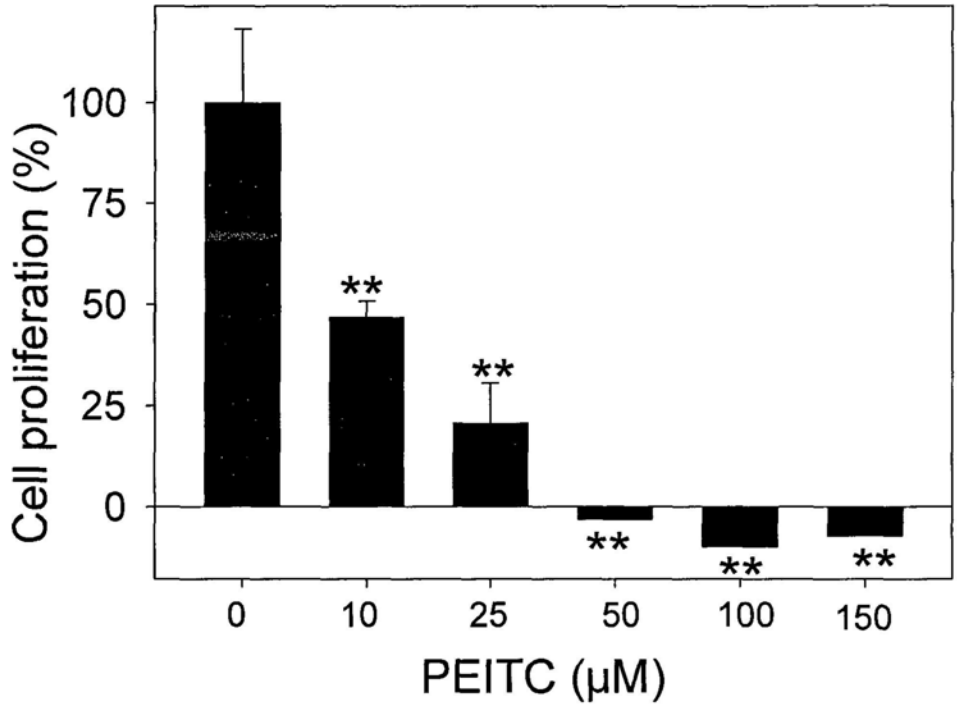

Figure 3.18 Effects of PEITC treatments for 24 h on SW620 cells as determined by BrdU assay. Results were expressed as mean ± S.D. of three independent experiments. Statistical differences between control and treatment groups were determined using two-tailed Student's *t*-test. The P-value of <0.05(*) or <0.01(**) was considered statistically significant.

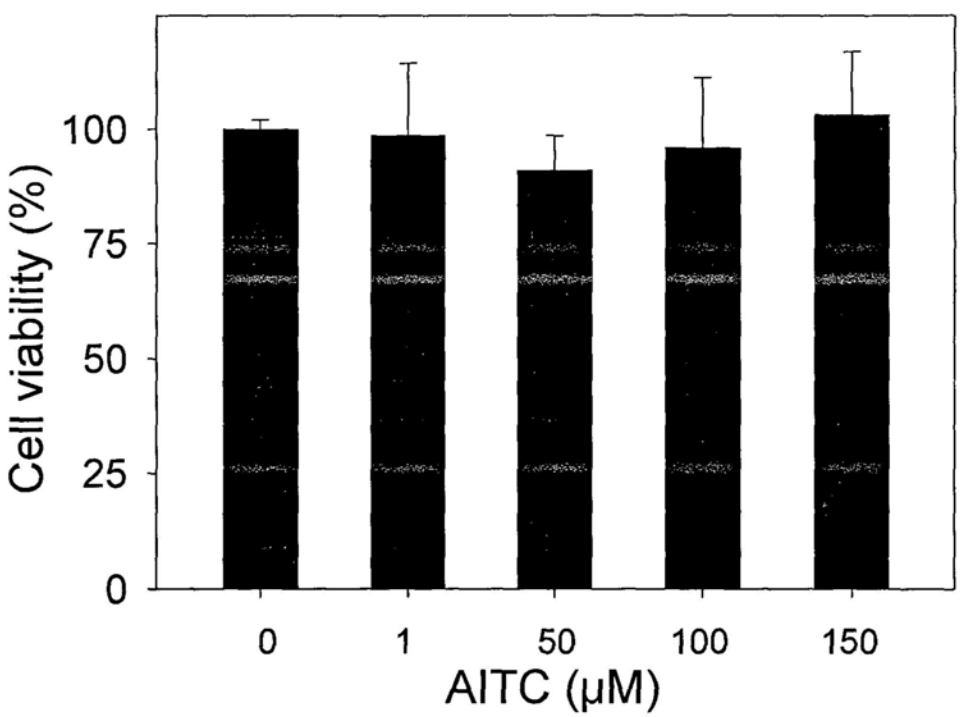

Figure 3.19 Effects of AITC treatments for 24 h on human skin fibroblast Hs68 as determined by MTT assay. Results were expressed as mean ± S.D. of three independent experiments.

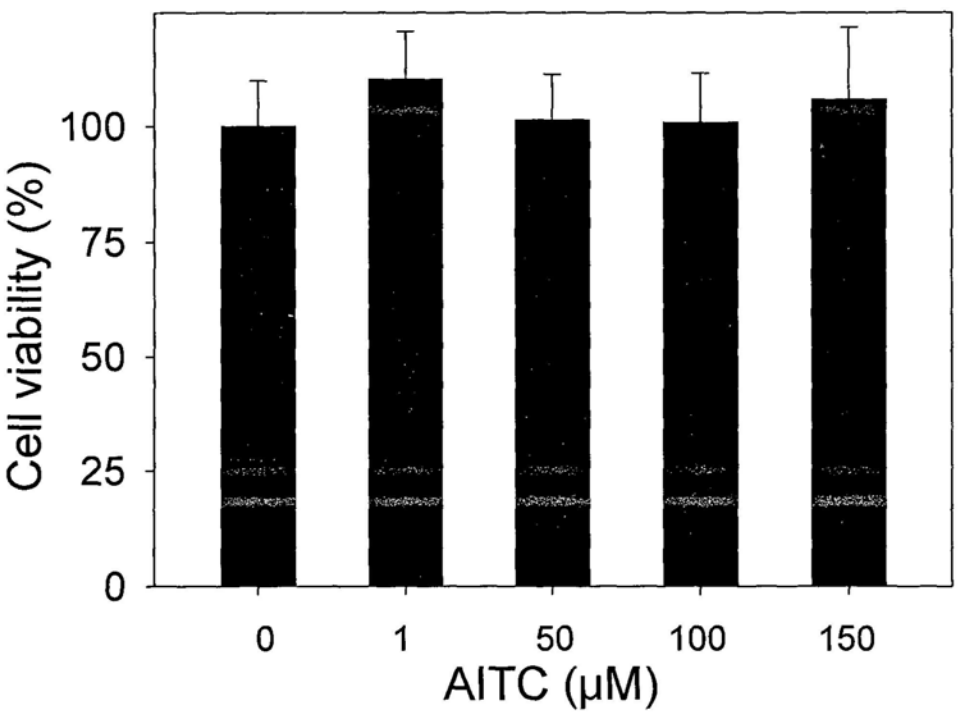

Figure 3.20 Effects of AITC treatments for 72 h on human skin fibroblast Hs68 as determined by MTT assay. Results were expressed as mean ± S.D. of three independent experiments.

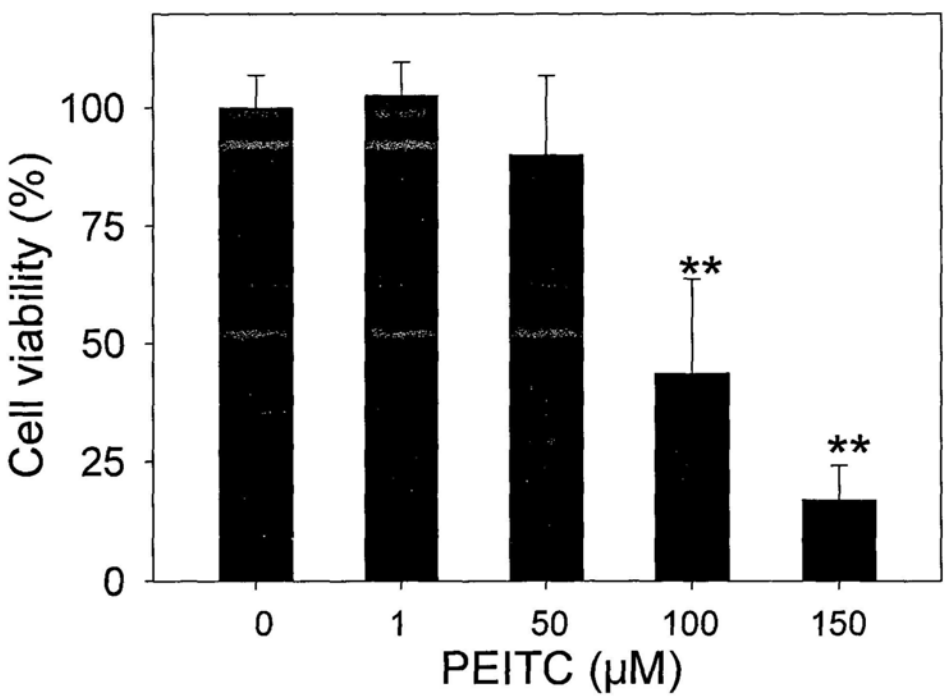

Figure 3.21 Effects of PEITC treatments for 24 h on human skin fibroblast Hs68 as determined by MTT assay. Results were expressed as mean ± S.D. of three independent experiments. Statistical differences between control and treatment groups were determined using two-tailed Student's *t*-test. The P-value of <0.05(*) or <0.01(**) was considered statistically significant.

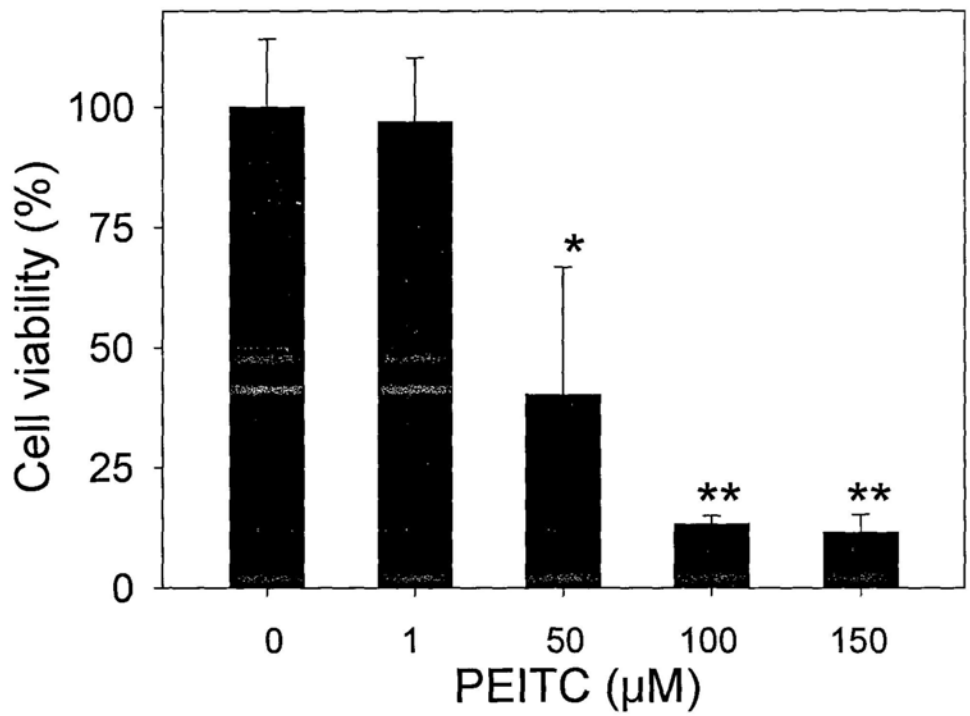

Figure 3.22 Effects of PEITC treatments for 72 h on human skin fibroblast Hs68 as determined by MTT assay. Results were expressed as mean ± S.D. of three independent experiments. Statistical differences between control and treatment groups were determined using two-tailed Student's *t*-test. The P-value of <0.05(*) or <0.01(**) was considered statistically significant.

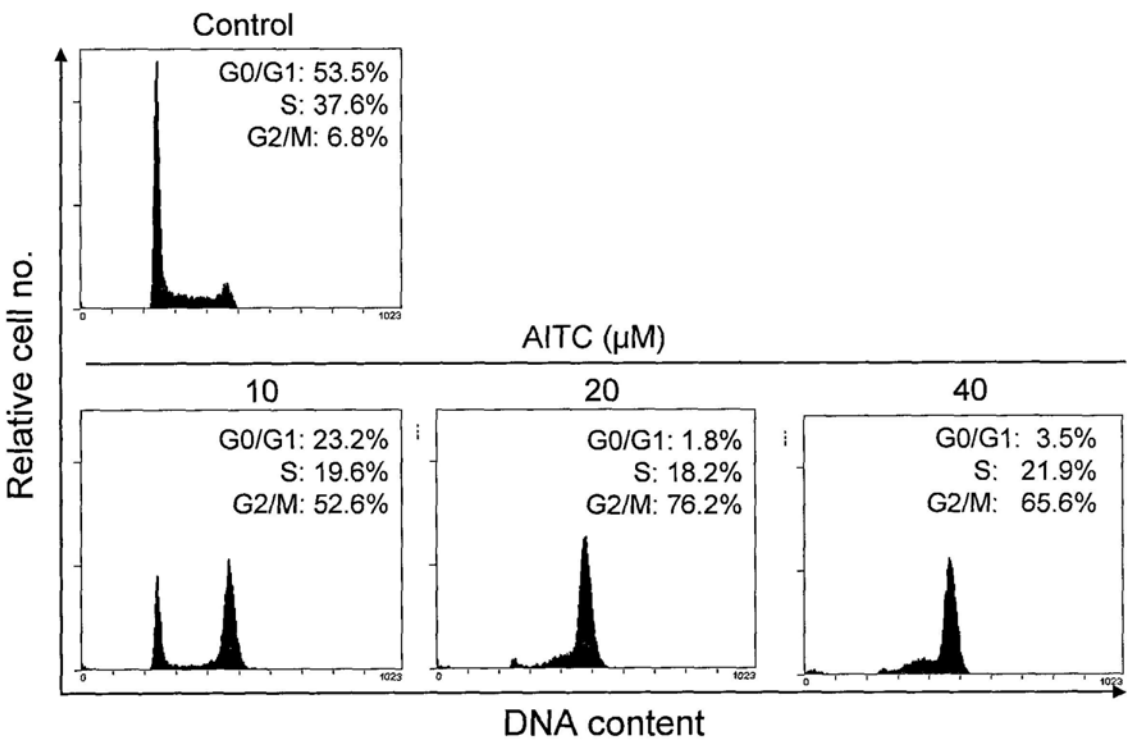

Figure 3.23 Representative DNA histograms of SW620 cells exposed to AITC treatments for 24 h.

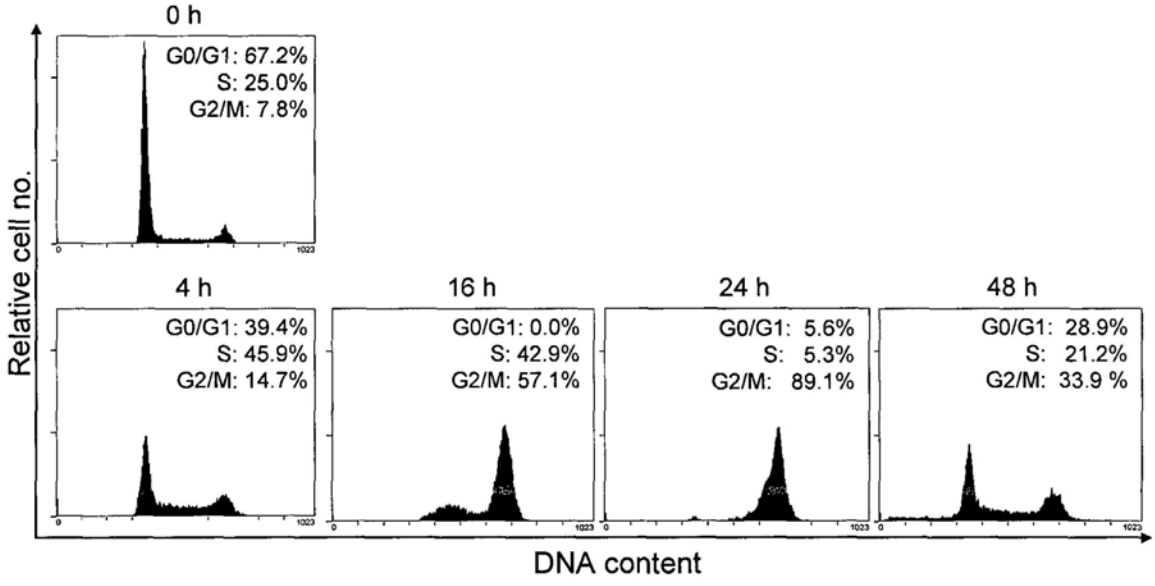

Figure 3.24 Representative DNA histograms of SW620 cells exposed to 20 μM AITC after different incubation periods.

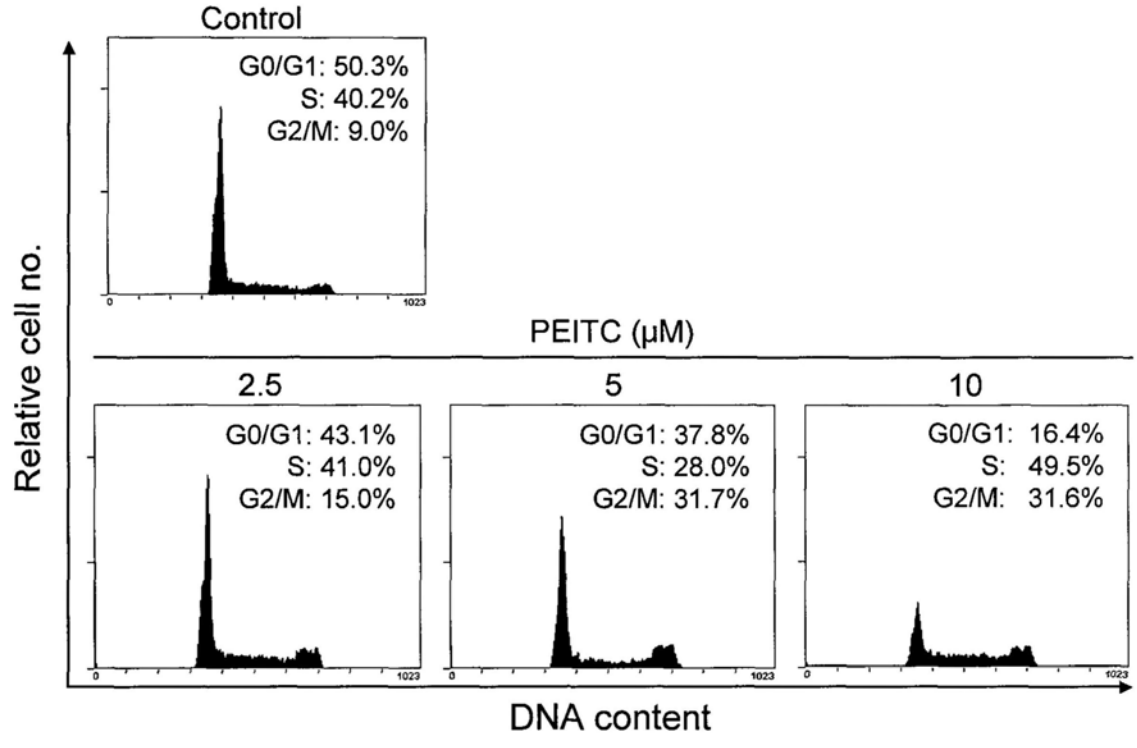

Figure 3.25 Representative DNA histograms of SW620 cells exposed PEITC treatments for 48 h.

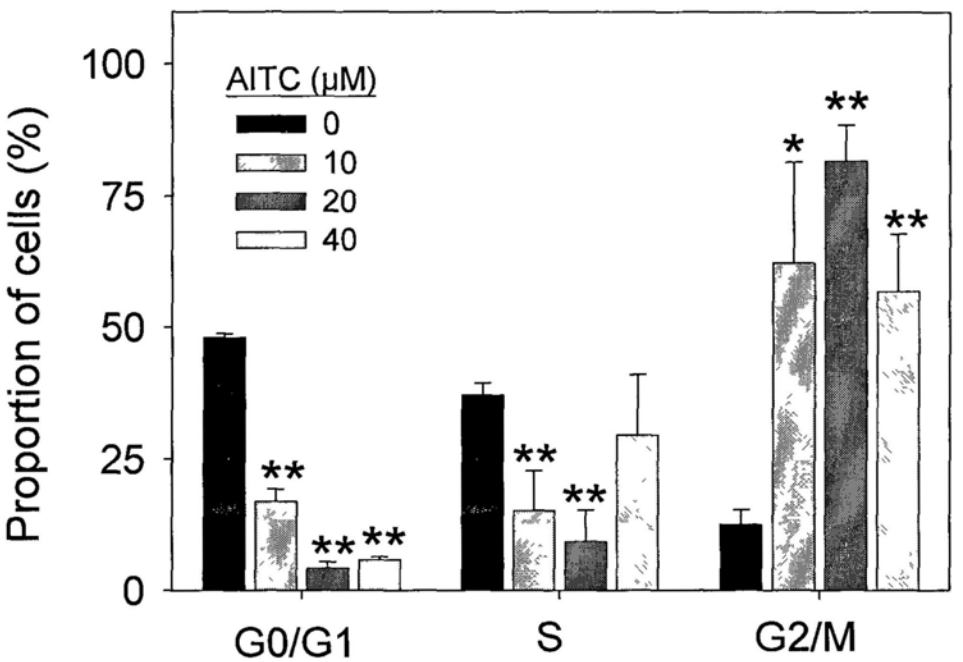

Figure 3.26 Effects of AITC treatments on cell cycle distribution for 24 h in SW620 cells as determined by flow cytometric assay. Results were expressed as mean ± S.D. of three independent experiments. Statistical differences between control and treatment groups were determined using two-tailed Student's *t*-test. The P-value of <0.05(*) or <0.01(**) was considered statistically significant.

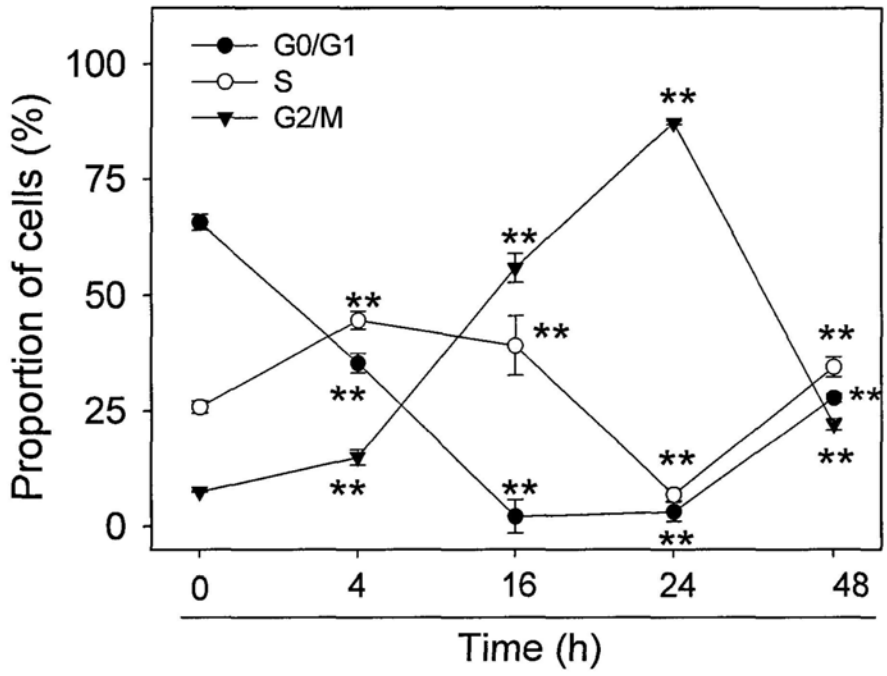

Figure 3.27 Time-dependent effects of AITC (20 μM) treatments on cell cycle distribution in SW620 cells as determined by flow cytometric assay. Results were expressed as mean ± S.D. of three independent experiments. Statistical differences between control and treatment groups were determined using two-tailed Student's *t*-test. The P-value of <0.05(*) or <0.01(**) was considered statistically significant.

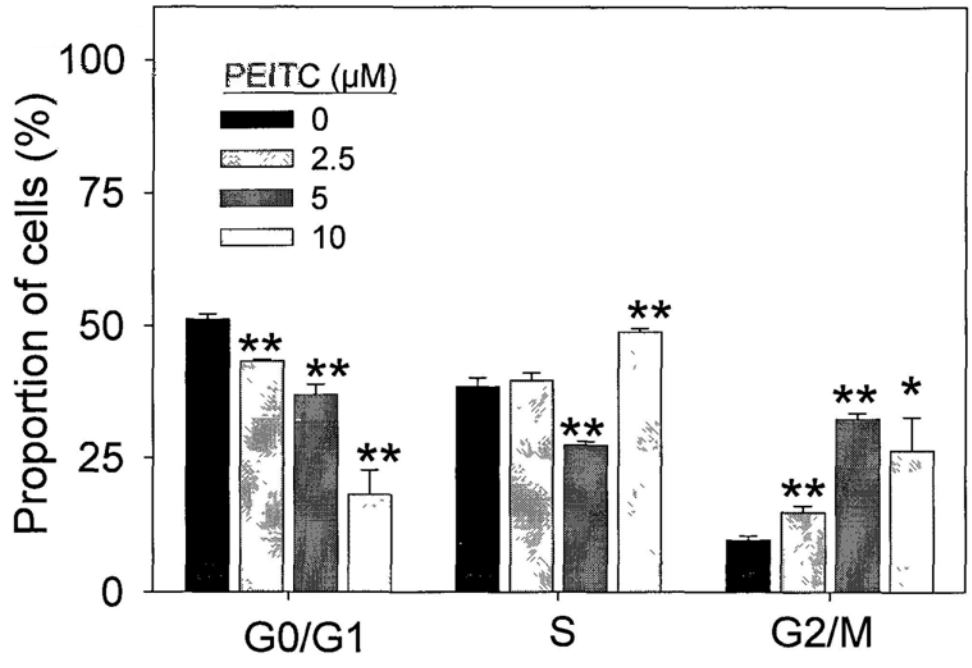

Figure 3.28 Effects of PEITC treatments for 24 h on cell cycle distribution in SW620 cells as determined by flow cytometric assay. Results were expressed as mean ± S.D. of three independent experiments. Statistical differences between control and treatment groups were determined using two-tailed Student's *t*-test. The P-value of <0.05(*) or <0.01(**) was considered statistically significant.

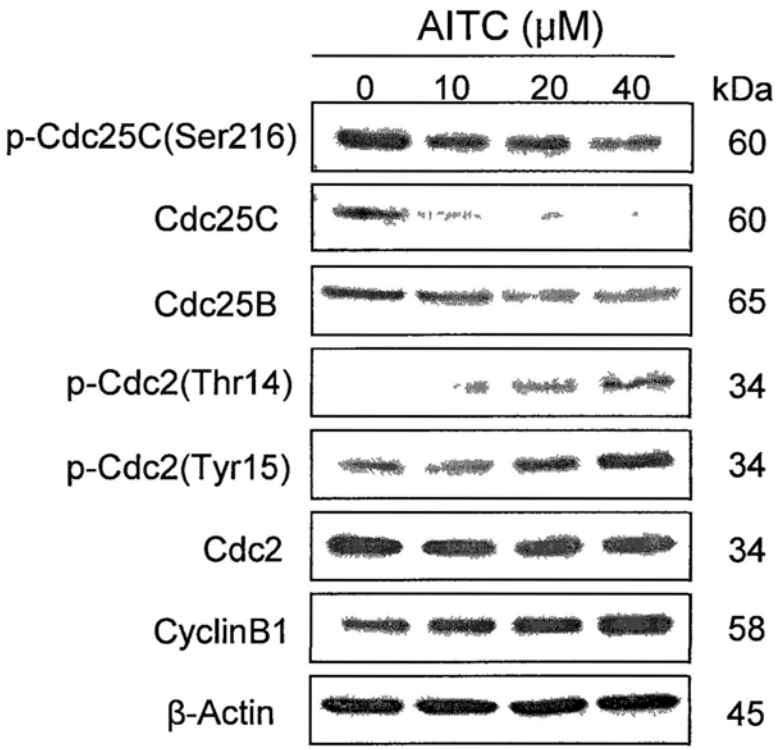

Figure 3.29 Effects of AITC treatments for 24 h on the expression of G_2 checkpoint proteins in SW620 cells as determined by western blot analysis. Data were representative of three independent experiments with similar results.

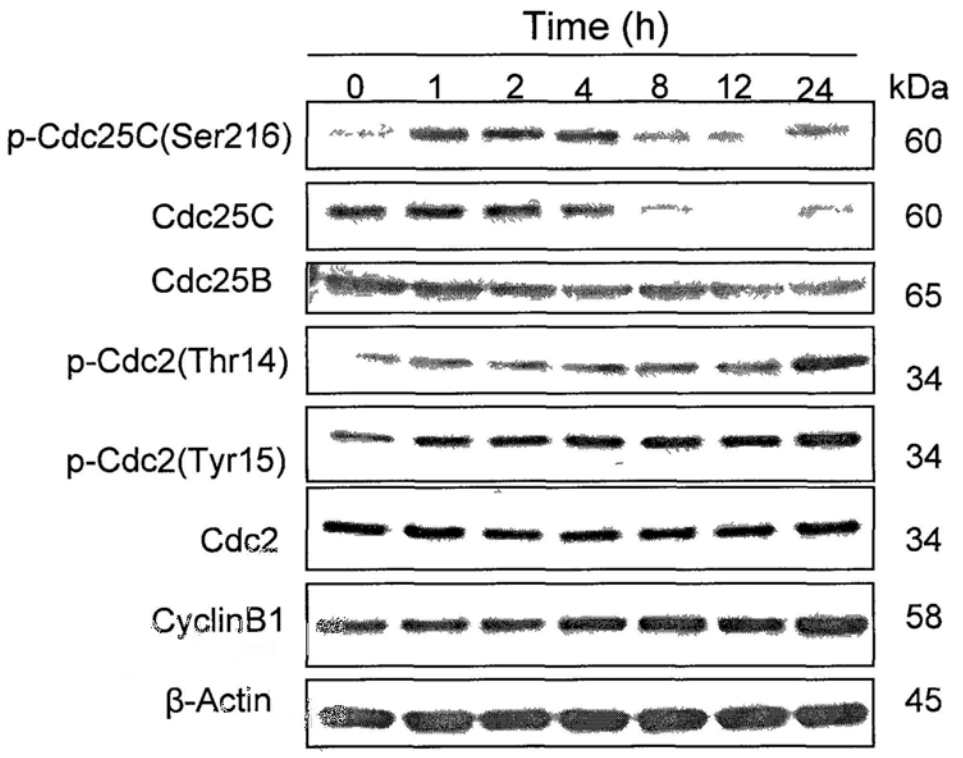

Figure 3.30 Time-dependent effects of AITC (20 μM) treatments on the expression of G_2 checkpoint proteins in SW620 cells as determined by western blot analysis. Data were representative of three independent experiments with similar results.

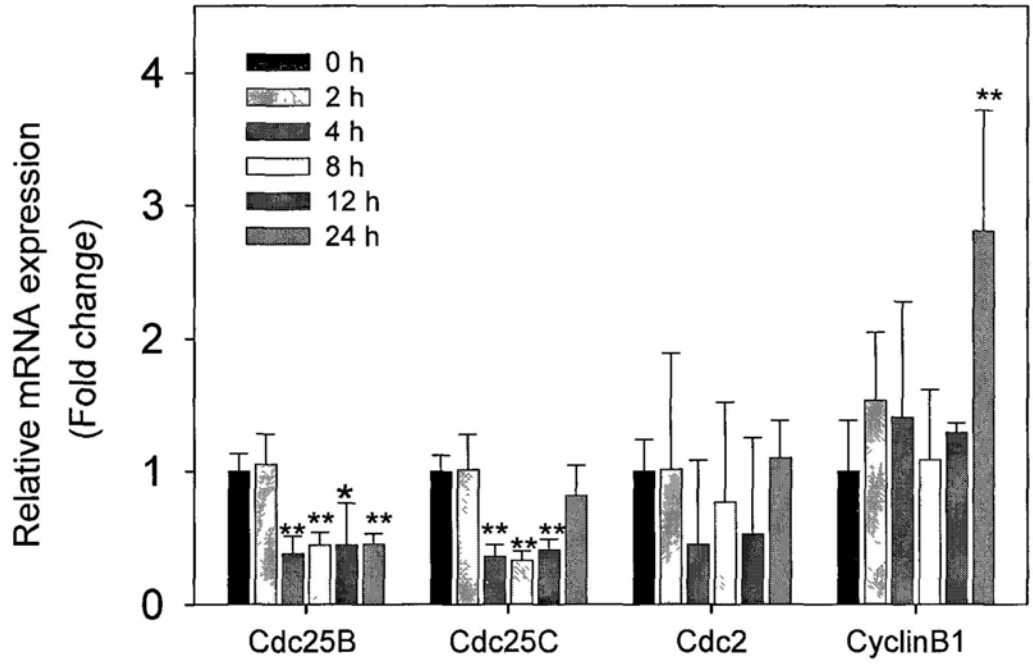

Figure 3.31 Time-dependent effects of AITC (20 μM) treatments on the relative mRNA expressions of G_2 checkpoint genes in SW620 cells as determined by real-time quantitative RT-PCR. The averages of each gene value was normalized by their corresponding GAPDH value and expressed as fold changes relative to time 0 (set to 1). Results were expressed as mean ± S.D.. Statistical differences between control and treatment groups were determined using two-tailed Student's *t*-test. The P-value of <0.05(*) or <0.01(**) was considered statistically significant. At least one independent experiment was performed with similar results.

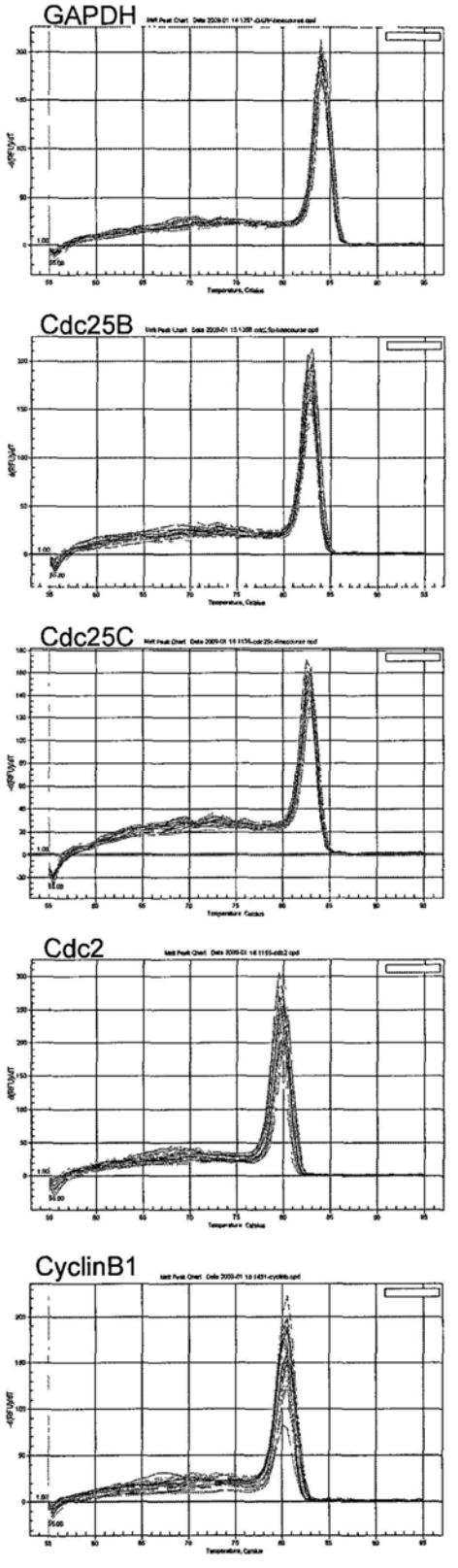

Figure 3.32 Representative dissociation curves obtained from the real-time quantitative RT-PCR assay.

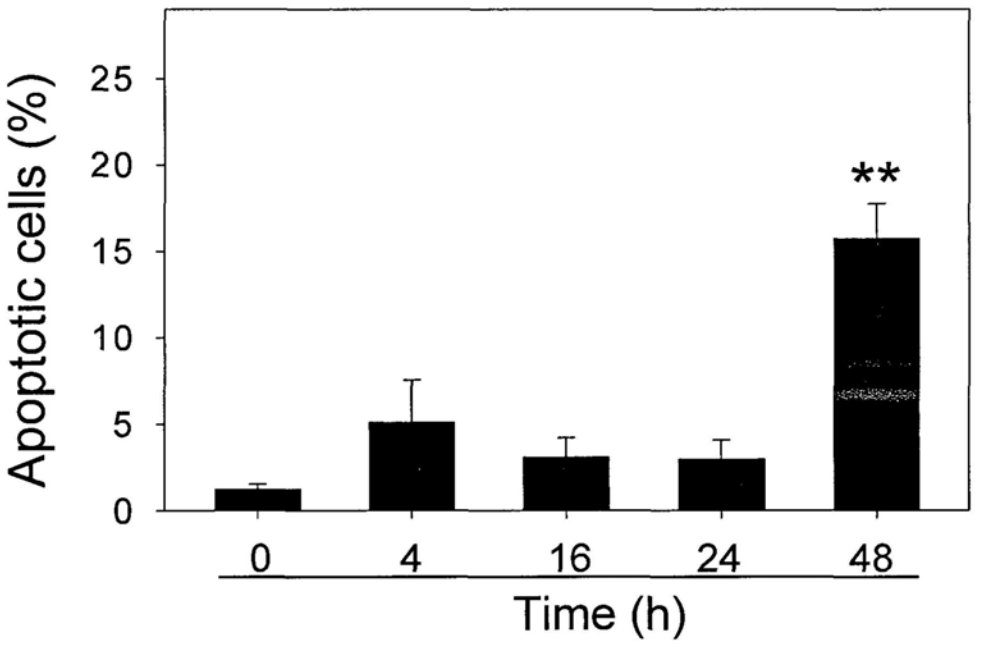

Figure 3.33 Time-dependent effects of AITC (20 μM) treatments on the induction of apoptosis in SW620 cells as determined by flow cytometric assay. Results were expressed as mean ± S.D. of three independent experiments. Statistical differences between control and treatment groups were determined using two-tailed Student's *t*-test. The P-value of <0.05(*) or <0.01(**) was considered statistically significant.

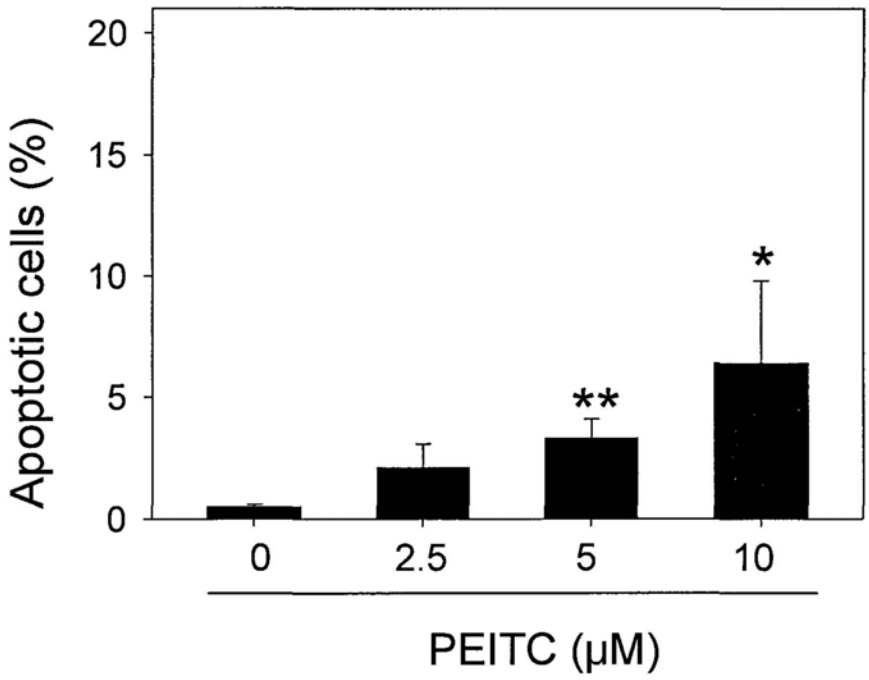

Figure 3.34 Effects of PEITC treatments on the induction of apoptosis in SW620 cells as determined by flow cytometric assay. Results were expressed as mean ± S.D. of three independent experiments. Statistical differences between control and treatment groups were determined using two-tailed Student's *t*-test. The P-value of <0.05(*) or <0.01(**) was considered statistically significant.

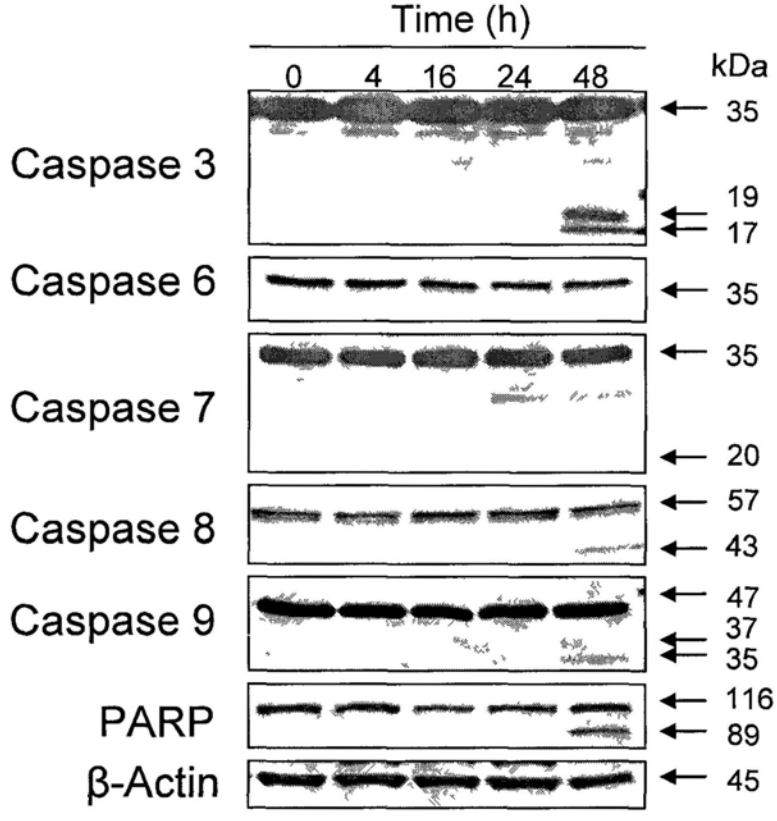

Figure 3.35 Time-dependent effects of AITC (20 μM) treatments on the expression of apoptotic proteins in SW620 cells as determined by western blot analysis. Data were representative of three independent experiments with similar results.

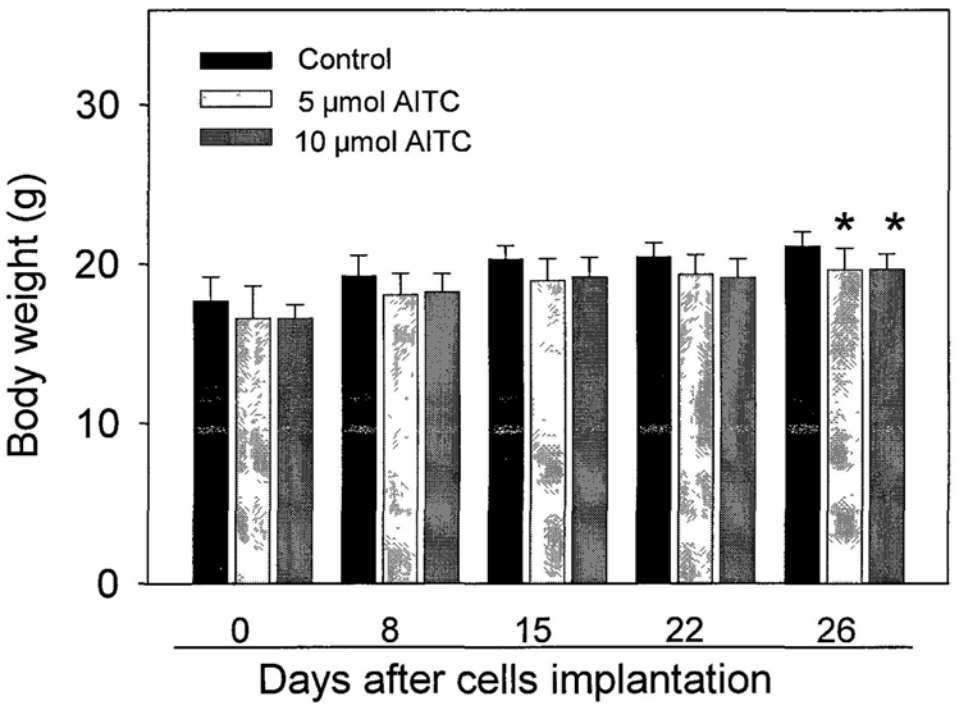

Figure 3.36 Body weights of control, 5 and 10 μmol AITC-treated mice during the course of experiment in the SW620 xenograft study. Results were expressed as mean ± S.D. (n = 8 mice/ group). Statistical differences between control and treatment groups were determined using two-tailed Student's *t*-test. The P-value of <0.05(*) or <0.01(**) was considered statistically significant.

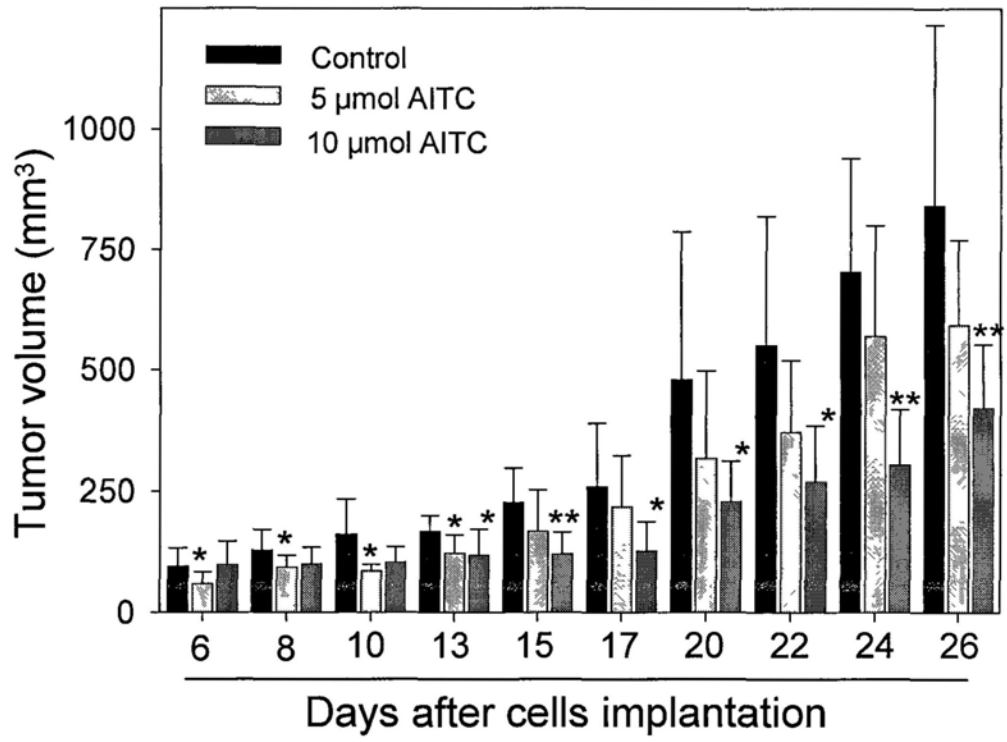

Figure 3.37 Tumor volumes of control, 5 and 10 μmol AITC-treated mice during the course of experiment in the SW620 xenograft study. Results were expressed as mean ± S.D. (n = 8 mice/ group). Statistical differences between control and treatment groups were determined using two-tailed Student's *t*-test. The P-value of <0.05(*) or <0.01(**) was considered statistically significant.

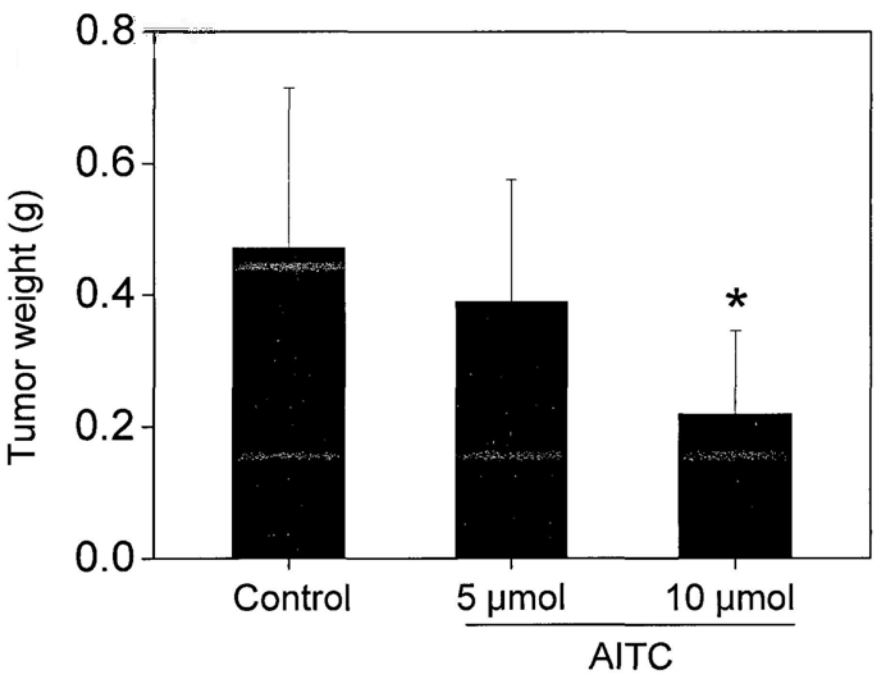

Figure 3.38 Wet tumor weights of control, 5 and 10 μmol AITC-treated mice obtained at the at of experiment in SW620 xenograft study. Results were expressed as mean ± S.D. (n = 8 mice/ group). Statistical differences between control and treatment groups were determined using two-tailed Student's *t*-test. The P-value of <0.05(*) or <0.01(**) was considered statistically significant.

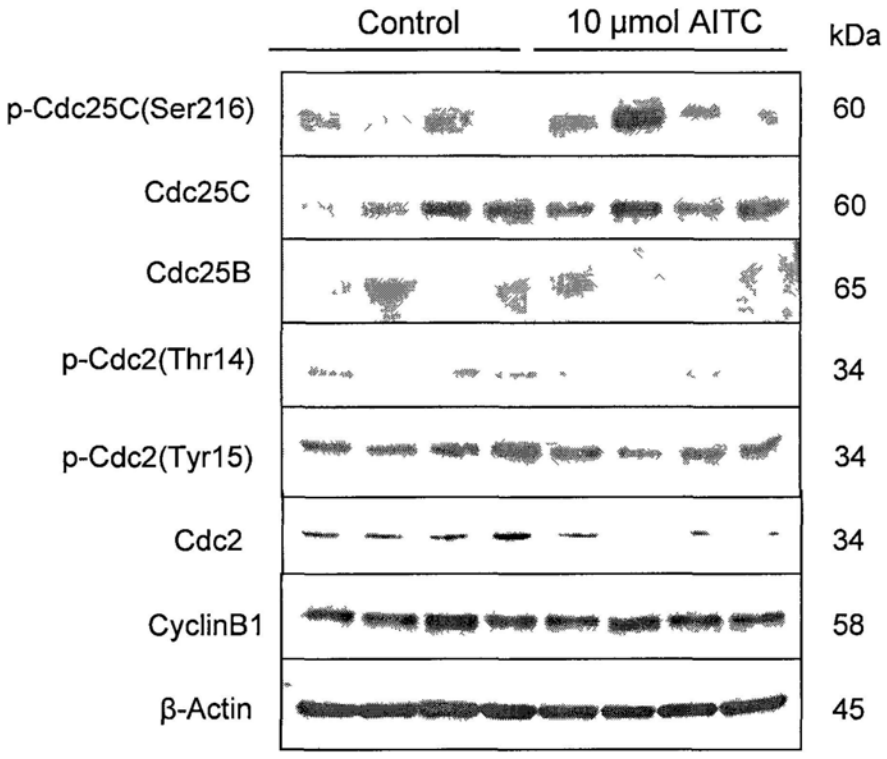

Figure 3.39 Effects of AITC treatment on the expression of G_2 checkpoint proteins in the mice as determined western blot analysis. Tumor lysates from four individual mice of both the control and 10 μmol AITC-treated groups were prepared separately. At least one independent western blot analysis was performed with similar results.

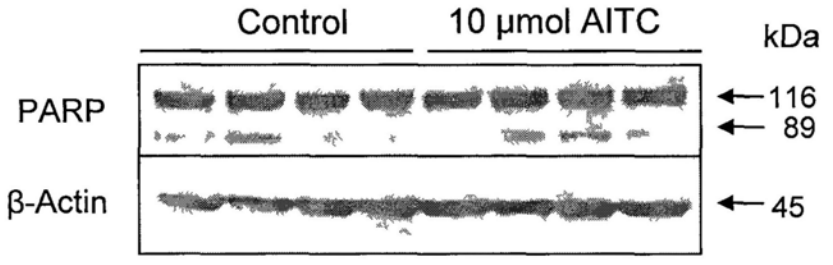

Figure 3.40 Effects of AITC treatment on the expression of apoptotic protein PARP in the mice as determined western blot analysis. Tumor lysates from four individual mice of both the control and 10 μmol AITC-treated groups were prepared separately. At least one independent western blot analysis was performed with similar results.

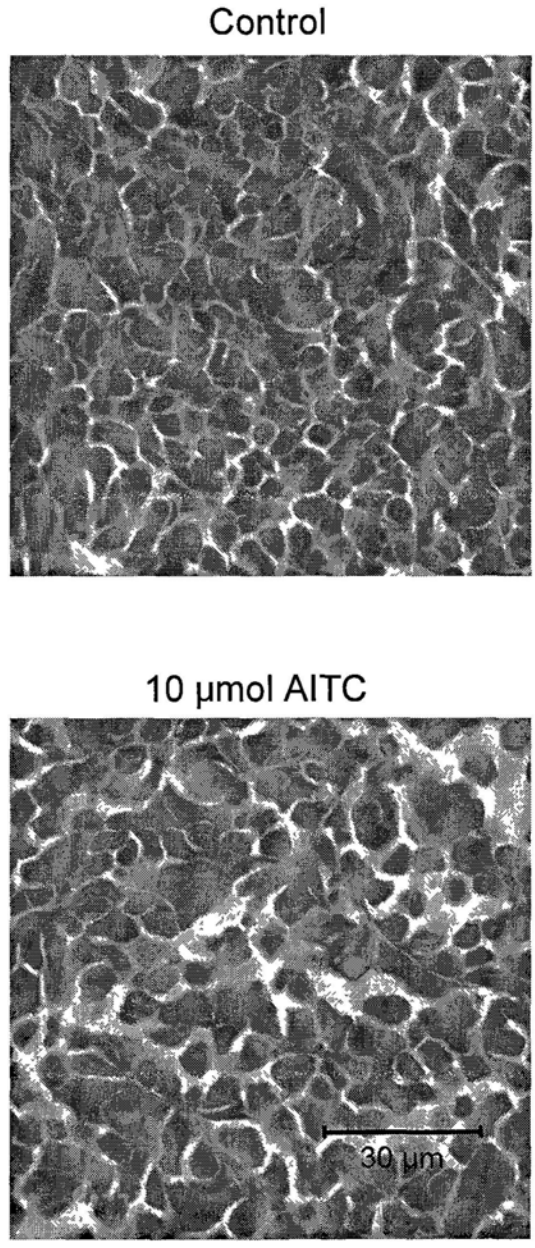

Figure 3.41 Representative photographs showed the tumor tissues from control and 10 µmol AITC-treated mice. Tumor tissues were collected for histological analysis. Fixed tissues embedded in paraffin wax were sectioned into 4 µm thick and stained with hematoxylin and eosin. The morphology of all the tumor tissues was observed under upright microscope.

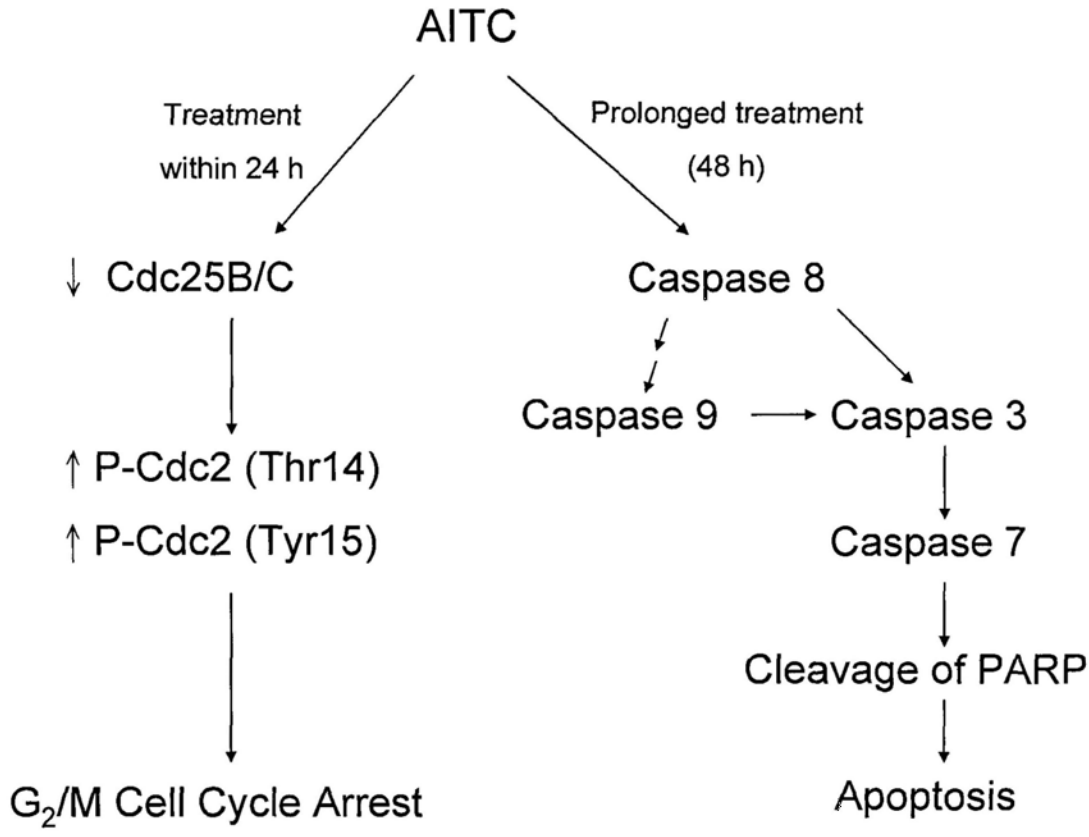

Figure 3.42 A schematic representation of the molecular mechanism of AITC induced cell cycle arrest and apoptosis in SW620 cells.

Table 3.1 Quantitative cell cycle analysis of SW620 cells after 24-h AITC treatments as determined by flow cytometric assay

	% of cells		
AITC treatments	**G_0 / G_1**	**S**	**G_2 / M**
Control	48.1 ± 1.3	37.3 ± 2.2	12.6 ± 2.8
10 μM	17.1 ± 10.2 **	15.2 ± 7.6 **	62.3 ± 19.2 *
20 μM	4.2 ± 5.6 **	9.3 ± 6.0 **	81.8 ± 6.7 **
40 μM	5.8 ± 2.6 **	29.6 ± 11.4	56.9 ± 11.0 **

Results were expressed as mean ± S.D. of three independent experiments. Statistical differences between control and treatment groups were determined using two-tailed Student's *t*-test. The P-value of <0.05(*) or <0.01(**) was considered statistically significant.

Table 3.2 Quantitative cell cycle analysis of SW620 cells after 20 μM AITC treatments for different incubation periods as determined by flow cytometric assay

	% of cells		
AITC treatments	**G_0 / G_1**	**S**	**G_2 / M**
0 h	65.6 ± 1.7	25.8 ± 1.3	7.4 ± 0.2
4 h	35.3 ± 2.1 **	44.6 ± 1.9 **	14.9 ± 1.6 **
16 h	2.1 ± 3.6 **	39.0 ± 6.4 **	55.8 ± 3.1 **
24 h	3.1 ± 2.1 **	6.8 ± 1.3 **	87.2 ± 0.4 **
48 h	30.4 ± 1.1 **	37.8 ± 2.4 **	24.4 ± 1.0 **

Results were expressed as mean ± S.D. of three independent experiments. Statistical differences between control and treatment groups were determined using two-tailed Student's *t*-test. The P-value of <0.05(*) or <0.01(**) was considered statistically significant.

Table 3.3 Quantitative cell cycle analysis of SW620 cells after 24-h PEITC treatments as determined by flow cytometric assay

	% of cells		
PEITC treatments	**G_0 / G_1**	**S**	**G_2 / M**
Control	50.3 ± 0.9	38.5 ± 1.6	9.7 ± 0.7
2.5 μM	43.3 ± 0.3 **	39.7 ± 1.4	14.9 ± 1.2 **
5 μM	37.0 ± 1.9 **	27.4 ± 0.7 **	32.4 ± 1.0 **
10 μM	18.2 ± 4.5 **	48.9 ± 0.6 **	26.4 ± 6.3 *

Results were expressed as mean ± S.D. of three independent experiments. Statistical differences between control and treatment groups were determined using two-tailed Student's *t*-test. The P-value of <0.05(*) or <0.01(**) was considered statistically significant.

Table 3.4 Relative mRNA expressions of G_2 checkpoint regulatory genes in SW620 cells after 20 μM AITC treatments for different incubation periods as determined by quantitative real-time PCR assay

	Relative mRNA expression (Fold change)			
AITC treatments	**Cdc25B**	**Cdc25C**	**Cdc2**	**CyclinB1**
0 h	1.00 ± 0.13	1.00 ± 0.12	1.00 ± 0.24	1.00 ± 0.39
2 h	1.05 ± 0.23	1.01 ± 0.27	1.02 ± 0.88	1.54 ± 0.51
4 h	0.38 ± 0.13**	0.36 ± 0.09**	0.45 ± 0.63	1.41 ± 0.87
8 h	0.44 ± 0.09**	0.33 ± 0.07**	0.77 ± 0.76	1.09 ± 0.53
12 h	0.45 ± 0.31*	0.41 ± 0.08**	0.53 ± 0.73	1.29 ± 0.07
24 h	0.45 ± 0.08 **	0.82 ± 0.23	1.10 ± 0.28	2.81 ± 0.91**

The averages of each gene value was normalized by their corresponding GAPDH value and expressed as fold changes relative to time 0 (set to 1). Results were expressed as mean ± S.D.. Statistical differences between control and treatment groups were determined using two-tailed Student's *t*-test. The P-value of <0.05(*) or <0.01(**) was considered statistically significant. At least one independent experiment was performed with similar results.

Table 3.5 Percentage of apoptotic cells after 20 μM AITC treatments in SW620 cells for different incubation periods as determined by flow cytometric assay

AITC treatments	% of apoptotic cells
0 h	1.2 ± 0.3
4 h	5.1 ± 2.4
16 h	3.1 ± 1.1
24 h	3.0 ± 1.1
48 h	15.7 ± 2.0 **

Results were expressed as mean ± S.D. of three independent experiments. Statistical differences between control and treatment groups were determined using two-tailed Student's *t*-test. The P-value of <0.05(*) or <0.01(**) was considered statistically significant.

Table 3.6 Percentage of apoptotic cells after 24-h PEITC treatments in SW620 cells as determined by flow cytometric assay

PEITC treatments	% of apoptotic cells
Control	0.5 ± 0.1
2.5 μM	2.1 ± 1.0
5 μM	$3.3 \pm 0.8^{**}$
10 μM	$6.4 \pm 3.4^{*}$

Results were expressed as mean $\pm$ S.D. of three independent experiments. Statistical differences between control and treatment groups were determined using two-tailed Student's *t*-test. The P-value of <0.05(*) or <0.01(**) was considered statistically significant.

Table 3.7 Body weights of control, 5 and 10 μmol AITC-treated mice during the course of experiment in the SW620 xenograft study

	Body weights (g)				
Treatments	**Day 1**	**Day 8**	**Day 15**	**Day 22**	**Day 26**
Control	17.7 ± 1.5	19.3 ± 1.3	20.3 ± 0.9	20.5 ± 0.9	21.2 ± 0.9
5 μmol	16.6 ± 0.8	18.3 ± 1.1	19.2 ± 1.2	19.2 ± 1.2	19.7 ± 1.0 *
10 μmol	16.6 ± 2.0	18.1 ± 1.3	19.0 ± 1.4	19.4 ± 1.2	19.7 ± 1.3 *

Results were expressed as mean ± S.D. (n = 8 mice/ group). Statistical differences between control and treatment groups were determined using two-tailed Student's *t*-test. Difference with P <0.05(*) or P <0.01(**) was considered statistically significant.

Table 3.8 Tumor volumes of control, 5 and 10 μmol AITC-treated mice during the course of experiment in the SW620 xenograft study

Treatments	Tumor weights (g)									
	Day 6	**Day 8**	**Day 10**	**Day 13**	**Day 15**	**Day 17**	**Day 20**	**Day 22**	**Day 24**	**Day 26**
Control	96.5 ± 36.8	130.4 ± 40.8	161.9 ± 72.3	168.2 ± 31.8	227.7 ± 68.9	260.6 ± 29.0	479.5 ± 308.1	552.0 ± 268.0	705.0 ± 243.7	843.2 ± 371.9
5 μmol	59.3 ± 24.4*	94.3 ± 23.8*	86.2 ± 13.2*	122.5 ± 37.9*	168.4 ± 84.9	218.6 ± 104.5	318.1 ± 179.9	371.6 ± 147.9	570.6 ± 230.6	593.5 ± 177.2
10 μmol	98.9 ± 48.8	101.1 ± 33.5	104.3 ± 32.0	118.8 ± 53.1*	121.4 ± 44.9**	127.0 ± 60.6*	229.5 ± 82.7*	269.4 ± 115.1*	304.4 ± 113.7**	420.7 ± 131.7*

Results were expressed as mean ± S.D. (n = 8 mice/ group). Statistical differences between control and treatment groups were determined using two-tailed Student's *t*-test. Difference with P <0.05(*) or P <0.01(**) was considered statistically significant.

Table 3.9 Wet tumor weights of control, 5 and 10 μmol AITC-treated mice obtained at the at of experiment in SW620 xenograft study

Treatments	Wet tumor weights (g)
Control	0.47 ± 0.24
5 μmol	0.39 ± 0.19
10 μmol	0.22 ± 0.13 *

Results were expressed as mean ± S.D. (n = 8 mice/ group). Statistical differences between control and treatment groups were determined using two-tailed Student's *t*-test. Difference with P <0.05(*) or P <0.01(**) was considered statistically significant.

Chapter Four

Discussion

Cancer is a leading cause of death in human populations over the world. It may affect people at all ages. Approximately 10 million people are diagnosed with cancer and more than 6 million people die of the disease every year (Stewart and Kleihues, 2003). In additional to the traditional therapies, it is now hypothesized that various naturally occurring phytochemicals from edible plants possess different antitumor activities (Baer-Dubowska *et al.*, 2006a-c; He, 2008; Ramos, 2007; Ramos 2008; Steinmetz and Potter, 1996; Surh, 2003). As a result, studies on these phytochemicals become a new direction in the anticancer drugs development. Now, ITCs attract more and more scientists' attention because of their potent antitumor activities. Recent reports showed that several ITCs could exert significant growth inhibitory effects on various human cancer cells (Gamet-Payrastre *et al.*, 2000; Hu *et al.*, 2003; Kuang *et al.*, 2004; Pappa *et al.*, 2007; Rose *et al.*, 2003; Satyan *et al.*, 2006; Singh *et al.*, 2004a; Singh *et al.*, 2004b; Tang *et al.*, 2004; Xiao *et al.*, 2003; Xiao *et al.*, 2004). Despite these findings, the sequence of molecular events leading to such effects is not yet defined. In this project, the growth inhibitory effect of sinigrin, one of the major naturally occurring glucosinolates on various human colorectal adenocarcinoma cells was studied. In fact, sinigrin has a high relative prevalence among the cruciferous vegetables (Fahey *et al.*, 2001; Fenwick *et al.*, 1983; Moreno *et al.*, 2006; Song *et al.*, 2005; Verkerk *et al.*, 2009). In Brussels sprouts, especially, the content of sinigrin can be up to 1.55 μmol/ g fresh weight (Table 1.2). On the other hand, another commonly found dietary glucosinolate, gluconasturtiin, is more commonly found in watercress (Fenwick *et al.*, 1983). Besides investigating the

effect of sinigrin, the growth inhibitory effects of its related digested products on different human colorectal adenocarinoma cells were further studied. Various *in vitro* assays using human cancer cell models and *in vivo* assay using animal model were employed to determine such effects.

4.1 Cytotoxic effects of sinigrin and the co-incubation of sinigrin with myrosinase on colorectal adenocarinoma cells

As shown in Figures 3.1 and 3.2, it was clear that sinigrin alone did not affect the survival of colorectal adenocarinoma cells, Caco-2 and SW620, even up to the concentration of 500 μM. Some other *in vitro* studies also indicated that native glucosinolates, such as gluconasturtiin, glucoraphanin and glucotropaeolin, did not exert any effect on the growth and survival in certain types of cancer cells (Fimognari *et al.*, 2002; Leoni *et al.*, 1997; Pappa *et al.*, 2006). Since sinigrin alone did not affect the survival of the tested cancer cells, a co-incubation assay of sinigrin with myrosinase was followed. Before performing the co-treatment, no alerting effect of myrosinase on the cells was counter-proved in our study (Figures 3.3 and 3.4). Similarly, myrosinase alone showed no effect on the cells as reported by others (Fimognari *et al.*, 2002; Leoni *et al.*, 1997; Pappa *et al.*, 2006). In this co-incubation assay, co-treatment of sinigrin with myrosinase demonstrated a clear dose-dependent effect on the survival of both SW620 and Caco-2 cells (Figures 3.5 - 3.8). This observation agreed with other studies on various cancer cells, which showed a similar inhibitory effect upon treatment (Fimognari *et al.*, 2002; Leoni *et al.*, 1997; Pappa *et al.*, 2006). Taken together, all these results suggested that the newly generated products possessed potent antitumor activities, in which the original precursors did not posses.

4.2 HPLC determination of sinigrin after *in vitro* enzyme digestion

In order to elucidate the digestion profile of sinigrin, an *in vitro* digestion of sinigrin by myrosinase was simulated. Only after 24 h of incubation, no sinigrin could be detected by the HPLC analysis (Figure 3.10). Therefore, all sinigrin should be broken down by myrosinase effectively. By considering the results from the co-incubation assay and availabilities of the digested products, it was expected that one or more of these digested product(s) from sinigrin should be the active components responsible for the inhibitory effect exerted on the tested colorectal adenocarinoma cells.

4.3 Cytotoxic and antiproliferative effects of ITCs on colorectal adenocarinoma cells

Among the breakdown products of glucosinolates, it is generally believed that ITCs are the major breakdown products under neutral pH (Cheung *et al.*, 2004; Elfoul *et al.*, 2001; Fimogonari *et al.*, 2002; Krul *et al.*, 2002). At the same time, recent studies showed that ITCs can selectively inhibit the growth of different human cancer cells (Gamet-Payrastre *et al.*, 2000; Hu *et al.*, 2003; Kuang *et al.*, 2004; Pappa *et al.*, 2007; Rose *et al.*, 2003; Satyan *et al.*, 2006; Singh *et al.*, 2004a; Singh *et al.*, 2004b; Tang *et al.*, 2004; Xiao *et al.*, 2003; Xiao *et al.*, 2004). However, little was known about their actual antitumor mechanisms, further investigations were required to fully elucidate the cellular signaling pathways involved. Therefore, AITC, the corresponding ITC of sinigrin, was chosen for study in this project. In addition, another commonly founded ITC, PEITC was also employed as a reference sample.

According to MTT assay, both AITC and PEITC exerted significant cytotoxic effects on different human colorectal adenocarcinoma cells, including Caco-2,

COLO 201 and SW620, in a dose- and time-dependent manner (Figures 3.11 - 3.14). Based on the sensitivity of these cells, the most vulnerable SW620 cells were chosen for mechanistic studies. Besides MTT assay, significant growth inhibitory effects of both AITC and PEITC on SW620 cells were further confirmed by BrdU assay (Figures 3.16 - 3.18). In fact, SW620 cells are categorized as stage C according to the Dukes' classification. It reflected a lymph-node metastasis had been occurred. In addition, a mutation of gene *p53* was also observed in SW620 cells. Usually, human tumor cells processes a *p53* mutation would result in a higher resistance towards chemotherapeutic treatments (Fisher, 2001). Therefore, it would be a meaningful finding if there is a new chemopreventive agent which possesses the ability to tackle this type of tumor cells. Recent reports have revealed the inhibitory effects of ITCs on different cancer cells with comparable dosages as we have employed in our study. The effective ITCs concentrations ranged form 5 - 20 μM (Gamet-Payrastre *et al.*, 2000; Hu *et al.*, 2003; Kuang *et al.*, 2004; Pappa *et al.*, 2007; Rose *et al.*, 2003; Satyan *et al.*, 2006; Singh *et al.*, 2004a; Singh *et al.*, 2004b; Tang *et al.*, 2004; Xiao *et al.*, 2003; Xiao *et al.*, 2004). Moreover, it was found that PEITC possessed a stronger inhibitory effect over the AITC in our study (Figures 3.11 - 3.14, 3.16 -3.18). Recent study suggested that the difference in anti-proliferative activities of ITCs on other types of cancer cells, including blood, breast, liver and skin, could be ITC-specific, but not cell-specific (Zhang *et al.*, 2003).

4.4 Cytotoxic effects of ITCs on normal skin fibroblast

Besides studying the growth inhibitory effects of ITCs on different cancer cells, their effects on normal cells were worth to be investigated. According to MTT assay, the survival of human skin fibroblast Hs68 was not affected by the 24 and 72-h periods of AITC treatment (up to 150 μM) (Figures 3.19 and 3.20). Similarly, low

cytotoxic effect of AITC was also reported in the detransformed non-tumorigenic colorectal cells (Musk and Johnson, 1993). At the same time, another commonly found ITC, SFN, also exerted minimal effects on human bronchical and prostate epithelial cells (Choi and Singh, 2005). On the other hand, it was found that the survival of skin fibroblast Hs68 was greatly affected by the PEITC treatment in a dose- and time-dependent manner (Figures 3.21 and 3.22). Although PETIC possessed a stronger growth inhibitory effect on the tested cancer cells in comparison to AITC (Figures 3.11 - 3.14), but it also showed a much stronger cytotoxic effect on normal cells at the same time (Figures 3.19 - 3.22). Therefore, it may suggest that the growth inhibitory effect of PEITC is not cell specific. Further investigations are required to study the effect of PEITC on other normal cell types.

4.5 Effects of ITCs on cell cycle progression and related proteins and genes expressions in colorectal adenocarinoma cells

After studying the growth inhibitory effects of ITCs on different cancer cells, a flow cytometric analysis using PI staining was employed to determine their effects on cell cycle distribution. As shown in the flow cytometric analysis, AITC-induced cell growth inhibition in SW620 cells was mainly caused by the arrested cell cycle progression at G_2/M phase (Figures 3.23 - 3.24). At the same time, treatment with PEITC also induced a similar blockage at G_2 transition in the cells (Figure 3.25). Our observations agreed with several studies illustrating similar ITCs-induced G_2/M arrest in other cancer cell types (Gamet-Payrastre *et al.*, 2000; Pappa *et al.*, 2007; Singh *et al.*, 2004b; Tang *et al.*, 2004; Xiao *et al.*, 2003; Xiao *et al.*, 2004).

In order to gain insights into the mechanisms, expression of checkpoint regulatory proteins in SW620 cells after AITC treatments were subjected to western

blot analysis. In the regulation of cell cycle, activation of Cdc2/CyclinB protein complex (also known as mitotic promoting factor) is required to drive cells to proceed into mitosis (Molinari, 2000; Shackelford *et al.*, 2000; Strausfeld *et al.*, 1991). Originally, the catalytic subunit Cdc2 is maintained in an inactive state by phosphorylation on Thr14 and Tyr15 by the actions of kinases Wee1 and Myt1. While at the G_2/M boundary, duel-specificity phosphatases Cdc25B and Cdc25C can remove the Thr14 and Tyr15 phosphorlaytions on Cdc2, and allows the cells to progress into mitosis. The importance of this passage could be further illustrated by recent studies (Guo *et al.*, 2004; Kudo *et al.*, 1997). An overexpression of Cdc25B was observed in human pancreatic and gastric cancer cells, when compared to their respective normal tissues (Guo *et al.*, 2004; Kudo *et al.*, 1997). In our study, it was found that the AITC-induced G_2/M cell cycle arrest was associated with the downregulation of both phosphatases Cdc25B and Cdc25C (Figures 3.29 and 3.30), which matched consistently with recent reports (Singh *et al.*, 2004b; Tang *et al.*, 2004; Xiao *et al.*, 2003; Xiao *et al.*, 2004). In addition, it was found that two Cdc25B inhibitors could inhibit the growth of pancreatic cancer cells in a dose dependent manner (Guo *et al.*, 2004). As majority of the related studies were focused on the post-translational level of regulation, our study tried to extend the investigation further into the transcriptional level. A significant time-dependent downregulation of both Cdc25B and Cdc25C mRNA expression was observed in AITC-treated cells (Figure 3.31). It was resembled to current studies revealing the low Cdc25B mRNA level in normal pancreatic tissue (Guo *et al.*, 2004), and downregulated Cdc25C mRNA level in G_2/M arrested cells (Nigam *et al.*, 2009; Prasad *et al.*, 2008). This consistency indicated the importance of transcriptional control in the AITC-induced cell cycle arrest. Furthermore, without the catalytic action of both phosphatases, an accumulation of inhibitory phosphorylation on Thr14 and Tyr15 of Cdc2 was

resulted (Figures 3.29 and 3.30), which blocked the G_2/M passage. Interestingly, upregulation of CyclinB1 at both mRNA and protein levels were observed (Figures 3.29 - 3.31). An upregulated CyclinB1 protein was also found in other G_2/M arrested cells. Such increment might be due to the increased proportion of cells at G_2/M phase in the arresting cells (Gamet-Payrastre *et al.*, 2000; Rose *et al.*, 2003).

4.6 Effects of ITCs on induction of apoptosis and related proteins expressions in colorectal adenocarinoma cells

Besides inducing G_2/M arrest, AITC could also induce apoptosis in the treated SW620 cells upon prolonged exposure (Figure 3.33). This finding agrees with studies employing other human colon cancer cells. A dynamic shift from the G_2/M arrest into subG1 phase was detected in colorectal cancer cells upon increased incubation time with SFN (Gamet-Payrastre *et al.*, 2000; Pappa *et al.*, 2007). Moreover, induction of apoptosis by PEITC (Figure 3.34) and other ITCs in different human cancer cells were observed, with an effective concentration ranged form 5 to 25 μM (Gamet-Payrastre *et al.*, 2000; Hu *et al.*, 2003; Kuang *et al.*, 2004; Rose *et al.*, 2003; Satyan *et al.*, 2006; Singh *et al.*, 2004a). To better determine which type of apoptotic pathway was involved, the expression of key apoptotic proteins was examined by western blot analysis. As shown in Figure 3.35, AITC-induced apoptosis was associated with an activation of caspase cascade. It triggered the activation of initiator caspases (caspase-8 and -9), and effector caspases (caspase-3 and -7), leading to the cleavage of PARP. Our findings agreed with other studies showing similar caspase-mediated apoptosis in ITCs-treated cells (Hu *et al.*, 2003; Satyan *et al.*, 2006; Singh *et al.*, 2004a, Tang and Zhang, 2004; Wu *et al.*, 2005). In additional to the involvement of caspases, other apoptotic biomakers induced by ITCs, such as the shift of mitochondrial membrane and the modulation of Bcl-2

family proteins, were also found (Gamet-Payrastre *et al.*, 2000; Satyan *et al.*, 2006; Singh *et al.*, 2004a). Subsequently, the release of other apoptogenic factors was followed (Choi *et al.*, 2005; Jakubikova *et al.*, 2005). Thus, our results, together with others, suggest that caspases may play an important role in ITCs-induced apoptotic cell death. Further investigations are required in order to get a better understanding on the ITCs-related apoptotic mechanisms.

4.7 Effects of AITC on the growth of xenograft *in vivo*

Apart from *in vitro* studies, nude mice xenograft assay was also employed to examine the *in vivo* effect of AITC. First of all, body weights of all mice were measured periodically in order to assess their health conditions. Although both groups of AITC-treated mice were marginally weighed less when compared with control, but these discrepancies were actually less than 7% (Figure 3.36). Similar reduction in body weight was also observed in the mice fed with PEITC-N-acetyl cysteine diet (Chiao *et al.*, 2004). Nevertheless, all the mice in our experiment were appeared healthy and did not show any impaired movements. As shown in Figure 3.37, AITC-treatment (10 μmol, 3 times/week) could effectively retard the growth of SW620 mice xenograft. Significant suppression effects of ITCs have also been shown in PC-3 xenograft (Singh *et al.*, 2004; Srivastava *et al.*, 2003). Moreover, tumor tissues of the mice were further subjected to western blot analysis. Downregulation of Cdc2 protein was found in the tumor tissues of the AITC-treated mice (Figure 3.39). It suggests that the AITC-mediated growth suppression in the xenografts may be partially associated with the impaired cell cycle progression at G_2/M transition. On the other hand, another AITC-treatment (5 μmol, 3 times/week) in our present study was effective only at early phase of the experiment (Figure 3.37). Besides concerning the AITC dosage employed, this might be a matter of frequency.

Recent studies showed that SFN supplemented diet (443 mg/ kg diet) for 10 weeks could significant suppress tumor formation in the *Apc*^{min} mice (Myazk *et al.*, 2006). Further investigations are required to explore the possibility to enhance the effectiveness of ITCs through adjusting the application frequency and the duration of treatment. By summarizing all together, the understanding of the *in vitro* and *vivo* antitumor activities of AITC in colorectal adeonocarcinoma cells would be beneficial in the design and development of novel chemopreventive agent in the future.

Chapter Five

Conclusion

Cruciferous vegetables are important parts of our diet. They provide us with energy, micronutrients, dietary fiber and even biologically active compounds. According to various epidemiological and animal studies, these suggested that the glucosinolates and related breakdown products in cruciferous vegetables possess potent antitumor activities. In this project, the growth inhibitory effects of sinigrin and its main digested product on various human colorectal adenocarcinoma cells were studied. Various *in vitro* cell model and *in vivo* animal assays were employed to determine such effects.

As determined by MTT assay, sinigrin alone did not affect the survival of colorectal adenocarinoma cells, Caco-2 and SW620. While in the following co-incubation assay, the co-treatment of sinigrin with myrosinase exerted dose-dependent cytotoxic effects on both SW620 and Caco-2 cells. Furthermore, in the HPLC determination of sinigrin after *in vitro* enzyme digestion, no sinigrin could be detected after 24 h of incubation. By considering the availabilities and the potency of the compounds, the corresponding ITC of sinigrin, AITC, was chosen for further investigation. In addition, another commonly founded ITC, PEITC, was employed as a reference sample. According to the MTT assay, both AITC and PEITC exerted significant dose- and time-dependent cytotoxic effects on different human colorectal adenocarcinoma cells, including Caco-2, COLO 201 and SW620. Based on the sensitivity of these cells, the most vulnerable SW620 cells were chosen for mechanistic studies. Besides MTT assay, significant growth inhibitory effects of both

AITC and PEITC on SW620 cells were further confirmed by BrdU assay. The IC_{50} values were determined to be 30.2 and 9.21 μM after 24-h AITC and PEITC treatments, respectively. In general, PEITC showed a stronger inhibitory effect on the cancer cells when compared with AITC. At the same time, the effects of AITC and PEITC on normal cells were also investigated. It was found that the survival of human skin fibroblast Hs68 cells was not affected by the treatments of AITC, whereas the survival of the cells was dose- and time-dependently affected by PEITC-treatments. It may suggest that the growth inhibitory effect of PEITC is not cell specific.

In order to gain insights into the underlying mechanisms, several methods including, flow cytometric, western blot and quantitative real-time PCR analyses were employed. From the flow cytometric analysis, it was found that the AITC-induced cell growth inhibition was mainly caused by G_2/M arrest. At the same time, this blockage at the G_2/M transition was accompanied by regulatory proteins modifications. Results of western blot analysis illustrated that AITC treatments led to a markedly reduced in both pivotal phosphatases Cdc25B and Cdc25C dose- and time-dependently. As majority of the related studies were focused on the post-translational level of regulation, our study tried to extend the investigation further into the transcriptional level. A significant time-dependent downregulation of both Cdc25B and Cdc25C mRNA expression was observed in the AITC-treated cells. Without the catalytic actions of these phosphatases, an accumulation of inhibitory phosphorylation of Cdc2 on Thr14 and Tyr15 was subsequently resulted. Furthermore, an AITC induced apoptosis after prolonged exposure was observed. After 48-h treatment of AITC, a clear caspase-mediated apoptosis was resulted. It was evidenced by the activation of initiator caspases (-8 and -9), effector caspases (-3

and -7) and cleavage of PARP. A schematic representation of the molecular mechanism of AITC induced cell cycle arrest and apoptosis in SW620 cells was shown in Figure 3.42. Besides *in vitro* studies, the antitumor activity of AITC was further illustrated by the nude mice xenograft experiment. Treatment with 10 μmol AITC could effectively suppress the growth of SW620 xenografts *in vivo.* At the end of the experiment, downregulation of Cdc2 in tumor tissues of AITC-treated mice was observed. This implies that the retarded growth of tumor induced by AITC may be partially associated with the G_2/M arrest in the tumor cells.

In summary, our study found that the AITC possessed significant antiproliferative activities on the human colorectal adenocarcinoma SW620 cells under both *in vitro* and *in vivo* conditions. In order to have a better understanding on the potential of AITC to work as a novel chemopreventive agent, some future works are proposed as follows:

1) Based on the mechanistic study, it was found that the AITC-induced cell growth inhibition was mainly caused by G_2/M arrest, which was accompanied by several regulatory proteins modifications. Specific *si*RNA transfection (e.g. on Chk1 and Chk2) may be employed to further confirm the importance of G_2/M blockage in the AITC-treated cells.

2) Recently, scientists are getting interested in the study on the combined effects of different chemopreventive agents. The aim is to enhance their effectiveness and minimize toxicity at the same time. Enhancement studies are required to explore the possibility of combining AITC with other agents.

References

Agudo, A., Ibáñez, R., Amiano, P., Ardanaz, E., Barricarte, A., Berenguer, A., Dolores Chirlaque, M., Dorronsoro, M., Jakszyn, P., Larrañaga, N., Martinez, C., Navarro, C., Pera, G., Quirós, J.R., Sanchéz, M.J., Tormo, M.J. and González, C.A. (2008). Consumption of cruciferous vegetables and glucosinolates in a Spanish adult population. *European Journal of Clinical Nutrition, 62, 324-331.*

Alabaster, O., Tang, Z. and Shivapurkar, N. (1996). Dietary fiber and the chemopreventive modelation of colon carcinogenesis. *Mutation Research. Fundamental and Molecular Mechanisms of Mutagenesis, 350,* 185-197.

Ames, B. and Wakimoto, P. (2002). Are vitamin and mineral deficiencies a major cancer risk. *Nature Reviews. Cancer, 2,* 694-704.

Asakage, M., Tsuno, N. H., Kitayama, J., Tsuchiya, T., Yoneyama, S., Yamada, J., Okaji, Y., Kaisaka, S., Osada, T., Takahashi, K. and Nagawa, H. (2006). Sulforaphane induces inhibition of human umbilical vein endothelial cells proliferation by apoptosis. *Angiogenesis, 9,* 83-91.

Baer-Dubowska, W., Bartoszek, A. and Malejka-Giganti, D. (2006a). Chemopreventive phenolic compounds in common species. In Surh, Y. J. (Ed.), *Carcinogenic and anticarcinogenic food components* (pp. 197-218). Boca Raton, FL: Taylor and Francis Group.

Baer-Dubowska, W., Bartoszek, A. and Malejka-Giganti, D. (2006b). Cancer prevention by tea and tea constituents. In Landau, J. M., Lambert, J. D., Lee, M. J., and Yang, C. S. (Ed.), *Carcinogenic and anticarcinogenic food components* (pp. 219-238). Boca Raton, FL: Taylor and Francis Group.

Baer-Dubowska, W., Bartoszek, A. and Malejka-Giganti, D. (2006c). Cancer chemoprevention by wine polyphenols and resveratrol. In Pezzuto, J. M., Kondratyuk, T. P., and Shalaev, E. (Ed.), *Carcinogenic and anticarcinogenic food components* (pp. 239-258). Boca Raton, FL: Taylor and Francis Group.

Berg, D. T. (2001a). Epidemiology and risk of cancer of the colon or rectum. In Berg, D. T. (Ed.), *Contemporary issues in colorectal cancer: a nursing perspective* (pp. 1-16). Sudbury, Mass.: Jones and Bartlett Publishers.

Berg, D. T. (2001b). Prevention strategies and the diet connection. In Christiansen, K. (Ed.), *Contemporary issues in colorectal cancer: a nursing perspective* (pp. 35-52). Sudbury, Mass.: Jones and Bartlett Publishers.

Berg, D. T. (2001c). Cellular characteristics, pathophysiology, and disease manifestations of colorectal cancer. In Griffin-Sobel, J. P. (Ed.), *Contemporary issues in colorectal cancer: a nursing perspective* (pp. 53-64). Sudbury, Mass.: Jones and Bartlett Publishers.

Berk, T. and Macrae, F. (2006a). Colorectal cancer can run in the family. In Dunlop, M. G. (Ed.), *What is inherited colorectal cancer?* (pp. 1-9). Wantirna, Vic.: Medcom Ltd.

Berk, T. and Macrae, F. (2006b). Colorectal cancer can run in the family. In Burt, R.W. (Ed.), *Why did this happened to me?* (pp. 22-35). Wantirna, Vic.: Medcom Ltd.

Bingham, S. and Riboli, E. (2004). Diet and cancer - the European prospective investigation into cancer and nutrition. *Nature Reviews. Cancer*, *4*, 208-216.

Bones, A. M. and Rossiter, J. T. (2006). The enzymatic and chemically induced decomposition of glucosinolates. *Phytochemistry*, *37*, 1053-1067.

Borek, C. Antioxidants and the prevention of hormonally regulated cancer. *The Journal of Men's Health and Gender*, *2*, 346-352.

Boysen, G., Kenney, P. M. J., Upadhyaya, P., Wang, M. and Hecht, S. S. (2003). Effects of benzyl isothiocyanate and 2-phenethyl isothiocyanate on benzo[a]pyrene and 4-(methylnitrosamino)-1-(3-pyridyl)-1-butanone metabolism in F-344 rats. *Carcinogenesis*, *24*, 517-525.

Brüsewitz, G., Cameron, B. D., Chasseaud, L. F., Görler, K., Hawkins, D. R., Koch, H. and Mennicke, W. H. (1977). The metabolism of benzyl isothiocyanate and its cysteine conjugate. *The Biochemical journal*, *162,* 99-107.

Callaway, E. C., Zhang, Y., Chew, W. and Chow, H. H. S. (2004). Cellular accumulation of dietary anticarcinogenic isothiocyanates is followed by transporter-mediated export as dithiocarbamates. *Cancer Letters*, *204*, 23-31.

Cheung, D. T., Hashimoto, K. and Uda, Y. (2004). In vitro digestion of sinigrin and glucotropaeolin by single strains of *Bifidobacterium* and identification of the digestive products. *Food and Chemical Toxicology*, *42*, 351-357.

Chiao, J. W., Wu. H., Ramaswamy, G., Conaway, C. C., Chung, F. L., Wang, L. and Liu, D. (2004). Ingestion of an isothiocyanate metabolite from cruciferous vegetables inhibits growth of human prostate cancer cell xenografts by apoptosis and cell cycle arrest. *Carcinogenesis*, *25*, 1403-1408.

Choi, S. and Singh, S. V. (2005). Bax and Bak are required for apoptosis induction by sulforaphane, a cruciferous vegetables-derived cancer chemopreventive agent. *Cancer Research, 65*, 2035-2043.

Clarke, J. D., Dashwood, R. H. and Ho, E. (2008). Multi-targeted prevention of cancer by sulforaphane. *Cancer Letters*, *269*, 291-304.

Conaway, C. C., Getahun, S. M., Liebes, L L., Pusateri, D. J., Topham, D. K. W., Botero-Omary, M. and Chung, F. (2000). Disposition of glucosionolates and sulforaphane in humans after ingestion of steamed and fresh broccoli. *Nutrition and Cancer*, *38*, 168-178.

Elfoul, L., Rabot, S., Khelifa, N., Quinsac, A., Duguay, A. and Rimbault, A. (2001). Formation of allyl isothiocyanate from sinigrin in the digestive tract of rats monoassociated with a human colonic strain of *Bacteroides thetaiotaomicron*. *FEMS Microbiology Letters*, *197*, 99-103.

Fahey, J. W., Zalcmann, A. T. and Talalay, P. (2001). The chemical diversity and distribution of glucosinolates and isothiocyanates among plants. *Phytochemistry*, *56*, 5-51.

Faivre, J., Bouvier, A. and Bonithon-Kopp, C. (2002). Epidemiology and screening of colorectal cancer. *Best Practice and Research Clinical Gastroenterolgy*, *16*, 187-199.

Fenwick, G. R., Heaney, R. K. and Mullin, W. J. (1983). Glucosinolates and their breakdown products in food and food plants. *Critical Reviews in Food Science and Nutrition, 18*, 123-201.

Fimognari, C. and Hrelia, P. (2007). Sulforaphane as a promising molecule for fighting cancer. *Mutation Research, 653*, 90-104.

Fimognari, C., Nösse, M., Cesari, R., Iori, R., Cantelli-Forti, G. and Hrelia, P. (2002). Growth inhibition, cell-cycle arrest and apoptosis in human T-cell leukemia by the isothiocyanate sulforaphane. *Carcinogenesis, 23*, 581-586.

Fisher, D. E. (2001). The p53 tumor suppressor: critical regulator of life and death in cancer. *Apoptosis*, 6, 7-15.

Fowke, J. H., Chung, F. L., Jin, F., Qi, D., Cai, Q., Conaway, C., Cheng, J. R., Shu, X. O., Gao., Y. T. and Zheng, W. (2003). Urinary isothiocyanate levels, *Brassica*, and human breast cancer. *Cancer Research, 63*, 3980-3986.

Franks, L. M and Teich, N. M. (1997b). Oncogenes and cancer. In Teich, N. M. (Ed.), *Introduction to the Cellular and Molecular Biology of Cancer (3rd Ed.)* (pp. 169-201). Oxford: Oxford University Press.

Franks, L. M. and Teich, N. M. (1997a). What is cancer. In Franks, L. M. (Ed.), *Introduction to the Cellular and Molecular Biology of Cancer (3rd Ed.)* (pp. 1-20). Oxford: Oxford University Press.

Gamet-Payrastre, L., Li, P., Lumeau, S., Cassar, G., Dupont, M. A., Chevolleau, S., Gasc, N., Tulliez, J. and Tercé, F. (2000). Sulforaphane, a naturally occurring isothioycanate, induces cell cycle arrest and apoptosis in HT29 human colon cancer cells. *Cancer Research, 60*, 1426-1433.

Getahun, S. M. and Chung, F. L. (1999). Conversion of glucosinolates into isothiocyanates in humans after ingestion of cooked watercress. *Cancer, Epidemiology, Biomarkers and Prevention, 8*, 447-451.

Görler, K., Krumbiegeel, G., Mennick, W. H. and Siehl, H. U. (1982). The metabolism of benzyl isothiocyanate and its cysteine conjugate in guinea-pigs and rabbits. *Xenibiotica, 12*, 535-542.

Guo, J., Kleeff, J., Li, J., Ding, J., Hammer, J., Zhao, Y., Giese, T., Korc, M., Büchler, M. W. and Friess, H. (2004). Expression and functional significance of Cdc25B in human pancreatic ductal adenocarinoma. *Oncogene*, *23*, 71-78.

Hanlon, N., Coldham, N., Sauer, M. and Ioannides, C. (2009). Modulation of rat pulmonary carcinogen-metabolising enzyme systems by the isothiocyanates erucin and sulforaphane. *Chemio-biological Interactions, 177*, 115-120.

Hartwell, L. H. and Kastan, M. B. (1994). Cell cycle control and cancer. *Science*, *266*, 1821-1828.

He, S., Sun, C. and Pan, Y. (2008). Red wine polyphenols for cancer prevention. *International Journal of Molecular Sciences*, *9*, 842-853.

Hu, R., Kim, B. R., Chen, C., Hebbar, V. and Kong, A. N. T. (2003). The roles of JNK and apoptotic signaling pathways in PEITC-mediated responses in human HT-29 colon adenocarcinoma cells. *Carcinogenesis*, *24*, 1361-1367.

Huong, P. L. T., Kolk, A. H. J., Eggelte, T. A., Verstijnen, C. P. H. J., Gilis, H. and Hendriks, J. T. (1991). Measurement of antigen specific lymphocyte proliferation using 5-bromo-deoxyuridine incorporation. An easy and low cost alternative to radioactive thymidine incorporation. *Journal of Immunological Methods*, *140*, 243-248.

Jakubikova, J., Bao, Y. and Sedlak, J. (2005). Isothiocyanate induce cell cycle arrest, apoptosis and mitochondrial potential depolarization in HK-60 and multidrug-resistant cell lines. *Anticancer Research, 25*, 3375-3386.

Ji, Y. and Morris, M. E. (2003). Determination of phenethyl isothiocyanate in human plasma and urine by ammonia derivatization and liquid chromatography-tandem mass spectrometry. *Analytical Biochemistry*, *232*, 39-47.

Johnson, I. T. (2002). Glucosinolates in the human diet. Bioavailablity and implications for health. *Phytochemistry Reviews*, *1*, 183-188.

Johnson, I. T., Williamson, G. and Musk, S. (1994). Anticarcinogenic factors in plant foods: A new class of nutrients? *Nutrition Research Reviews*, *7*, 175-204.

King, R. J. B. (2000a). What is cancer. In King R. J. B. (Ed.), *Cancer Biology (2nd Ed.)* (pp. 1-7). Harlow: Pearson Education Ltd..

King, R. J. B. (2000b). Natural history: the life of a cancer. In King, R. J. B. (Ed.), *Cancer Biology (2nd Ed.)* (pp. 8-30). Harlow: Pearson Education Ltd..

King, R. J. B. (2000c). Oncogenes, repressor genes and viruses. In King, R. J. B. (Ed.), *Cancer Biology (2nd Ed.)* (pp. 71-95). Harlow: Pearson Education Ltd..

King, R. J. B. (2000d). Invasion and metastasis. In King, R. J. B. (Ed.), *Cancer Biology (2nd Ed.)* (pp. 213-232). Harlow: Pearson Education Ltd..

Klein, E. A., Lippman, S. M., Thompson, I. M., Goodman, P. J., Albanes, D., Taylor, P. R. and Coltman, C. (2003). The selenium and vitamin E cancer prevention trial. *World Journal of Urology*, *21*, 21-27.

Kris-Etherton. P. M., Hecker, K. D., Bonanome, A., Coval, S. M., Binkoski, A. E., Hilpert, K. F., Griel, A. E. and Etherton, T. D. (2002). Bioactive compounds in foods: their role in the prevention of cardiovascular disease and cancer. *The American Journal of Medicine*, *113*, 71S-88S.

Krul, C., Humblot, C., Philippe, C., Vermeulen, M., van Nuenen, M., Havenaar, R. and Rabot, S. (2002). Metabolism of sinigrin (2-propenyl glucosinolate) by the human colonic microflora in a dynamic *in vitro* large-intestinal model. *Carcinogenesis*, *23*, 1009-1016.

Kuang, Y. F. and Chen, Y. H. (2004). Induction of apoptosis in a non-small cell human lung cancer cell line by isothiocyanates is associated with P53 and P21. *Food Chemical Toxicology*, *42*, 1711-1718.

Kudo, Y., Yasui, W., Ue, T., Yamamoto, S. and Yokozaki, H. (1997). Overexpression of cyclin-dependent kinase-activating Cdc25B phosphatase in human gastric carcinomas. *Japanese Journal of Cancer Research: Gann*, *88*, 947-952.

Kune, G. and Watson, L. (2006). Colorectal cancer protective effects and the dietary micronutrients folate, methionine, vitamins B6, B12, C, E, selenium, and lycopene. *Nutrition and Cancer*, 56, 11-21.

Lazebnik, Y. A., Kaufmann, S. H., Desnoyers, S., Poirier, G. G. and Earnshaw, W. C. (1994). Cleavage of poly(ADP-ribose) polymerase by a proteinase with properties like ICE. *Nature*, *371*, 346-347.

Leoni, O., Iori, R., Palmieri, S., Esposito, E., Menegatti, E., Cortesi, R. and Nastruzzi, C. (1997). Myrosinase-generated isothiocyanate from glucosinolates: isolation, characterization and in vitro antiproliferative studies. *Bioorganic and Medicinal Chemistry*, *9*, 1799-1806.

Li, P., Nijhawan, D., Budihardjo, I., Srinivasula, S. M., Ahmad, M., Alnemari, E. S. and Wang, X. (1997). Cytochrome c and dATP-dependent formation of Apaf-1/caspase-9 complex initiates an apoptosis protease cascade. *Cell*, *91*, 479-489.

Lin, H. J., Probst-Hensch, N. M., Louie, A. D., Kau, I. H., Witte, J. S., Ingles, S. A., Frankl., H. D., Lee, E. R. and Haile, R. W. (1998). Glutathione transferase null genotype, broccoli, and lower prevalence of colorectal adenomas. *Cancer Epidemiology, Biomarkers and Prevention*, *7*, 647-652.

Livak, K. J. and Schmittgen, T. D. (2001). Analysis of relative gene expression data using real-time quantitative PCR and the $2^{-\Delta\Delta CT}$ method. *Methods*, *25*, 402-408.

Lowe, J. F. and Frazee, L. A. (2006). Update on prostate cancer chemoprevention. *Pharmacotherapy*, *26*, 353-359.

Marques-Vidal, P., Ravasco, P. and Camilo, M. E. (2006). Foodstuffs and colorectal cancer risk: a review. *Clinical Nutrition*, *25*, 14-36.

McKinnell, R. G., Parchment, R. E., Perantoni, A. O., Pierce, G. B. and Damjanov, I. (2006a). Cacinogenesis. In Perantoni, A. O. (Ed.), *The Biological Basis of Cancer (2nd Ed.)*. (pp. 80-125). Cambridge: Cambridge University Press.

McKinnell, R. G., Parchment, R. E., Perantoni, A. O., Pierce, G. B. and Damjanov, I. (2006b). Cancer-associated genes. In Perantoni, A. O. (Ed.), *The Biological Basis of Cancer (2nd Ed.)*. (pp. 145-194). Cambridge: Cambridge University Press.

McKinnell, R. G., Parchment, R. E., Perantoni, A. O., Pierce, G. B. and Damjanov, I. (2006c). Lifestyle: is there anything more important. In McKinnell, R. G. (Ed.), *The Biological Basis of Cancer (2nd Ed.)*. (pp. 248-265). Cambridge: Cambridge University Press.

McKinnell, R. G., Parchment, R. E., Perantoni, A. O., Pierce, G. B. and Damjanov, I. (2006d). Oncology: the difficult task of eradicating caricatures of normal tissue renewal in the human patient. In Parchment, R. E. (Ed.), *The Biological Basis of Cancer (2nd Ed.)*. (pp. 307-354). Cambridge: Cambridge University Press.

McMillan, M., Spinks, E. A. and Fenwick, G. R. (1986). Preliminary observations on the effect of dietary Brussels sprouts on thyroid function. *Human Toxicology*, *5*, 15-19.

McNaughton, S. A. and Marks, G. C. (2003). Development of a food compositon database for the estimation of dietary intakes of glucosinolates, the biologically active constituents of cruciferous vegetables. *British Journal of Nutrition*, *90*, 687-697.

Mennicke, W.H., Görler, K. and Krumbiegel, G. (1983). Metabolism of some naturally occurring isothiocyanates in the rat. *Xenobiotica, 13*, 203-207.

Mennicke, W.H., Görler, K., Krumbiegel, G., Lorenz, D. and Rittmann, N. (1988). Studies on the metabolism and excretion of benzyl isothiocyanate in man. *Xenobiotica, 18*, 441-447.

Mithen, R. F., Dekker, M., Verkerk, R., Rabot, S. and Johnson, I. T. (2000). The nutritional significance, biosynthesis and bioavailability of glucosinolates in human foods. *Journal of the Science of Food and Agriculture*, *80*, 967-984.

Molinari, M. (2000). Cell cycle checkpoints and their inactivation in human cancer. *Cell proliferation*, *33*, 261-274.

Moreno, D A., Carvajal, M., López-Berenguer, C. and García-Viguera, C. (2006). Chemical and biological characterization of nutraceutical compounds of broccoli. *Journal of Pharmaceutical and Biomedical Analysis*, *41*, 1508-1522.

Mosmann, T. (1983). Rapid colorimetric assay for cellular growth and survival: application to proliferation and cytotoxicity assays. *Journal of Immunological Methods*, 65, 55-63.

Musk, S. R. R. and Johnson, I. T. (1993). Allyl isothiocyanate is selectively toxic to transformed cells of human colorectal tumor line HT29. *Carcinogenesis*, *14*, 2079-2083.

Myzak, M. C., Dashwood, W. M., Orner, G. A., Ho, E. and Dashwood, R. H. (2006). Sulforaphane inhibits histone deacetylase in vivo and suppresses tumorigenesis in Apc-minus mice. *FASEB Journal*, *20*, 506-508.

Nigam, N., Prasad, S., George, J. and Shukla, Y. (2009). Lupeol induces p53 and cyclin-B-mediated G_2/M arrest and targets apoptosis through activation of caspase in mouse skin. *Biochemical Biophysical Research Communication*, *381*, 253-258.

Nishikawa, A., Furukawa, F., Uneyama, C., Ikezaki, S., Tanakamaru, Z, Y., Chung, F. L., Takahashi, M. and Hayashi, Y. (1996). Chemopreventive effects of phenethyl isothiocyanate on lung and pancreatic tumorigenesis in *N*-nitrosobis(2-oxopropyl)amine-treated hamsters. *Carcinogenesis*, *17*, 1381-1384.

Palop, M. L., Smiths, J. P. and ten Brink, B. (1995). Degradation of sinigrin by *Lactobacillus agilis* strain R16. *International Journal of Food Microbiology*, 26, 219-229.

Pappa, G., Bartsch, H. and Gerhäuser, C. (2007). Biphasic modulation of cell proliferation by sulforaphane at physiologically relevant exposure times in a human colon cancer cell line. *Molecular Nutrition and Food Research*, *51*, 977-984.

Pappa, G., Lichtenberg, M., Iori, R., Barillari, J., Bartsch, H. and Gerhäuser, C. (2006). Comparison of growth inhibition profiles and mechanisms of apoptosis induction in human colon cancer cell lines by isothiocyanates and indoles from *Brassicaceae*. *Mutation Research*, *599*, 76-87.

Pennington, J. A. T. (2002). Food composition databases for bioactive food components. *Journal of Food Components and Analysis*, *15*, 419-434.

Porstmann, T., Ternynck, T. and Avrameas, S. (1985). Quantitation of 5-bromo-2-deoxyuridine incorporation into DNA: an enzyme immunoassay for the assessment of the lymphoid cell proliferative response. *Journal of Immunological Methods*, *82*, 169-179.

Prasad, S., Nigam, N., Kalra, N. and Shukla, Y. (2008). Regulation of signaling pathways involved in lupeol induced inhibition of proliferation and induction of apoptosis in human prostate cancer cells. *Molecular Carcinogenesis*, *47*, 916-924.

Prawan, A., Saw, C. L. L., Khor, T. O., Keum, Y., Yu, S., Hu, L. and Kong, A. (2009). Anti-NF-κB and anti-inflammatory activities of synthetic isothiocyanates: effect of chemical structures and cellular signaling. *Chemico-Biological Interactions*, *179*, 202-211.

Pucillo, C., Salzano, D., Pepe, S., Vitale, M., Formisano, S. and Rossi, G. (1990). Regulation of expression of low-affinity IgE receptor (FcεRII) in the human monocyte-like cell line (U937) by phorbol esters and IgE. *International Archives of Allergy and Applied Immunology*, *93*, 330-337.

Ramos, S. (2007). Effects of dietary flavonoids on apoptotic pathways related to cancer chemoprevention. *Journal of Nutritional Biochemistry, 18*, 427-442.

Ramos, S. (2008). Cancer chemoprevention and chemotherapy: dietary polyphenols and signaling pathways. *Molecular Nutrition and Food Research*, *52*, 507-526.

Reddy, B. S. (1999). Role of dietary fiber in colon cancer: an overview. The *American Journal of Medicine*, *106*, 16-19.

Rose, P., Whiteman, M., Huang, S. H., Halliwell, B. and Ong, C. N. (2003). β-phenylethyl isothiocyanate-mediated apoptosis in hepatoma HepG2 cells. *Cellular and Molecular Life Sciences*, *60*, 1489-1503.

Rungapamestry, V., Duncan, A. J., Fuller , Z. and Ratcliffe, B. (2007). Effect of meal composition and cooking duration on the fate of sulforaphane following consumption of broccoli by healthy human subjects. *British Journal of Nutrition*, *97*, 644-652.

Satyan, K. S., Swamy, N., Dizon, D. S., Singh, R., Granai, C. O. and Brard, L. (2006). Phenethyl isothiocyanate (PEITC) inhibits growth of ovarian cancer cells by inducing apoptosis: role of caspase and MAPK activation. *Gynecologic Oncology*, *103*, 261-270.

Shackelford, R. E., Kaufmann, W. K. and Paules, R. S. (2000). Oxidative stress and cell cycle checkpoint function. *Free Radical Biology and Medicine*, *28*, 1387-1404.

Sherr, C. (2004). Principles of tumor suppression. *Cell*, *116*, 235-246.

Singh, A. V., Xiao, D., Lew, K. L., Dhir, R. and Singh, S. V. (2004a). Sulforaphane induces caspase-mediated apoptosis in cultured PC-3 human prostate cancer cells and retards growth of PC-3 xenografts in vivo. *Carcinogenesis*, *25*, 83-90.

Singh, S. V., Herman-Antosiewicz, A., Singh, A. V., Lew, K. L., Srivastava, S. K., Kamath, R., Brown, K. D., Zhang, L. and Baskaran, R. (2004b). Sulforaphane-induced G_2/M phase cell cycle arrest involves checkpoint kinase 2-mediated phosphorylation of cell division cycle 25C. The *Journal of Biological Chemistry*, *279*, 25813-25822.

Singh, S. V., Mohan, R. R., Agarwal, R., Benson, P. J., Hu, X., Rudy, M. A., Xia, H., Katoh, A., Srivastava, S. K., Mukhtar, H., Gupta, V. and Zaren, H. A. (1996). Novel anti-carcinogenic activity of an organosulfide from garlic: inhibition of H-*RAS* oncogene transformed tumor growth *in vivo* by diallyl disulfide is associated with inhibition of $p^{21H\text{-}ras}$ processing. *Biochemical Biophysical Research Communications*, *225*, 660-665.

Song, L., Iori, R. and Thornalley, P. J. (2006). Purification of major glucosinolates from *Brassicaceae* seeds and preparation of isothiocyanate and amine metabolites. *Journal of the Science of Food and Agriculture*, *86*, 1271-1280.

Song, L., Morrison, J. J., Botting, N. P. and Thornalley, P. J. (2005). Analysis of glucosinolates, isothiocyanates, and amine degradation products in vegetable extracts and blood plasma by LC-MS/MS. *Analytical Biochemistry*, *347*, 234-243.

Srivastava, S. K., Xiao, D., Lew, K. L., Hershberger, P., Kokkinakis, D. M., Johnson, C. S., Trump, D. L. and Singh, S. V. (2003). Allyl isothiocyanate, a constituent of cruciferous vegetables, inhibits growth of PC-3 human prostate cancer xenografts in vivo. *Carcinogenesis*, *24*, 1665-1670.

Staretz, M. E., Koenig, L. and Hecht, S. S. (1997). Effects of long term dietary phenethyl isothiocyanate on the microsomal metabolism of 4-(methylnitrosamino)-1-(3-pyridyl)-1-butanone and 4-(methylnitrosamino)-1-(3-pyridyl)-1-butanol in F344 rats. *Carcinogenesis*, *18*, 1715-1722.

Steinmetz, K. A. and Potter, J. D. (1996). Vegetables, fruit, and cancer prevention: a review. *Journal of the American Dietetic Association*, *96*, 1027-1039.

Stewart, B. W. and Kleihues, P. (2003). International Agency for Research on Cancer. World. In Stewart, B. W. and Kleihues, P. (Ed.), *Cancer Report*. Lyon: IARC Press.

Strausfeld, U., Labbé, J. C., Fesquet, D., Cavadore, J. C., Picard, A., Sadhu, K., Russell, P. and Dorée, M. (1991). Dephosphorylation and activation of a $p34^{cdc2}$/ cyclin B complex *in vitro* by human CDC25 protein. *Nature*, *351*, 242-245.

Surh, Y. J. (2003). Cancer chemoprevention with dietary phytochemicals. *Nature Reviews. Cancer*, *3*, 768-780.

Tang, L. and Zhang, Y. (2004). Dietary isothiocyanates inhibit the growth of human bladder carcinoma cells. *The Journal of Nutrition*, *134*, 2004-2010.

Tannock, I. F., Hill, R. P., Bristow, R. G. and Harrington, L. (2004a). Chemical and radiation carcinogenesis. In Okey, A. B., Harper, P. A., Grant, D. M., and Hill, R. P. (Ed.). *The Basic Science of Oncology* (4th Ed) (pp. 25-48). New York: McGraw-Hill Companies, Inc..

Tannock, I. F., Hill, R. P., Bristow, R. G. and Harrington, L. (2004b). Oncogenes and tumor suppressor genes. In Oster, S., Penn, L., and McGlade, J. (Ed.). *The Basic Science of Oncology* (4th Ed) (pp. 123-141). New York: McGraw-Hill Companies, Inc..

Tannock, I. F., Hill, R. P., Bristow, R. G. and Harrington, L. (2004c). Angiogenesis. In Sturk, C., and Dumont, D. (Ed.). *The Basic Science of Oncology* (4th Ed) (pp. 123-141). New York: McGraw-Hill Companies, Inc..

Terry, P., Lagergren, J., Ye, W., Wolk, A. and Nyrén, O. (2001). Inverse association between intake of cereal fiber and risk of gastric cardia cancer. *Gastroenterology*, *120*, 387-391.

Thejass, P. and Kuttan, G. (2007). Allyl isothiocyanate (AITC) and phenyl isothiocyanate (PITC) inhibit tumor-specific angiogenesis by downregulating nitric oxide (NO) and tumor necrosis factor-α (TNF-α) production. *Nitric Oxide*, *16*, 247-257.

Tian, Q., Rosselot, R. A. and Schwartz, S. J. (2005). Quantitative determination of intact glucosinolates in broccoli, broccoli sprouts, Brussels sprouts, and cauliflower by high-performance liquid chromatography-electrospray ionization-tandem mass spectrometry. *Analytical Biochemistry, 343*, 93-99.

Towbin, H., Staehelin, T. and Gordon, J. (1979). Electrophoretic transfer of proteins from polyacrylamide gels to nitrocellulose sheets: procedure and some applications. *Proceedings of the National Academy of Sciences of the United States of America, 76*, 4350-4354.

Verhoeven, D. T. H., Goldbohm, R. A., van Poppel, G., Verhagen, H. and van Den Brandt, P. A. (1996). Epidemiological studies on Brassica vegetables and cancer risk. *Cancer Epidemiology, Biomarkers and Prevention, 5*, 733-748.

Verkerk, R., Schreiner, M., Krumbein, A., Ciska, E., Holst, B., Rowland, I., De Schrijver, R., Hansen, M., Gerhäusher, C., Mithen, R. and Dekker, M. (2009). Glucosinolates in Brassica vegetables: the influence of the food supply chain on intake, bioavailability and human health. *Molecular Nutrition and Food Research, In press*.

Winawer, S. J. (2007). Colorectal cancer screening. Best Practice and Research *Clinical Gastroenterology, 21*, 1031-1048.

Wolf, F., Wandke, C., Isenberg, N. and Geley, S. (2006). Dose-dependent effects of stable cyclin B1 on progression through mitosis in human cells. *EMBO Journal, 25*, 2802–2813.

Wu, S. J., Ng, L. T. and Lin. C. C. (2005). Effects of antioxidants and caspase-3 inhibitor on the phenylethyl isothiocyanate-induced apoptotic signaling pathways in human PLC/PRF/5 cells. *European Journal of Pharmacology, 518*, 96-106.

Xiao, D., Johnson, C. S., Trump, D. L. and Singh, S. V. (2004). Proteasome-mediated degradation of cell division cycle 25C and cyclin-dependent kinase 1 in phenethyl isothiocyanate-induced G_2/M-phase cell cycle arrest in PC-3 human prostate cancer cells. *Molecular Cancer Therapeutics, 3*, 567-575.

Xiao, D., Srivastava, S. K., Lew, K. L., Zeng, Y., Hershberger, P., Johnson, C. S., Trump, D. L. and Singh, S. V. (2003). Allyl isothiocyanate, a constituent of cruciferous vegetables, inhibits proliferation of human prostate cancer cells by causing G_2/M arrest and inducing apoptosis. *Carcinogenesis*, *24*, 891-897.

Xu, C., Shen, G., Yuan, X., Kim, J., Gopalkrishnan, A., Keum, Y., Nair, S. and Kong, A. T. (2006). ERK and JNK signaling pathways are involved in the regulation of activator protein 1 and cell death elicited by three isothioycanates in human prostate cancer PC-3 cells. *Carcinogenesis*, *27*, 437-445.

Ye, L., Dinkova-Kostova, A. T., Wade, K. L., Zhang, Y., Shapiro, T. A. and Talalay, P. (2002). Quantitative determination of dithiocarbamates in human plasma, serum, erythrocytes and urine: pharmocokinetics of broccoli sprout isothiocyanates in humans. *Clinica Chimica Acta*, *316*, 43-53.

Yeh C. T. and Yen G. C. (2005). Effect of sulforaphane on metallothionein expression and induction of apoptosis in human hepatoma HepG2 cells. *Carcinogenesis*, *26*, 2138-2148.

Zhang, Y. (2000). Role of glutathione in the accumulation of anticarcinogenic isothiocyanates and their glutathione conjugates by murine hepatoma cells. *Carcinogenesis, 21*, 1175-1182.

Zhang, Y. (2001). Molecular mechanism of rapid cellular accumulation of anticarcinogenic isothiocyanates. *Carcinogenesis, 22*, 425-431.

Zhang, Y. and Callaway, E. C. (2002). High cellular accumulation of sulfhoraphane, a dietary anticarcinogen, is followed by rapid transporter-mediated export as a glutathione conjugate. *The Biochemical journal, 364*, 301-307.

Zhang, Y., Tang, L. and Gonzalez, V. (2003). Selected isothiocyanates rapidly induce growth inhibition of cancer cells. *Molecular Cancer Therapeutics*, *10*, 1045-1052.

Zhang, Y., Yao, S. and Li, J. (2006). Vegetable-derived isothiocyanates: anti-proliferative activity and mechanism of action. *Proceedings of the Nutrition Society*, *65*, 68-75.